

Rare-Earth Complexes in Ionic Liquids

Structures, Electrochemical and Optical Properties

Inaugural-Dissertation
zur Erlangung des Doktorgrades
der Mathematisch-Naturwissenschaftlichen Fakultät
der Universität zu Köln

vorgelegt von

Arash Babai
aus Trier

Köln 2006

Die vorliegende Arbeit wurde im Zeitraum von Oktober 2004 bis August 2006 am Institut für Anorganische Chemie der Universität zu Köln unter der Anleitung von Priv.-Doz. Dr. Anja-Verena Muding angefertigt.

Berichterstatter: Priv.-Doz. Dr. Anja-Verena Muding
Prof. Dr. Gerd Meyer

Tag der mündlichen Prüfung: 08.11.2006

“These Elements (rare earth) perplex us in our researches, baffle us in our speculations, and haunt us in our very dreams. They stretch like an unknown sea before us – mocking, mystifying and murmuring strange revelations and possibilities.”

Sir William Crookes (Address to the British Association, 1876)

Acknowledgements

First of all, I would like to thank my supervisor Priv.-Doz. Dr. Anja-Verena Mudring for her great support, fruitful discussions and providing an excellent environment to prepare this thesis. It is a privilege to be part of her team.

I am grateful to Professor Dr. Gerd Meyer for supporting me during my studies at the university and showing me the appeal of inorganic chemistry.

Special thanks to my colleagues for good collaboration and for providing a great working environment in all respects. It was a pleasure to work with them; I enjoyed the good ambience in the laboratory.

Furthermore, I would like to thank the whole *Meyer* group, especially Dr. I. Pantenburg and I. Müller for single-crystal XRD and H. Schuhmacher for powder XRD measurements.

Sincere thank goes to my family and my partner. Their support made this project possible. I am grateful to be surrounded by such persons.

Abstract.– The thesis presented here deals with solvent-solute interactions of rare-earth ions in bis(trifluoromethanesulfonyl)amide ([Tf₂N]⁻) and trifluoromethanesulfonate ([OTf]⁻)-based ionic liquids (IL). In order to elucidate the process of solvation, rare earth iodides, triflates and bis(trifluoromethanesulfonyl)amides are synthesized as precursors and reacted with [Tf₂N]⁻ and [OTf]⁻-based ionic liquids, containing substituted pyrrolidinium or imidazolium heterocycles as cations.

Interaction of NdI₃ with the room temperature ionic liquid (RTIL) 1-butyl-1-methylpyrrolidinium [Tf₂N] ([bmpyr][Tf₂N]) leads to the formation of the sparingly soluble compound [bmpyr]₄[NdI₆][Tf₂N], the anion of the RTIL being incorporated in the structure in a non-coordinating fashion. By displacing the butyl chain in [bmpyr]⁺ by a methyl group, the compound [mppyr]₃[NdI₆], a [Tf₂N]-free compound is obtained. The solvation of the other trivalent iodides of the rare-earth elements leads to similar compounds with the composition [bmpyr]₄[LnI₆][Tf₂N] (Ln = La, Pr, Sm, Dy, Er) in which the metals are coordinated octahedrally by iodine atoms. A structural change is observed between Pr and Nd, which is manifested in the arrangement of the [LnI₆]-octahedra with respect to each other.

The coordination mode of the [Tf₂N]⁻-anion was determined by reaction of Ln(Tf₂N)₃ with [bmpyr][Tf₂N]. X-Ray structure determinations reveal that [bmpyr]₂[Ln(Tf₂N)₅] is formed for the larger lanthanides (La-Tb), whereas the smaller ones (Dy-Lu) are coordinated by four ligands in [bmpyr][Ln(Tf₂N)₄]. The RTIL 1-butyl-1-methylimidazolium [Tf₂N] ([bmim][Tf₂N]) reacts with Eu(Tf₂N)₃ to give a lanthanide-based RTIL [bmim][Eu(Tf₂N)₅] (glass-transition point: -50°C). Ligand exchange examinations reveal that [OTf]⁻-anions are able to displace [Tf₂N]⁻-ligands. For example the compound [bmpyr]₄[Yb(OTf)₆][Tf₂N] can be crystallized from Yb(Tf₂N)₃ and [bmpyr][OTf]. Simple halides of the salt-like divalent rare-earth dissolve in [Tf₂N]-based ILs under complete ligand exchange as can be shown by the formation of [mppyr]₂[Yb(Tf₂N)₄] from YbI₂ and [mppyr][Tf₂N]. In addition, [mppyr]₂[AE(Tf₂N)₄] (AE = Ca, Sr) and [mppyr][Ba(Tf₂N)₃] were synthesized as model compounds for the larger divalent lanthanides (Eu, Sm).

Zusammenfassung.– In der vorliegenden Arbeit werden Solvens-Solvat Wechselwirkungen von Lanthanid-Ionen in Bis(trifluoromethansulfonyl)amide ([Tf₂N])- und Trifluoromethansulfonate ([OTf])-basierten Ionischen Flüssigkeiten (IL = ionic liquids) untersucht. Zu diesem Zweck wurden die dreiwertigen Iodide, Triflate und Bis(trifluormethansulfonyl)amide der Seltenen-Erden, und die wasserfreien Diodide des Yb, Sm, Ca, Sr und Ba als Ausgangsverbindungen synthetisiert. Die Untersuchten Ionischen Flüssigkeiten bestehen aus [Tf₂N]- oder [OTf]-Anionen, als Kationen dienen bisubstituierte N-Heterocyclen (Pyrrolidinium oder Imidazolium). Durch die Reaktion von NdI₃ mit der RTIL (room temperature ionic liquid) 1-Butyl-1-methylpyrrolidinium [Tf₂N] ([bmpyr][Tf₂N]) wurde die schwerlösliche Verbindung [bmpyr]₄[NdI₆][Tf₂N] erhalten. Das Anion der IL ist hierbei nicht koordinierend in die Struktur eingebaut, die Verbindung kann daher als Solvat Addukt gemäß [bmpyr]₃[NdI₆]·[bmpyr][Tf₂N] aufgefasst werden. Durch Austausch des Butyl-Substituenten am Kation der IL durch eine Propyl-Seitenkette ([mppyr]) konnte die [Tf₂N]-freie Verbindung [mppyr]₃[NdI₆] erhalten werden. Systematische Untersuchungen zum Solvatationsverhalten der weiteren Lanthanidiodide führte zu Produkten der gleichen Zusammensetzung, [bmpyr]₄[LnI₆][Tf₂N] (Ln = La, Pr, Sm, Dy, Er), wobei der Effekt der Lanthanidenkontraktion zu einem strukturellen Übergang von *P*₄*3**2*₁*2* (La-Pr) zu *I*₄*1*/*a* (Nd-Er) führt, bei dem sich die Anordnung der [LnI₆]³⁻ Oktaeder entlang der kristallographischen *c*-Achse ändert. Anhand der Praseodym-Verbindungen [bmpyr]₄[PrI₆][Tf₂N] und [bmpyr][Pr(Tf₂N)₅] wurden die luminophoren Eigenschaften in Lösung und in Festphase untersucht. Dabei lässt sich in Lösung eine bemerkenswerte Population der hochenergetischen Zustände nachweisen, die in konventionellen Lösemitteln weitestgehend strahlungslos deaktiviert wird. Die Koordination der [Tf₂N]-Anionen wurde durch Reaktion von Ln(Tf₂N)₃ (Ln = Pr, Nd, Sm, Eu, Tb, Dy, Tm, Yb, Lu) mit [bmpyr][Tf₂N] nachgewiesen. Bei den größeren Lanthaniden entsteht die Verbindung [bmpyr]₂[Ln(Tf₂N)₅] (Ln = La-Dy) während die kleineren lediglich vier Anionen gemäß

[bmpyr][Ln(Tf₂N)₄] koordinieren. Die Koordinationsmodi wurden eingehend an der Eu- und Yb- Verbindung spektroskopisch und elektrochemisch untersucht. Durch Reaktion von Yb(Tf₂N)₃ mit der Triflat-basierten Ionischen Flüssigkeit [bmpyr][OTf] konnte die Verbindung [bmpyr]₄[Yb(OTf)₆][Tf₂N] kristallisiert werden. Die stärker basischen Triflat-Liganden verdrängen in dieser Verbindung alle [Tf₂N]-Liganden aus der Koordinationssphäre des Yb-Ions. Die [Tf₂N]-Einheit ist wiederum als Solvens-Addukt gemäß [bmpyr]₃[Yb(OTf)₆]·[bmpyr][Tf₂N] in die Struktur eingebaut. Durch cyclovoltammetrische Untersuchungen konnte der Ligandenaustausch auch in Lösung nachgewiesen werden. Hierbei ließ sich die stärkere Lewis-Basizität der Triflat-Liganden gegenüber den Bis(trifluormethansulfonyl)amiden feststellen. Die [Tf₂N]-freie Verbindung [bmpyr]₃[Yb(OTf)₆] konnte durch Umsetzung von Yb(OTf)₃ mit [bmpyr][OTf] erhalten werden. Im Bereich der zweiwertigen Seltenerd-Verbindungen konnte durch Reaktion von YbI₂ mit [mppyrr][Tf₂N] die homoleptische Verbindung [mppyrr][Yb(Tf₂N)₄] isoliert werden, bei der analog zur dreiwertigen Verbindung vier Anionen das Metallion koordinieren. Für die analoge Samarium-Verbindung konnte eine zweiwertige Spezies lediglich spektroskopisch in Lösung nachgewiesen werden. NdI₂ zeigt gegenüber Pyrrolidinium-basierten ILs keine Reaktivität, ein Übergang zu Triethylsulfonium-Kationen führt zur Zersetzung der Ionischen Flüssigkeit. Durch Reaktion von NdI₂ und SmI₂ mit [S(Et)₃][Tf₂N] konnte das dreiwertige Zersetzungsprodukt [S(Et)₃]₃[LnI₆] (Ln = Nd, Sm) kristallographisch nachgewiesen werden. Als strukturemisches Modell für die zweiwertigen Ionen des Sm und Eu wurden Erdalkalimetallionen herangezogen. Die Umsetzung von CaI₂ und SrI₂ mit [mppyrr][Tf₂N] führte zu Yb-analogen Verbindungen [mppyrr][AE(Tf₂N)₄] (AE = Ca, Sr). Die Umsetzung mit BaI₂ ergab die Verbindung [mppyrr][Ba(Tf₂N)₃], in der die [Tf₂N]-Liganden Barium-Ionen zu unendlichen Ketten verknüpfen. Die unterschiedlichen Koordinationsmodi wurden Raman-spektroskopisch bestätigt.

Index

I. General considerations.....	12
1. Introduction.....	12
2. State of the art	13
2.1 What is an ionic liquid?.....	13
2.2 Divalent lanthanide-mediated organic reactions	14
2.3 Trivalent lanthanide-catalyzed organic reactions.....	15
2.4 Spectroscopy of rare-earth compounds in ionic liquids	16
2.5 Electrochemistry of rare-earth compounds in ionic liquids	17
3. Literature.....	18
II. Ln(III)-compounds in ionic liquids	21
1. NdI₃ in Tf₂N-based ionic liquids.....	21
1.1 Introduction	21
1.2 Preparation	21
1.3 Structural aspects.....	23
1.4 Discussion	26
1.5 Literature	27
2. Pr(III)-compounds in [bmpyr][Tf₂N] – structural and optical aspects.....	29
2.1 Introduction	29
2.2 Preparation	30
2.3 Structural aspects.....	30
2.3.1 Comparison of [bmpyr] ₄ [PrI ₆][Tf ₂ N] and [bmpyr] ₄ [NdI ₆][Tf ₂ N].....	30
2.3.2 The coordination mode of the [Tf ₂ N]-anion in [bmpyr] ₂ [Pr(Tf ₂ N) ₅].....	34
2.4 Spectroscopical aspects	36
2.4 Discussion	39
2.5 Literature	40
3. Behaviour of Ln(Tf₂N)₃ in [bmpyr][Tf₂N]	41
3.1 Introduction	41
3.2 Preparation	41
3.3 Structural aspects.....	43
3.4 Thermal investigations	49
3.4 Spectroscopical investigations	51
3.5 Ligand exchange reactions	53
3.5.1 Structural investigations.....	53
3.5.2 Electrochemical investigations.....	57
3.6 Literature	59
III. Divalent (pseudo) rare-earth compounds in ILs	60
1. YbI₂ in Tf₂N-based ionic liquids	60
1.1 Introduction	60
1.2 Preparation	61
1.3 Structural aspects.....	61
1.4 Literature	64

2.	SmI₂ and NdI₂ in [S(Et)₃][Tf₂N]	66
2.1	Introduction	66
2.2	Preparation	66
2.3	Structural aspects.....	67
2.4	Literature	69
3.	Alkaline-earth diiodides in [mppy_r][Tf₂N]	71
3.1	Introduction	71
3.2	Preparation	71
3.3	Structural aspects.....	72
3.4	Raman investigations	82
3.5	Discussion	83
3.6	Literature	84
IV	Summary	86
V	Appendix	93
1.	General Methods	93
1.1	Experimental techniques	93
1.2	XRD-methods.....	93
1.3	Absorption-, Emission- and Raman-spectroscopy	94
1.4	DSC and cyclic voltammetry	94
2.	VIS-Spectrum of Sm²⁺ in [bmpyr][Tf₂N]	95
3.	List of Abbreviations	96
4.	Chemicals	97
5.	Publications	98
	Curriculum Vitae	101

I. General considerations

1. Introduction

The aim of this work is to gain a better understanding of the interaction of rare earth ions with triflate- and bis(trifluoromethanesulfonyl)amide-based ionic liquids. These systems have received considerable attention over the last few years in several fields of chemistry, whereas most of the published work in this field appeared in the last two years. This indicates the growing interest in this class of compounds and their high potential for different applications.

Gaillard *et al.* investigated the behaviour of Eu(III) and its halides in RTILs in the context of actinide/lanthanide separation [1]. Already in 1999, a patent had been filed for the recovery of uranium and plutonium from spent nuclear fuels [2]. Especially Tf₂N⁻ based RTILs (Tf₂N⁻ = bis(trifluoromethanesulfonyl)-amide) are expected to be applicable to various uses in electrochemistry such as batteries, electroplating and electrochemical syntheses [3]. Also in organic chemistry rare-earth/ionic liquid-based systems are identified as very useful catalysts e.g. in the Friedel-Crafts acylation of aromatics with Yb(Tf₂N)₃/[bmim][Tf₂N] [4]. However, one major application of rare-earth compounds follows from its luminescence properties which are widely applied. Lighting devices (economical luminescent lamps, light emitting diodes), television and computer displays, optical fibres, optical amplifiers, lasers, as well as responsive luminescent stains for biomedical analysis, medical diagnosis, and cell imaging rely heavily on lanthanide ions [5]. Their optical properties can be modified by the use of ionic liquids. For example, high quantum yields and enhanced photostability have been recently reported for Eu(III) in a weakly coordinating imidazolium ionic liquid [6]. Since there is very little known about complexation effects of rare earth ions in ionic liquids, the aim of this work is to get deeper insights into the dissolution process of rare-earth compounds in certain ionic liquids as they crucially determine the material's properties.

The main focus is set on the electrochemical and optical properties of these systems, and the structure determination of newly composed complexes.

2. State of the art

2.1 What is an ionic liquid?

According to a common definition, ionic liquids (ILs) are compounds which consist entirely of ions and have a melting point below 100°C. The definition of a melting point < 100°C comes from the patent literature in order to distinguish this class of compounds from traditional high temperature molten salts. Many are even liquid at room temperature (RTIL's – room temperature ionic liquids). Because of their salt-like nature, ionic liquids have a high Coulomb potential which can be used to stabilize other ionic compounds. But not only! It has been well established that ionic liquids can even dissolve metals [7]. The character of an ionic liquid can be comparatively easily tuned (and thus tailored for a certain application) by the choice of the respective cation/anion combination. Physical and chemical properties that are dependent on the cation/anion combination include miscibility of the IL with water, organic solvents, dissolution of gases, basicity, coordination power, viscosity, thermal stability and many further properties [8]. The unique constituency of ionic liquids allows not only the choice between different cations and anions (c.f. Figure 1) but also further functionalization of the ionic liquid via modification of the cationic alkyl chain. For example, it has already been shown that air-sensitive transition metal catalysts can be kinetically stabilized in certain ionic liquids [9]. Furthermore, ionic liquids as a solvent for synthetic reactions have the advantage of a negligible vapour pressure, which offers, aside from “green chemistry” aspects (low volatility, no flammability etc.), the possibility to distill off any volatile reaction products and at the same time keep the catalyst cation in solution.

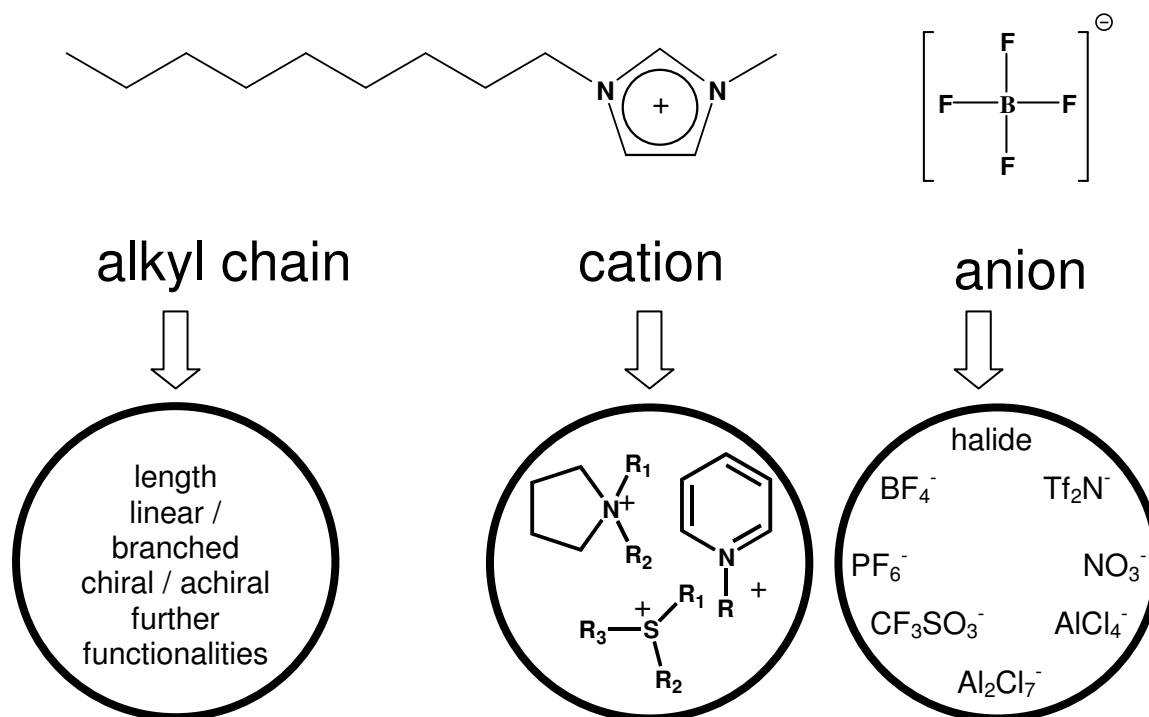


Fig. 1: The ionic liquid "construction kit"

2.2 Divalent lanthanide-mediated organic reactions

Rare-earth Compounds in the oxidation states +III are widely applied in conventional solvents for numerous organic transformations. For the +II state, the most prominent is the Kagan-reagent, SmI₂. This compound is usually synthesized *in situ* in THF from Sm metal and CH₂I₂ [10]. It is used for selective reduction of functional groups and reductive C-C coupling (e.g. Pinacol-coupling, Barbier-Grignard-reaction [11], cleavage of C-heteroatom-bonds [12]). Sm(II) together with Sm(III) is used for selective reduction of carboxylic acids in presence of aldehydes [13] and also in cascade-Aldol-Tishchenko-reaktionen [14]. Eu(II) und Yb(II) are less investigated due to their lower redox-potential. The more reducing divalent species are too reactive to be utilized in molecular solvents at ambient temperatures. Nd(II) for example decomposes in THF above -20°C. Divalent organometallic species of Tm are stable as solid compounds, but decompose in solution in about several hours [15-22]. Recently it was shown, that DyI₂(THF)₅, due to its higher reduction potential, can be utilized for reductive coupling of alkyl-halides which are not coupled by SmI₂ [23]. Also the system NdI₃/Na yields interesting coupling reactions,

although the route of the transformation and the active species is not determined clearly [24]. Yet, ionic liquids are not utilized as a reaction media for divalent rare-earth species, although the effect of the Coulomb potential could stabilize metal-ions in solution. Only one work appeared before the start of this work, dealing with the spectroscopical investigation of EuI_2 in a $[\text{PF}_6]^-$ based ionic liquid [25].

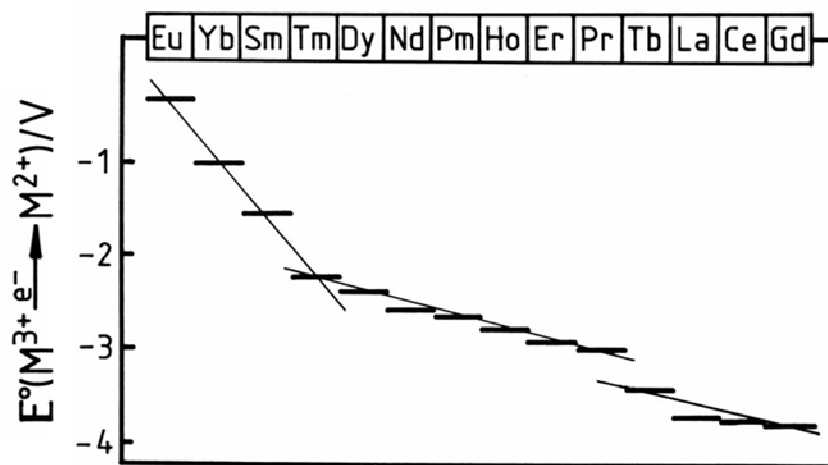


Fig. 2: Reduction potentials Ln(III)/Ln(II) [26]

2.3 Trivalent lanthanide-catalyzed organic reactions

Trivalent lanthanide compounds can be used like to AlCl_3 as a Lewis-acid-catalyst and are utilized for C-C and C-heteroatom bond formation [27] (c.f. Michael-reaction [28], Tishchenko-reduction [29], Baeyer-Villiger-reaction [30], (Mukaiyama) aldol-condensation [31], Diels-Alder-reaction or Claisen-reaction). Stereoselective transformations can be accomplished with chiral rare-earth compounds e.g. with Lanthanum-BINOL [32]. Regarding the effectiveness as a catalyst several rare-earth trihalides were compared and investigated in reactivity towards the Meerwein-Ponndorf-Verley-reduction [33] and Hetero-Diels-Alder-reactions [34]. There is a direct connection between the ionic radius and the catalytic activity in these systems. By choosing the size of the metal-ion, the acidity and therefore the reactivity is tuneable.

Lewis-acid catalysis with rare-earth compounds in ionic liquids is known, e.g. with triflates of Sc, used for cyclodimerization [35], 1,3-dienes, for Aza-Diels-Alder-reactions [36] and Claisen-rearrangements [37]. Lanthanoid-triflates in ionic liquids can be used for a three-component reaction of aldehyde, amine und $P(OEt)_3$ to yield α -aminophosphonates, an important class of pharmaceutical products [39]. This reaction is catalyzed by $M(OTf)_3$, $M=Yb, Sc, Dy, Sm$ in $[bmim][PF_6]$, $[bmim][SbF_6]$, $[bmim][BF_4]$ und $[bmim][OTf]$ in high yields (>90% in ionic liquid compared with 70% in dichloromethane) [40]. $M(OTf)_3$ ($M=Y, Ho, Tm$ and Lu) catalyze the Friedel-Crafts-alkylation of arenes if they are dissolved in ionic liquids; in molecular solvents they exhibit no catalytic activity [41]. In the Friedel-Crafts acylation of aromatic compounds with carboxylic acids and aldehydes, rare-earth $[Tf_2N]$ -compounds can be utilized [42]. In all cases, the structure of the catalytic active species is to a great extent unknown.

2.4 Spectroscopy of rare-earth compounds in ionic liquids

Ionic liquids with weakly coordinating anions are solvents with interesting properties to study the luminescence of rare-earth ions. In conventional solvents, the excited state can be easily quenched by multiphonon relaxation due to high frequency oscillators (e.g., O-H, N-H, C-H bonds) which can transfer the energy from the luminescent centre to vibronic modes of the ligands. Especially low energy transitions in the near-infrared (1-1.6 μm) are quenched effectively. However, lanthanide near-infrared emitters are of huge interest as potential stains for immunoassays or for the imaging of biological cells, since biological tissues are to a great extent transparent in this range [43]. By designing the ionic liquid, luminescent properties can be tuned in a way that is desired for the respective application. For example, NdI_3 and ErI_3 dissolved in a hydrophobic imidazolium ionic liquid show an intense luminescence in the near-infrared [44]. By designing the ionic liquid in a way that there are no high frequency oscillators present in the coordination sphere of the dissolved metal-species, it is possible to enhance the

efficiency of photoemission. In conventional solvents this is partially achieved by the use of deuterated carbohydrates [45] or by the use of sterical demanding, well shielding podant-systems [46].

2.5 Electrochemistry of rare-earth compounds in ionic liquids

Bhatt *et al.* were the first to report on the reduction of Eu(II) to Eu(0) in $[\text{Me}_4\text{X}][\text{Tf}_2\text{N}]$ molten salts, where X = N, P, As [47]. These salts are solid at room-temperature, but become liquid below 170°C. Since the Eu(II)/Eu(0) couple is more negative than the U(III)/U(0) or Pu(III)/Pu(0) couple, there is a potential for U/Pu or An/Ln separation. In 2005 Bhatt *et al.* investigated the electrochemistry of La, Sm and Eu in the ionic liquid $[\text{Me}_3\text{N}^n\text{Bu}][\text{Tf}_2\text{N}]$ and the reduction of the hydrated lanthanide cations to the zerovalent state is claimed. For Sm(III) and Eu(III) the reductions were achieved via the divalent species, whereas the La(III) was directly reduced to La(0). In the same context further groups investigated the behavior of U(IV)-hexachloro complexes [48] and Th(IV)- $[\text{Tf}_2\text{N}]$ complexes in $[\text{Me}_3\text{N}^n\text{Bu}][\text{Tf}_2\text{N}]$, also Np(IV) and Pu(IV) were investigated in the imidazolium- based ionic liquid $[\text{bmim}][\text{Tf}_2\text{N}]$ [49].

Katayama *et al.* reported on the electrochemical behavior of Eu(III), Sm(III) and Yb(III) as models of the half-cell reactions for redox-flow batteries with $[\text{Tf}_2\text{N}]$ -based RTIL's [50]. The reduction to the trivalent state was in all cases quasi- or irreversible which was interpreted by the shielding of the $[\text{Tf}_2\text{N}]$ -ligand which is surrounding the redox-centre. Formation of Ln- $[\text{Tf}_2\text{N}]$ species was suggested from chronoamperometric and chronopotentiometric data and the donor-number of the solvent was estimated from the half-wave potentials of the divalent and trivalent lanthanides to be 7 ± 2 . The effect of anion exchange in RTILs is not reported and will be investigated in this work.

3. Literature

- [1] C. Gaillard, I. Billard, A. Chaumont, S. Mekki, A. Ouadi, M. A. Denecke, G. Moutiers, G. Wipff, *Inorg. Chem.* **2005**, *44*, 8355.
- [2] R.C. Thied, K.R. Seddon, W.R. Pitner, D. Rooney *WO 99/41752* **1999**.
- [3] M. Yamagata, Y. Katayama, T. Miura, *J. Electrochem. Soc.* **2006**, *153*, E5.
- [4] M.J. Earle, U. Hakala, B.J. McAuley, M. Nieuwenhuyzen, A. Ramani and K.R. Seddon, *Chem. Commun.* **2004**, 1368.
- [5] J.-C. G. Bünzli, *Acc. Chem. Res.* **2006**, *39*, 53; J.-C. G. Bünzli, C. Piguet, *Chem. Soc. Rev.* **2005**, *34*, 1048.
- [6] P. Nockemann, E. Beurer, K. Driesen, R. Van Deun, K. Van Hecke, L. Van Meervelt, K. Binnemans, *Chem. Commun.* **2005**, 4345.
- [7] W.J. Whitehead, G.A. Lawrence, A. McCluskey, *Green Chem.* **2004**, *6*, 313.
- [8] For example: T. Welton, *Chem. Rev.* **1999**, *99*, 2071; P. Wasserscheidt, W. Keim, *Angew. Chem.* **2000**, *112*, 3926; A. Blanchard D. Hancu, E.J. Beckmann, J.F. Brenecke, *Nature* **1999**, *399*, 28.
- [9] S. Guernik, A. Wolfson, M. Herskowitz, N. Greenspoon, S. Geresh, *Chem. Commun.* **2001**, 2314.
- [10] W.J. Evans, *J. Alloys Compd.* **1993**, *109*, 1074.
- [11] A. Kreif, A.M. Laval, *Chem. Rev.* **1999**, *99*, 745.
- [12] S.L. Zhang, Y.M. Zhang, *Synth. Commun.* **2000**, *30*, 285 and references cited therein.
- [13] Y. Kamochi, T. Kudo, *Tetrahedron Lett.* **2000**, *41*, 341.
- [14] L. Lu, H.Y. Chang, J. M. Fang, *J. Org. Lett.* **1999**, *1*, 1989.
- [15] W.J. Evans, N.T. Allen, *J. Am. Chem. Soc.* **2000**, *122*, 2118.
- [16] W.J. Evans, N.T. Allen, J.W. Ziller, *J. Am. Chem. Soc.* **2000**, *122*, 11749.
- [17] M.N. Bochkarev, I.L. Fedushkin, A.A. Fagin, T.V. Petrovskaya, J.W. Ziller, R.N.R. Broomhal-Dillard, W.J. Evans, *Angew. Chem.* **1997**, *109*, 123.

- [18] W.J. Evans, N.T. Allen, J.W. Ziller, *J. Am. Chem. Soc.* **2000**, *122*, 11749.
- [19] M.N. Bochkarev, I.L. Fedushkin, S. Dechert, A.A. Fagin, H. Schumann, *Angew. Chem.* **2001**, *113*, 3268.
- [20] M.C. Cassani, M.L. Lappert, F. Sasaki, *Chem. Commun.* **1997**, 1563.
- [21] M.C. Cassani, D.J. Duncalf, M.L. Lappert, *J. Am. Chem. Soc.* **1998**, *120*, 12958.
- [22] *In situ* generated Ce(II) is supposed to play a role in the diastereoselective Pinacol-coupling of aldehydes: U. Groth, M. Jeske, *Synlett* **2001**, 129; U. Groth, M. Jeske, *Angew. Chem.* **2000**, *39*, 574.
- [23] W.J. Evans, *Coord. Chem. Rev.* **2000**, *206/207*, 263.
- [24] W.J. Evans, P. S. Workman, *Organometallics*, **2005**, *24*, 1989.
- [25] I. Billard, G. Moutiers, A. Labet, A. El Azzi, C. Gaillard, C. Mariet, K. Lutzenkirchen, *Inor. Chem.* **2003**, *42*, 1726.
- [26] G. Meyer, *Chem. Rev.* **1988**, *88*, 93.
- [27] S. Kobayashi (Ed.), *Lanthanides: Chemistry and Use in Organic Synthesis*, Springer, Berlin, **1999**.
- [28] S. Matsubara, M. Yoshioka, K. Utimoto, *Chem. Lett.* **1994**, 827.
- [29] K.M. Gillespie, I.J. Munslow, P. Scott, *Tetrahedron Lett.* **1999**, *40*, 9371.
- [30] F. Bonadies, A. Lattanzi, L.R. Orelli, S. Pesci, A. Scettri, *Tetrahedron Lett.* **1993**, *34*, 7649.
- [31] S. Fukuzawa, T. Tsuchimoto, T. Kanai, *Bull. Chem. Soc. Jpn.* **1994**, *67*, 2227.
- [32] H. Sasai, S. Watanabe, M. Shbasaki, *Enantiomer*, **1997**, *2*, 267.
- [33] C.B. Castellani, O. Cargo, A. Perotti, D. Sacchi, A.G. Invernizzi, G. Vidari, *J. Mol. Catal.* **1993**, *85*, 65.
- [34] R.P.C. Cousins, W.C. Ding, R.G. Pritchard, R.J. Stoodley, *Chem. Commun.* **1997**, 2171.
- [35] C.E. Song, W.H. Shim, E.J. Roh, S. Lee, J. H. Choi, *Chem. Commun.* **2001**, 1122.
- [36] F. Zulfiqar, T. Kitazume, *Green Chemistry*, **1999**, *1*, 23.

- [37] F. Zulfiqar, T. Kitazume, *Green Chemistry*, **2000**, 2, 296.
- [38] A. Chaumont, G. Wipff, *PCCP*, **2003**, 5, 3481.
- [39] P. Kafarski, B. Lejczak, *Phosphorus Sulfur Silicon*, **1991**, 63, 193.
- [40] S. Lee, J.H. Park, J. Kang, J.K. Lee, *Chem. Commun.* **2001**, 1698.
- [41] C.E. Song, W.H. Shim, E.J. Roh, J.H. Choi, *Chem. Commun.* **2000**, 1695.
- [42] M. Kawamura, D.-M. Cui, T. Hayashi, S. Shimada, *Tetrahedron Lett.* **2003**, 44, 7715.
- [43] M.H.V. Werts, R.H. Woudenberg, P.G. Emmerink, R. van Gassel, J.W. Hofstraat, J.W. Verhoeven, *Angew. Chem. Int. Ed.* **2000**, 39, 4542; D. Imbert, M. Cantuel, J.-C. Bünzli, G. Bernardinelli, C. Piguet, *J. Am. Chem. Soc.* **2003**, 125, 15698.
- [44] S. Arenz, A. Babai, K. Binnemans, K. Driesen, R. Giernoth, A.-V. Mudring, P. Nockemann, *Chem. Phys. Lett.* **2005**, 402, 75.
- [45] Y. Hasegawa, T. Ohkubo, K. Sogabe, Y. Kawamura, Y. Wada, N. Nakashima, S. Yanagida, *Angew. Chem.* **2000** 112, 365.
- [46] S. Petoud, S.M. Cohen, J.-C. Bünzli, K.N. Raymond, *J. Am. Chem. Soc.* **2003**, 125, 13326.
- [47] A.I. Bhatt, I. May, A.V. Volkovich, M.E. Hetherington, B. Lewin, *Dalton Trans.* **2002**, 4532.
- [48] S.I. Nikitenko, C. Cannes, C. Le Naour, P. Moisy, D. Trubert, *Inorg. Chem.* **2005**, 44, 9497.
- [49] S.I. Nikitenko, P. Moisy, *Inorg. Chem.* **2006**, 45, 1235.
- [50] A.I. Bhatt, N.W. Duffy, D. Collison, I. May, R.G. Lewin, *Inorg. Chem.* **2006**, 45, 1677.

II. Ln(III)-compounds in ionic liquids

1. NdI₃ in Tf₂N-based ionic liquids

1.1 Introduction

Already in 2005 we showed that anhydrous neodymium(III)iodide and erbium(III) iodide dissolved in carefully dried batches of the ionic liquid 1-dodecyl-3-methylimidazoliumbis(trifluoromethanesulfonyl)amide, [C₁₂mim][Tf₂N] exhibit intense near-infrared luminescence [1]. In order to investigate this system further, the cation is modified in a way that it is possible to obtain single crystals of a composed Nd-ionic liquid-compound. The general route to obtain crystalline samples of sufficient quality for single-crystal X-ray analysis in this systems is to completely dissolve the educts in the heat (~393 K) and to subsequently cool the solution slowly to room temperature (1-2 K/h). By using two different ionic liquids which only slightly differ in the length of the alkyl chain of the pyrrolidinium-cation ([mppyr]⁺ and [bmpyr]⁺) two new rare-earth ionic liquid compounds ([mppyr]₄[LnI₆] and ([bmpyr]₄[NdI₆][Tf₂N]) were obtained, which point an interesting crystallographic correlation.

The products were structurally characterized in terms of single-crystal and powder X-ray structure analysis.

1.2 Preparation

NdI₃: To synthesize NdI₃, the respective amounts of the elements were placed in a silica tube which was sealed off under vacuum and subsequently heated for 30 h at 200 °C. The crude product was purified by sublimation under high vacuum at 800°C [2].

[mppyr][Tf₂N] and [bmpyr][Tf₂N]: Both ionic liquids were synthesized in a similar manner following a modified literature procedure [3]. First, the tetraalkyl-ammoniumhalide was obtained by solvent-free alkylation of N-methylpyrrolidin with 1-bromo-butane(-methane) respectively at 80°C. The crude product was recrystallized

from acetonitrile/toluene, dried in vacuum to remove the solvent mixture and subsequently dissolved in water. One equivalent of lithium bis(trifluoromethanesulfonyl)amide in water was added and the mixture was stirred for 24 h at room temperature. The product which formed a second phase to water was separated, purified by addition of activated charcoal and filtration through aluminum oxide. It was dissolved in dichloromethane and washed with small aliquots of water until no halide residues could be detected in the extract (AgNO_3 test). The ionic liquid was dried for 48 h in a Schlenk tube at 150°C under reduced pressure and rigorous stirring. Anal. Calc. for $\text{C}_{11}\text{H}_{20}\text{F}_6\text{N}_2\text{O}_4\text{S}_2$ ([bmpyr][Tf₂N]): C, 31.28; H, 4.77; N, 6.63%. Found: C, 31.53; H, 5.88; N, 6.63%. Anal. Calc. for $\text{C}_9\text{H}_{18}\text{F}_6\text{N}_2\text{O}_4\text{S}_2$ ([mppyr][Tf₂N]): C, 29.41; H, 4.44; N, 6.86%. Found: C, 29.42; H, 4.90; N, 7.31%.

[mppyr]₃[NdI₆]: NdI_3 (~52 mg, 0.1 mmol) was put in a silica tube (11 mm in diameter), then [mppyr][Tf₂N] (~ 0.5 ml, 0.73 g, 1.8 mmol) was added. The tube was sealed off under dynamic vacuum and heated to 393 K until the rare earth salt was completely dissolved. To obtain [mppyr]₃[NdI₆], the solutions was subsequently cooled to room temperature (2 K/min). Under these conditions, crystals of the composition [mppyr]₃[NdI₆] precipitated from the solution. The product was separated by canula-filtration. Estimated yield: 40%.

[bmpyr]₄[NdI₆][Tf₂N]: NdI_3 (~ 52 mg, 0.1 mmol) were put in a silica tube (11 mm in diameter), then [bmpyr][Tf₂N] (~ 0,5 ml, 0.7 g, 1.67 mmol) was added. The tube was sealed off under dynamic vacuum and heated to 393 K until the rare earth salts were completely dissolved. To obtain [bmpyr]₄[LnI₆][Tf₂N], the solutions was subsequently cooled to room temperature (2 K/min). Under these conditions, crystals of the composition [bmpyr]₄[LnI₆][Tf₂N] precipitated from the solution. The product was separated by canula-filtration. Estimated yield: 75%.

To obtain a powder for powder-XRD measurements, the samples were cooled rapidly in a water bath and the pale greenish solid transferred to a glass-capillary.

1.3 Structural aspects

The compound $[\text{mppyr}]_3[\text{NdI}_6]$ crystallizes in the tetragonal noncentrosymmetric space group $P4_12_12$ (no. 92) with eight formula units in the unit cell (Figure 1a). The asymmetric unit contains two symmetry-independent neodymium cations which are each surrounded by an only slightly distorted octahedron of iodine anions with a mean neodymium-iodide interatomic distance of about 311.4 pm (Figure 1a and c). It is noteworthy that the acentricity of the whole crystal structure is introduced by these (highly symmetric) octahedra which are tilted with respect to the c crystallographic axis and wind themselves along the parallel 4_1 screw axis. Above each of the triangular faces of the $[\text{NdI}_6]^{3-}$ -octahedron a $[\text{mppyr}]$ cation is located tangentially (Figure 2b) like it was already predicted from molecular dynamic studies for hexachlorocomplexes of trivalent lanthanide cations [4].

Table 1: Crystallographic and refinement details for $[\text{mppyr}]_3[\text{NdI}_6]$ and $[\text{bmpyr}]_4[\text{NdI}_6][\text{Tf}_2\text{N}]$

	$[\text{mppyr}]_3[\text{NdI}_6]$	$[\text{bmpyr}]_4[\text{NdI}_6][\text{Tf}_2\text{N}]$
Empirical formula	$\text{C}_{24} \text{H}_{54} \text{I}_6 \text{N}_3 \text{Nd}$	$\text{C}_{36} \text{H}_{80} \text{I}_6 \text{Nd S}_2 \text{F}_6 \text{N}_5 \text{O}_4$
Formula weight	1290.34	1446.69
Crystal system	tetragonal	tetragonal
Space group	$P4_12_12$ (no. 92)	$I4_1/a$ (no. 88)
Unit cell dimensions	$a = b = 1888.10(8)$ pm $c = 2198.39(10)$ pm	$a = b = 1496.85(6)$ pm $c = 2853.91(14)$ pm
Volume	$7.83709(6)$ nm ³	$6.38582(5)$ nm ³
Z	8	4
Density (calculated)	2.19 g·cm ⁻³	1.88 g·cm ⁻³
Absorption coefficient	6.068 mm ⁻¹	1.362 mm ⁻¹
Reflections collected	121794	25654
Independent reflections / R_{int}	8543 / 0.1138	2759 / 0.0538
Absorption correction	numerical	numerical
Parameters	316	91 (62 restraints)
GooF on F^2	0.963	0.953
Final R indices [$I > 2\sigma(I)$]	$R_1 = 0.046$, $wR_2 = 0.105$	$R_1 = 0.0439$, $wR_2 = 0.1228$
R indices (all data)	$R_1 = 0.0654$, $wR_2 = 0.1136$	$R_1 = 0.0646$, $wR_2 = 0.1312$

A small change of the ionic liquid, from $[\text{mppyr}][\text{Tf}_2\text{N}]$ to $[\text{bmpyr}][\text{Tf}_2\text{N}]$ ($\text{bmpyr} = 1$ -butyl-1-methyl-pyrrolidinium), results surprisingly in single crystals of a (at first sight) rather different compound, $[\text{bmpyr}]_4[\text{NdI}_6][\text{Tf}_2\text{N}]$ (Figure 2c). That exclusively either

[mppyr]₃[NdI₆] or [bmpyr]₄[NdI₆][Tf₂N] are formed depending on the choice of the ionic liquid, hence the cation of the ionic liquid, is reliable, as confirmed by X-ray powder diffraction. The powder diffractograms of the respective bulk samples are well matched with the from single-crystal data expected one. [bmpyr]₄[NdI₆][Tf₂N] crystallizes in the (centrosymmetric) space group I4₁/a (no. 88) with four formula units in the unit cell.

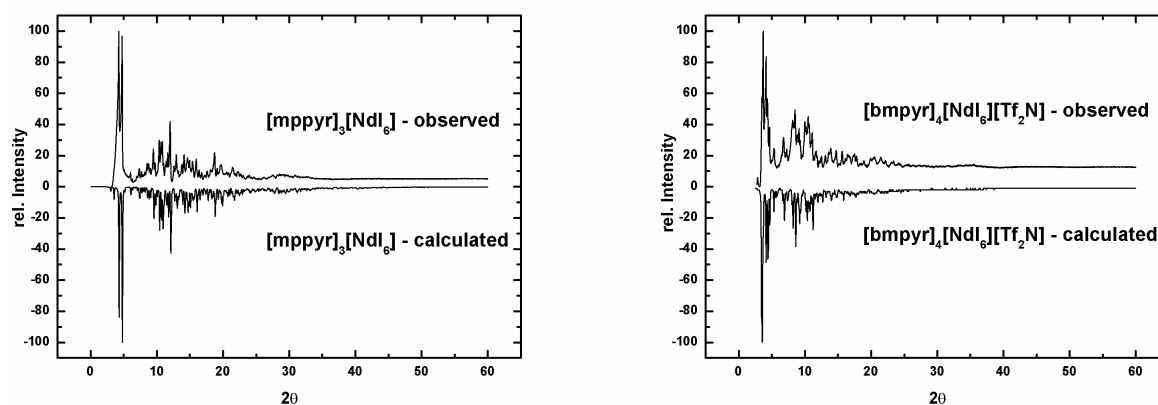


Fig. 1: XRD-pattern of [mppyr]₃[NdI₆] and [bmpyr]₄[NdI₆][Tf₂N]

Again, the main structural feature is neodymium cations surrounded by a nearly ideal octahedron of iodine anions (mean neodymium-iodine interatomic distance $d(\text{Nd-I})$ 310.6 pm). Not only is the first coordination sphere around the neodymium cation in [bmpyr]₄[NdI₆][Tf₂N] the same as in [mppyr]₃[NdI₆] but also the second. Again, eight cations of the ionic liquid (here: bmpyr) are residing tangentially above the faces of the [NdI₆]³⁻ octahedron (Figure 1d). The most important difference between both crystal structures is that in case of [bmpyr]₄[NdI₆][Tf₂N] not only the cation of the ionic liquid participates in the structure but also the anion, [Tf₂N]⁻, is incorporated in the crystal structure. By extending the alkyl side chain of the quaternary 1-methylpyrrolidinium cation by one carbon atom, optimal space filling for a structure containing only pyrrolidinium cations and [NdI₆]³⁻ octahedra seems not to be possible. The cation has become too large. To get optimal packing in the solid, one formula unit of the ionic

liquid itself has to get included into the structure. This is, thereby, an example of chemospecific crystal engineering [5].

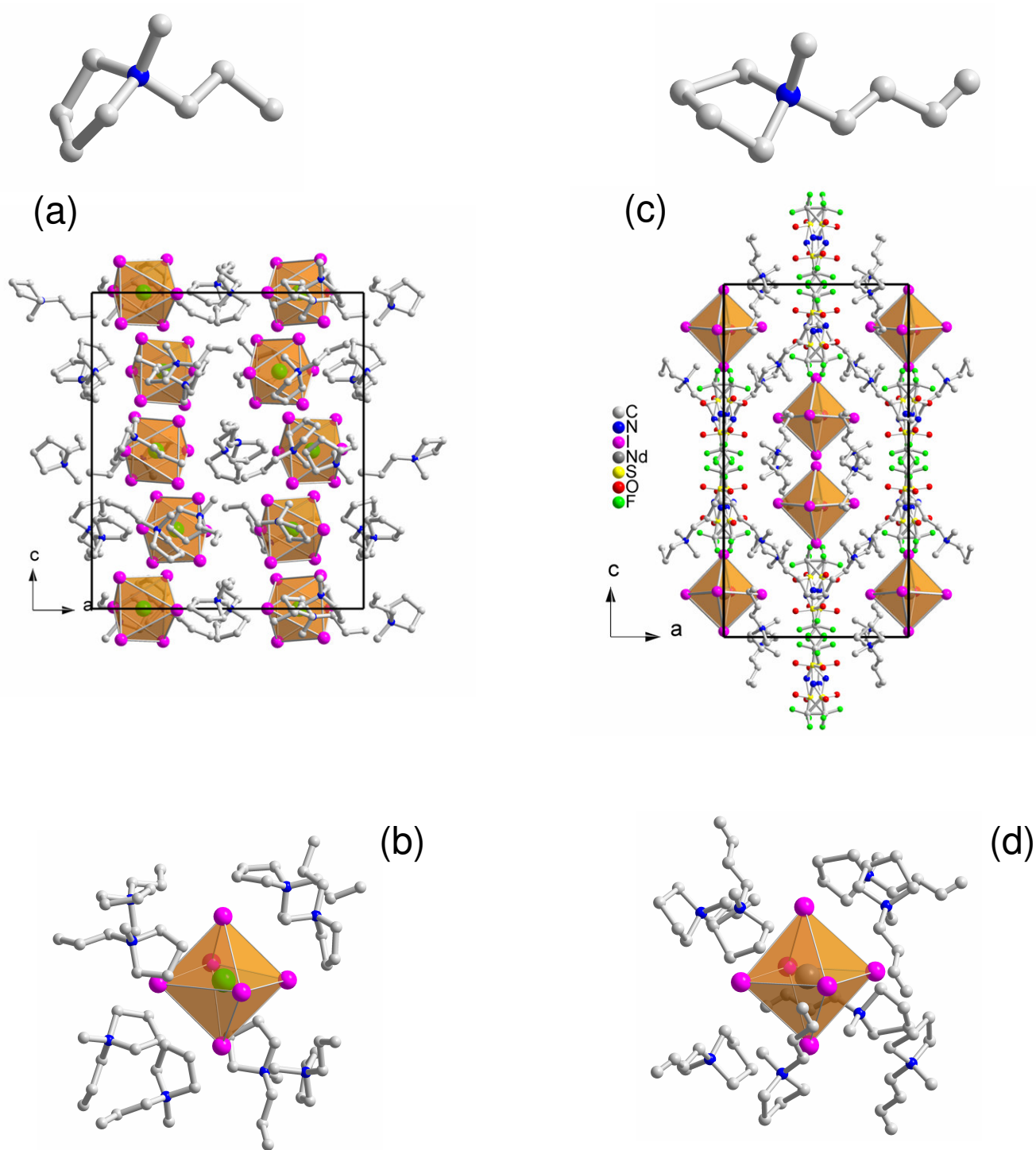
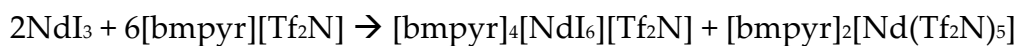


Fig. 2 a-d: Molecular and crystal-structures of [mppyr][NdI₆] and [bmpyr]₄[NdI₆][Tf₂N]

1.4 Discussion

By rewriting the formula $[\text{bmpyr}]_4[\text{NdI}_6][\text{Tf}_2\text{N}]$ as $[\text{bmpyr}]_3[\text{NdI}_6] \cdot [\text{bmpyr}][\text{Tf}_2\text{N}]$ not only the relationship to $[\text{mppyr}]_3[\text{NdI}_6]$ becomes obvious but this formulation also shows that the compound may be viewed as $[\text{bmpyr}]_3[\text{NdI}_6]$ with one formula of the “solvent”, $[\text{bmpyr}][\text{Tf}_2\text{N}]$, added. This view is backed by the fact that the bis(trifluoromethanesulfonyl)amide anion gets incorporated in a non-coordinating mode. It has been well established that the bis(trifluoromethanesulfonyl)amide anion shows the essential feature that is necessary for a low tendency to coordinate: delocalization of negative charge over an extended area of functional groups [6]. After many unsuccessful attempts [7] to crystallize rare earth complexes with the Tf_2N -ligand bonded to the metal-center only recently the first structure determinations appeared, featuring La^{3+} in $\text{La}(\text{Tf}_2\text{N})_3 \cdot 3\text{H}_2\text{O}$ [8], Pr^{3+} , Nd^{3+} , Tm^{3+} in $[\text{bmpyr}]_3[\text{Ln}(\text{Tf}_2\text{N})_5]$, Tm^{3+} , Lu^{3+} in $[\text{bmpyr}][\text{Ln}(\text{Tf}_2\text{N})_4]$ [9], and Yb^{2+} in $[\text{mppyr}]_2[\text{Yb}(\text{Tf}_2\text{N})_4]$ [10]. In $[\text{bmpyr}]_4[\text{NdI}_6][\text{Tf}_2\text{N}]$, the bis(trifluoromethanesulfonyl)amide anion is disordered over two positions which are occupied equally, and adopts a transoid conformation with respect to the $-\text{CF}_3$ groups (Figure 2c), which is generally preferred in the absence of suitable coordination centers as structure determinations of ILs show [11]. The transoid conformation of the $-\text{CF}_3$ groups is also found in the free acid $[\text{Tf}_2\text{N}]\text{H}$ (i.e., $(\text{CF}_3\text{SO}_2)_2\text{NH}$) [12]. Recent theoretical calculations revealed that transoid $[\text{Tf}_2\text{N}]\text{H}$ is about 8 kJ/mol more stable than cisoid $[\text{Tf}_2\text{N}]\text{H}$ and that transoid $[\text{Tf}_2\text{N}]^-$ compared to cisoid $[\text{Tf}_2\text{N}]^-$ about 4 kJ/mol [10]. During the formation of both $[\text{bmpyr}]_3[\text{NdI}_6]$ and $[\text{bmpyr}]_4[\text{NdI}_6][\text{Tf}_2\text{N}]$, the ionic liquid solution depletes of iodide. According to the stoichiometrical reaction equations



aside from the two insoluble reactions products which both have the $[\text{NdI}_6]^{3-}$ octahedron in common, a second neodymium complex which features the lanthanide cation in a coordination of bis(trifluoromethanylsulfonyl)amide must form. In chapter 3.3 this

species is characterized in case of the [bmpyr]-ionic liquid. The compound [bmpyr]₂[Nd(Tf₂N)₅] is formed. Here, the neodymium-ion is surrounded by five Tf₂N-ligands.

1.5 Literature

- [1] S. Arenz, A. Babai, K. Binnemans, K. Driesen, R. Giernoth, A.-V. Mudring, P. Nockemann, *Chem. Phys. Lett.* **2005**, 75.
- [2] J.D Corbett, *Inorg. Synth.* **1983**, 22, 31-36; G. Meyer, in: *Synthesis of Lanthanide and Actinide Compounds* (G. Meyer, L.R. Morss, eds.), Kluwer Acad. Publ., Dordrecht/NL **1991**, 135.
- [3] R. Giernoth, M.S. Krumm, *Adv. Synth. Catal.* **2004**, 346, 989.
- [4] A. Chaumont, G. Wipff, *J. Phys. Chem. B* **2004**, 108, 3311.
- [5] B. Kahr, J. M. McBride, *Angew. Chem., Int. Ed. Engl.* **1992**, 31, 1.
- [6] I. Krossing, I. Raabe, *Angew. Chem.* **2004**, 116, 2116; S. H. Strauss, *Chem. Rev.* **1993**, 93, 927.
- [7] K. Mikami, O. Kotera, Y. Motoyama, M. Tanaka, *Inorg. Chem. Commun.* **1998**, 1, 10.
- [8] A.I. Bhatt, I. May, V.A. Volkovich, D. Collision, M. Helliwell, I.B. Polovov, R.G. Lewin, *Inorg. Chem.* **2005**, 44, 4934.
- [9] A. Babai, A.-V. Mudring, *Chem. Mater.* **2005**, 17, 6230; A. Babai, A.-V. Mudring, *Dalton Trans.* **2006**, 1828.
- [10] A.-V. Mudring, A. Babai, S. Arenz, R. Giernoth, *Angew. Chem. Int. Ed.* **2005**, 44, 5485.
- [11] J.J. Golding, D.R. MacFarlane, L. Spiccia, M. Forsyth, B.W. Skelton, A.H. White, *Chem. Commun.* **1998**, 15, 1593; V. Montanari, D.D. DesMarteau, W.T. Pennigton, *J. Mol. Struct.* **2000**, 550/551, 337; C.M. Forsyth, D.R. MacFarlane, J.J. Golding, J. Huang, J. Sun, M. Forsyth, *Chem. Mater.* **2002**, 14, 2103; M.G. Davidson, P.R. Raithby, A.L. Johnson, P.D. Bolton, *Eur. J. Inorg. Chem.* **2003**, 3445;

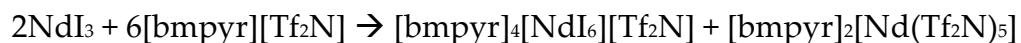
D.D. DesMarteau, W.T. Pennington, V. Montanari, B.H. Thomas, *J. Fluorine Chem.* **2003**, *122*, 57.

[12] A. Haas, C. Klare, P. Betz, J. Bruckmann, C. Kruger, Y.-H. Tsay, F. Aubke, *Inorg. Chem.* **1996**, *35*, 1918.

2. Pr(III)-compounds in [bmpyr][Tf₂N] – structural and optical aspects

2.1 Introduction

Considering the equation from the last chapter



it becomes obvious, that there must be beside the crystallographic characterized $[\text{bmpyr}]_4[\text{NdI}_6][\text{Tf}_2\text{N}]$ also a Nd-species present, which is coordinated by the $[\text{Tf}_2\text{N}]$ -anions of the ionic liquid. Apart from XRD, such ligand effects can be studied well utilizing optical spectroscopic methods. Since Nd(III) has no optical transitions in the visible region, the analogue Pr(III) compounds can be regarded as model compounds, which are examined by emission spectroscopy.

Lanthanide contraction leads to a slightly smaller ionic radius for Nd^{3+} (11.23 pm) compared to Pr^{3+} (11.3 pm) for the coordination number six [1], which is negligible considering the coordination environment of the metal-ions dissolved in the ionic liquid. Astonishingly, the solid state structures of $[\text{bmpyr}]_4[\text{NdI}_6][\text{Tf}_2\text{N}]$ and $[\text{bmpyr}]_4[\text{PrI}_6][\text{Tf}_2\text{N}]$ differ significantly. Emission spectra of the latter compound are compared with solutions of PrI_3 in $[\text{bmpyr}][\text{Tf}_2\text{N}]$. To verify the coordination of the $[\text{Tf}_2\text{N}]$ -entity to the rare-earth ion, $\text{Pr}(\text{Tf}_2\text{N})_3$ was synthesized and its interaction with $[\text{bmpyr}][\text{Tf}_2\text{N}]$ studied by XRD and emission spectroscopy. The crystal structure of the compound $[\text{bmpyr}]_3[\text{Pr}(\text{Tf}_2\text{N})_5]$, which is isostructural to the respective neodymium-compound, proves unequivocally the coordination of the $[\text{Tf}_2\text{N}]$ -anion to the metal ion, viz five ligands completing the coordination sphere around the rare earth ions.

2.2 Preparation

Solution of Pr³⁺ in [bmpyr][Tf₂N]: PrI₃ (~ 26 mg, 0.05 mmol) was put in a silica tube (11 mm in diameter), then [bmpyr][Tf₂N] (~ 0,5 ml, 0.75 g, 1.8 mmol) was added. The tube was sealed off under dynamic vacuum and heated to 120°C until the rare-earth salt was completely dissolved. All spectra were recorded with the substance sealed in the silica tube.

[bmpyr]₄[PrI₆][Tf₂N]: PrI₃ (~ 52 mg, 0.1 mmol) was put in a silica tube (11 mm in diameter), then [bmpyr][Tf₂N] (~ 0,5 ml, 0.75 g, 1.8 mmol) was added. The tube was sealed off under dynamic vacuum and by heating the reaction mixture to 393 K and subsequent cooling to room temperature (2 K/min), crystals of the composition [bmpyr]₄[PrI₆][Tf₂N] precipitated from the solution. The solid was isolated by cannula-filtration.

Pr(Tf₂N)₃: The compound was synthesised by dissolving the praseodym metal in aqueous HTf₂N and subsequent removal of the liquid phase [2]. The crude products were sublimed at 280 °C under reduced pressure (10⁻³ mbar) to give Pr(Tf₂N)₃.

[bmpyr]₂[Pr(Tf₂N)₅] was synthesised from Pr(Tf₂N)₃ (123 mg, 0.125 mmol) and [bmpyr][Tf₂N] (355 mg, 0.25 ml, 0.8 mmol). The educts were placed in a silica tube which was sealed under vacuum. The reaction was carried out at 120°C for 36 h. Single crystals form as an insoluble product after cooling the reaction mixture to room temperature (5 K/min). The product was separated by cannula-filtration from the ionic liquid.

2.3 Structural aspects

2.3.1 Comparison of [bmpyr]₄[PrI₆][Tf₂N] and [bmpyr]₄[NdI₆][Tf₂N]

The praseodym compound [bmpyr]₄[PrI₆][Tf₂N] crystallizes in the axial space group *P*4₃2₁2 (no. 96) with four formula units in the unit cell, while the neodymium compound [bmpyr]₄[NdI₆][Tf₂N] crystallizes in the centrosymmetric space group *I*4₁/*a* (no. 88), with

four formula units in the unit cell as well (see Table 1). In both cases, the asymmetric unit – corresponding to one formula unit of $[\text{bmpyr}]_4[\text{LnI}_6][\text{Tf}_2\text{N}]$ – contains four cations of the ionic liquid, $[\text{bmpyr}]^+$, one (slightly distorted) $[\text{LnI}_6]^{3-}$ octahedron (Fig. 1, Tab. 2) and one anion of the ionic liquid, $[\text{Tf}_2\text{N}]^-$. Formally, the compound can thus be seen as a solvent adduct of the pseudo-binary salt $[\text{bmpyr}]_3[\text{LnI}_6]$ with the ionic liquid $[\text{bmpyr}][\text{Tf}_2\text{N}]$ (“crystal solvent”) itself according to the formula $[\text{bmpyr}]_3[\text{LnI}_6] \cdot [\text{bmpyr}][\text{Tf}_2\text{N}]$.

Table 2: Crystallographic and refinement details for $[\text{bmpyr}]_4[\text{PrI}_6][\text{Tf}_2\text{N}]$ and $[\text{bmpyr}]_4[\text{NdI}_6][\text{Tf}_2\text{N}]$

	$[\text{bmpyr}]_4[\text{PrI}_6][\text{Tf}_2\text{N}]$	$[\text{bmpyr}]_4[\text{NdI}_6][\text{Tf}_2\text{N}]$
Empirical formula	Pr I ₆ S ₂ F ₆ O ₄ N ₅ C ₃₆ H ₈₀	Nd I ₆ S ₂ F ₆ O ₄ N ₅ C ₃₆ H ₈₀
Formula weight	1751.5	1754.8
Crystal system	tetragonal	tetragonal
Space group	$P4_32_12$ (no. 96)	$I4_1/a$ (no. 88)
Unit cell dimensions	$a = b = 1454.52(7)$ pm $c = 2852.4(2)$ pm	$a = b = 1496.85(6)$ pm $c = 2853.91(14)$ pm
Volume	$6034.6(6) \cdot 10^6$ pm ³	$6385.82(5) \cdot 10^6$ pm ³
Z	4	4
Density (calculated)	1.839 g·cm ⁻³	1.88 g·cm ⁻³
Absorption coefficient	3.998 mm ⁻¹	1.362 mm ⁻¹
Reflections collected	55865	25654
Independent reflections / R_{int}	6731 / 0.1524	2759 / 0.0538
Absorption correction	numerical	numerical
Parameters	348	91
GooF on F^2	1.027	0.953
Final R indices [$I > 2\sigma(I)$]	$R_1 = 0.0582$, $wR_2 = 0.1116$	$R_1 = 0.0439$, $wR_2 = 0.1228$
R indices (all data)	$R_1 = 0.0924$, $wR_2 = 0.1223$	$R_1 = 0.0646$, $wR_2 = 0.1312$

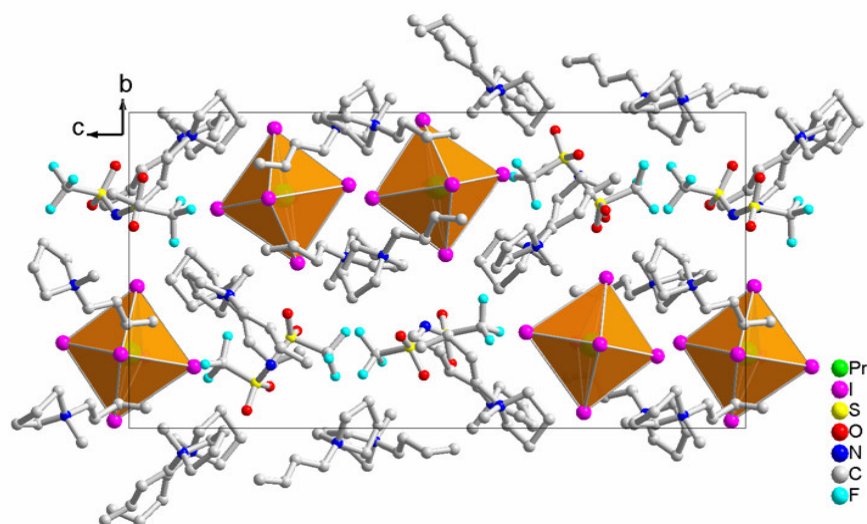


Fig. 1: Crystal structure of $[\text{bmpyr}]_4[\text{PrI}_6][\text{Tf}_2\text{N}]$, view along $[100]$. H-atoms are omitted for clarity

The local surrounding of each $[\text{LnI}_6]^{3-}$ octahedron is comparable for both compounds as described in 1.3. Also the orientation of the [bmpyr]-cations is similar, which are situated above the faces of the $[\text{LnI}_6]^{3-}$ octahedra such that the pyrrolidinium rings are almost parallel to the octahedral faces. The Tf_2N^- anions fill the gaps of the $\{[\text{PrI}_6]@8[\text{bmpyr}]\}^{5+}$ units winding also along the 4_3 screw axis parallel to the crystallographic c -axis. The anions are displaced against the cationic fragment. The Tf_2N^- anions themselves are strongly disordered (Figure 2). High conformational flexibility and a strong tendency to packing frustrations of both the cation and anion are believed to be the key to low melting salts and thus, to (room temperature) ionic liquids. This is aggravating to obtain a crystal of sufficient quality for single crystal X-ray structure analysis. Many specimens showed an extreme disorder of the cation and anion belonging to the included "solvent". The crystal structure refinement of the best specimen that is reported here exhibits even at 170(2) K large displacement factors for the [bmpyr] cations and the $[\text{Tf}_2\text{N}]$ anions.

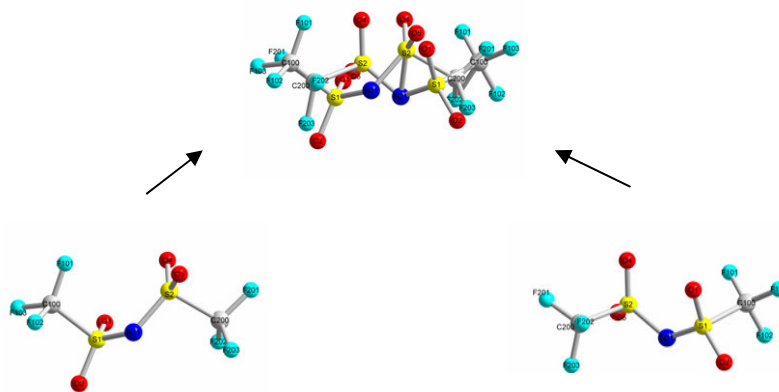


Fig 2: Disorder of the Tf_2N -anion in $[\text{bmpyr}]_4[\text{PrI}_6][\text{Tf}_2\text{N}]$

The main structural difference between the praseodymium and neodymium-compound becomes clear by comparing the heavy-atom positions in the two compounds.

In the praseodymium-compound, the $[\text{PrI}_6]^{3-}$ octahedra wind themselves along the 4_3 screw axis parallel to the crystallographic c -axis. The octahedra are tilted from the c axis

as can be seen from Figure 3. In case of the neodymium-compound, the $[\text{NdI}_6]^{3-}$ octahedra orient themselves parallel to the crystallographic c -axis. Thus, the latter compound has a higher symmetry and crystallizes in the space group $I4_1/a$, a supergroup of $P4_32_12$. In both crystal structures, the $[\text{Tf}_2\text{N}]$ -anions fill in the gaps between two $[\text{LnI}_6]$ units along the crystallographic c -axis. It is therefore clear why the $[\text{LnI}_6]$ octahedra are tilted in one compound and not in the other. In case of the smaller Nd^{3+} cations the size between the $\{[\text{LnI}_6] @ 8 \text{ bmpyr}\}^{5+}$ units is just right to accommodate the Tf_2N - anions in the remaining voids, whereas in the larger Pr^{3+} analogue the cavity would be too large for the Tf_2N -groups. Thus, the space is reduced by tilting of the $[\text{PrI}_6]^{3-}$ octahedra to allow for an appropriate fit of the Tf_2N -unit. The metal-iodine distances are listed in Table 2 and indicate the larger size of the $[\text{PrI}_6]^{3-}$ compared to the neodymium one. This assumption is supported by the observation that the analogous lanthanum compound crystallizes isotypically with the $[\text{bmpyr}]_4[\text{PrI}_6][\text{Tf}_2\text{N}]$ and that there exists an erbium-compound [3], isotypic with the neodymium analogue. Thus, the borderline for the structural transition from $P4_32_12$ to $I4_1/a$ of $[\text{bmpyr}]_4[\text{LnI}_6][\text{Tf}_2\text{N}]$ compounds is in between Pr^{3+} and Nd^{3+} .

Table 3: Metal-iodine distances (pm) in $[\text{bmpyr}]_4[\text{LnI}_6][\text{Tf}_2\text{N}]$

Pr(1)-I(1)	Pr(1)-I(2)	Pr(1)-I(3)	Nd(1)-I(1)	Nd(1)-I(2)
315.91(10)	311.71(8)	311.64(10)	310.02(10)	310.99(8)

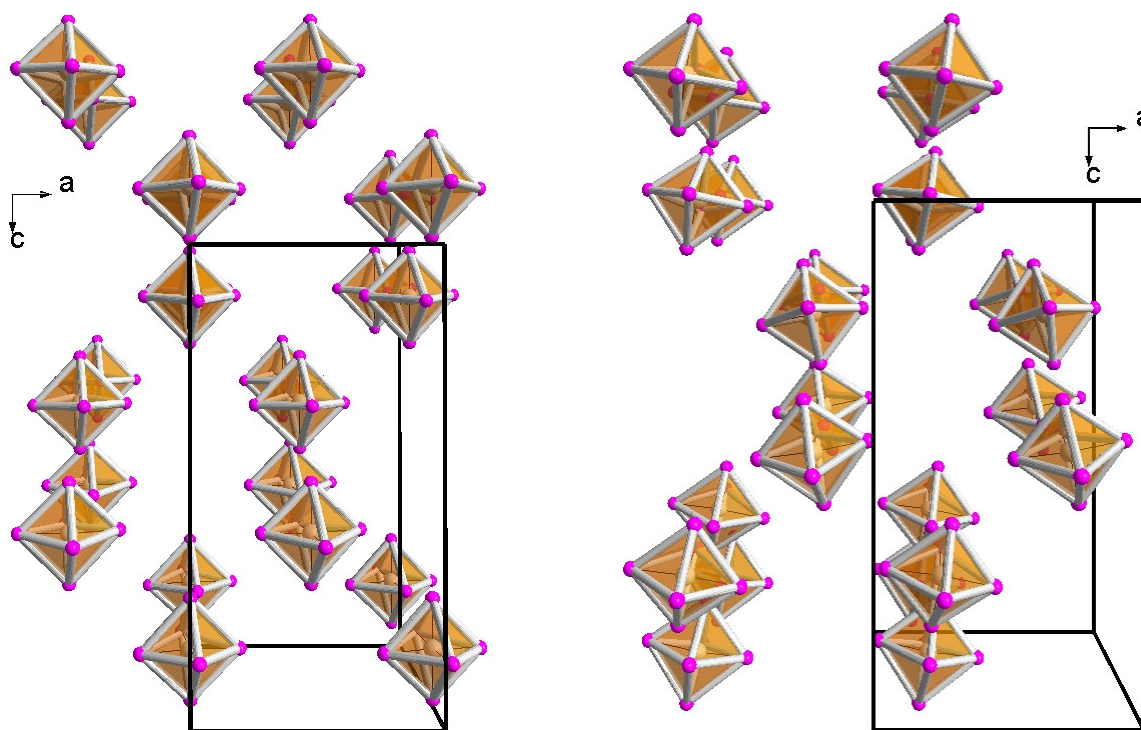


Fig. 3: Arrangement of the $[\text{NdI}_6]^{3-}$ units (left) and the $[\text{PrI}_6]^{3-}$ (right) in $[\text{bmpyr}]_4[\text{LnI}_6][\text{Tf}_2\text{N}]$

2.3.2 The coordination mode of the $[\text{Tf}_2\text{N}]^-$ -anion in $[\text{bmpyr}]_2[\text{Pr}(\text{Tf}_2\text{N})_5]$

In order to achieve an exclusive coordination of Pr^{3+} by $[\text{Tf}_2\text{N}]^-$, $\text{Pr}(\text{Tf}_2\text{N})_3$ was reacted with the ionic liquid $[\text{mppyr}][\text{Tf}_2\text{N}]$ and a compound of the composition $[\text{bmpyr}]_2[\text{Pr}(\text{Tf}_2\text{N})_5]$ was obtained. The compound crystallizes in the triclinic centrosymmetric space group $P\bar{1}$ with two formula units in the unit cell. The structure of $[\text{bmpyr}]_2[\text{Pr}(\text{Tf}_2\text{N})_5]$ is built up by $[\text{Pr}(\text{Tf}_2\text{N})_5]^{2-}$ complex anions which are forming sheets parallel to the crystallographic a - b -plane and are separated in the c -direction by $[\text{bmpyr}]$ cations (Fig. 4). By this – as often observed in the case of Tf_2N^- -complex compounds – separate hydrophobic (Tf_2N^-) and hydrophilic (bmpyr) regions are formed in the structure. The praseodymium cation itself is coordinated by five bis(trifluoromethanesulfonyl)amide ligands in the form of a (distorted) monocapped square antiprism. Four Tf_2N^- ligands coordinate bidentately, one just monodentately

(Fig. 4) with an average Pr-O distance of 249 pm. Three of the bidentate ligands adopt a *trans*-conformation while one exhibits *cis*- conformation (with respect to the $-\text{CF}_3$ groups).

Table 3: Crystallographic details for $[\text{bmpyr}]_2[\text{Pr}(\text{Tf}_2\text{N})_5]$

	$[\text{bmpyr}]_2[\text{Pr}(\text{Tf}_2\text{N})_5]$
Empirical formula	Pr S ₁₀ F ₃₀ O ₂₀ N ₇ C ₂₆ H ₄₀
Formula weight	1802.16
Crystal system	triclinic
Space group	$P\bar{1}$ (no. 2)
Unit cell dimensions	$a = 1232.04(12)$ pm $b = 1242.61(14)$ pm $c = 2264.0(2)$ pm $\alpha = 94.440(9)^\circ$ $\beta = 102.632(8)^\circ$ $\gamma = 105.792(8)^\circ$
Volume	$3219.8(6) \cdot 10^6$ pm ³
Z	2
Absorption coefficient	1.235 mm^{-1}
Reflections collected	40163
Independent reflections / R_{int}	11337 / 0.1106
Absorption correction	numerical
Data/Parameters	11337/894
Goof on F^2	0.954
Final R indices [$I > 2\sigma(I)$]	$R_1 = 0.0743$, $wR_2 = 0.0827$
R indices (all data)	$R_1 = 0.1316$, $wR_2 = 0.1742$

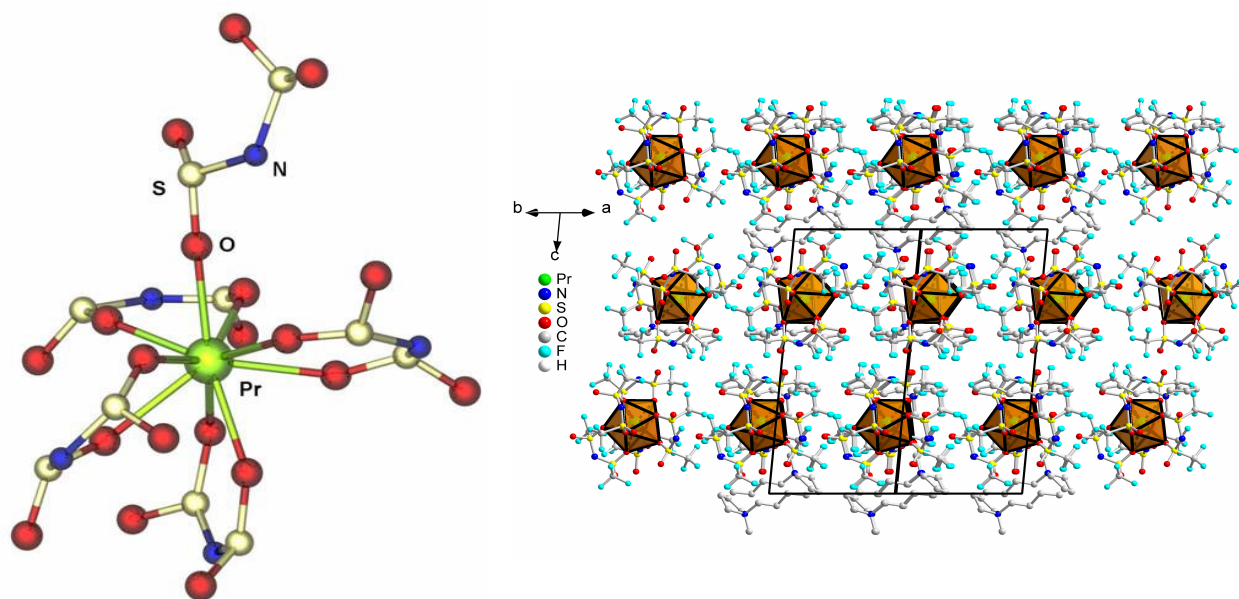


Fig. 4: Coordination sphere of Pr³⁺ in $[\text{bmpyr}]_2[\text{Pr}(\text{Tf}_2\text{N})_5]$ (l.) and the respective crystal structure (r.)

The monodentate ligand shows *trans*-conformation. Coordination of oxygen atoms influences the S-O bonding distance. For S-O bonds involving a coordinating oxygen atom, a mean interatomic S-O distance of 145 pm is found while for “free” oxygen atoms a shorter mean S-O distance of 143 pm is observed.

2.4 Spectroscopical aspects

By dissolving PrI_3 and $\text{Pr}(\text{Tf}_2\text{N})_3$ in $[\text{bmpyr}][\text{Tf}_2\text{N}]$ in both cases transparent, pale yellow green solutions are obtained. The absorption spectrum of the solutions shows the expected transitions from the $^3\text{H}_4$ ground level to $^3\text{P}_0$, $^3\text{P}_1$, $^3\text{P}_2$, $^1\text{D}_2$ levels according to the well-known energy level diagram of trivalent rare earth elements [4]. The strong absorption above 400 nm can be assigned to ligand→metal charge transfer absorptions which are stronger in case of iodide containing solution. Above 245 nm, absorptions of the ionic liquid itself are observed.

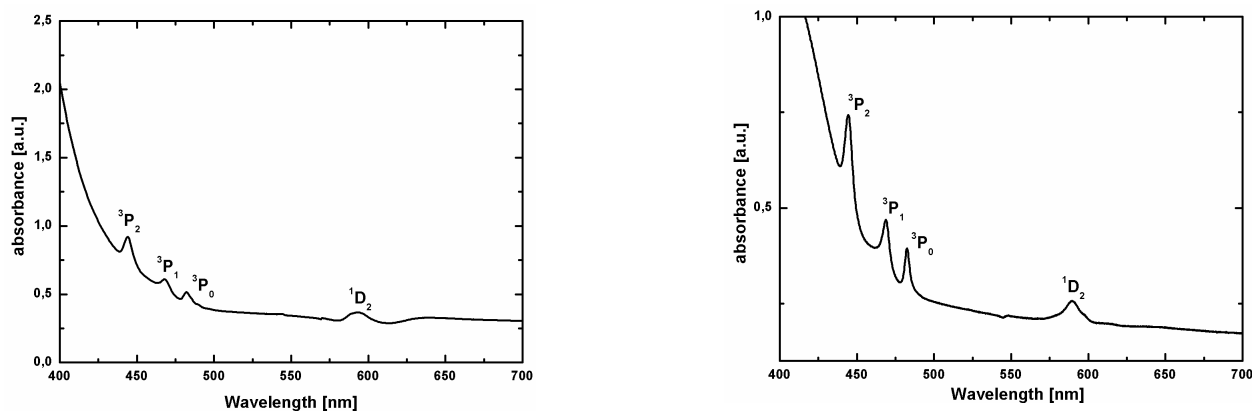


Fig. 5: Absorption spectra of PrI_3 (left) and $\text{Pr}(\text{Tf}_2\text{N})_3$ (right) in $[\text{bmpyr}][\text{Tf}_2\text{N}]$

In principle, transitions from the $^3\text{P}_1$, $^3\text{P}_0$ and the $^1\text{D}_2$ level can be observed for Pr^{3+} in the visible region of light. The luminescence spectra of PrI_3 (Fig. 6) and $\text{Pr}(\text{Tf}_2\text{N})_3$ (Fig. 7) dissolved in $[\text{bmpyr}][\text{Tf}_2\text{N}]$ as well as those of $[\text{bmpyr}]_4[\text{PrI}_6][\text{Tf}_2\text{N}]$ (Fig. 9) and $[\text{bmpyr}]_2[\text{Pr}(\text{Tf}_2\text{N})_5]$ (Fig. 10) were recorded at room temperature under excitation into the $^3\text{H}_4 \rightarrow ^3\text{P}_2$ level (corresponding to a wavelength of 443 nm). The emission spectra of

both a solution of PrI_3 (Fig. 7) and $\text{Pr}(\text{Tf}_2\text{N})_3$ (Fig. 8) dissolved in $[\text{bmpyr}][\text{Tf}_2\text{N}]$ show similar features.

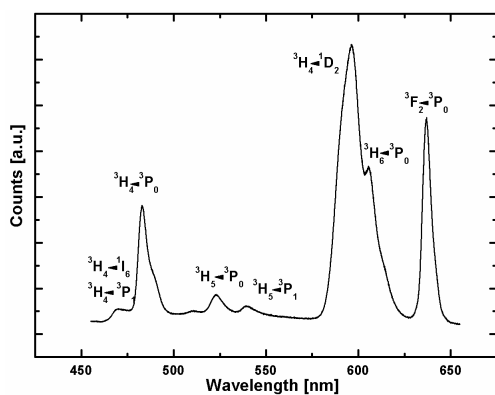


Fig. 6: Emission spectrum of PrI_3 dissolved in $[\text{bmpyr}][\text{Tf}_2\text{N}]$

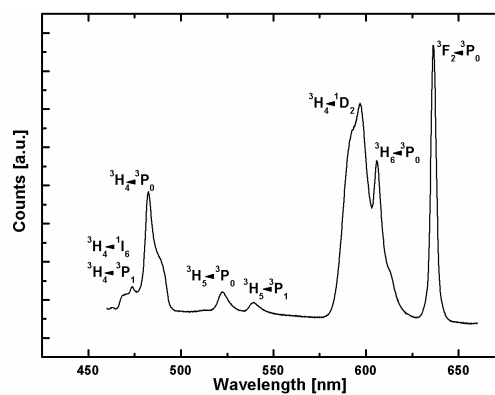


Fig. 7: Emission spectrum of $\text{Pr}(\text{Tf}_2\text{N})_3$ dissolved in $[\text{bmpyr}][\text{Tf}_2\text{N}]$

This is not astonishing taking into consideration that both solutions must contain Pr^{3+} solvated by Tf_2N^- . Most probably the complex is $[\text{Pr}(\text{Tf}_2\text{N})_5]^{3-}$ as can be concluded from the single crystal X-ray structure analysis (see above). In addition the solution of PrI_3 in $[\text{bmpyr}][\text{Tf}_2\text{N}]$ should contain Pr^{3+} in the form of $[\text{PrI}_6]^{3-}$, as can again be deduced from the single crystal X-ray structure analysis.

As previously reported, for Pr^{3+} the $^1\text{D}_2 \rightarrow ^3\text{H}_4$ transition generally yields the most intense emission [5]. Radiative transitions from the $^1\text{D}_2$ level are more probable than transitions from the $^3\text{P}_j$ levels as radiative transitions are more likely to occur when energy gaps are larger. The $^1\text{D}_2$ level exhibits the largest energy gap ($\sim 6.500 \text{ cm}^{-1}$, compared to 3.500 cm^{-1} for $^3\text{P}_0 \rightarrow ^1\text{D}_2$) to the next lower lying level in the region under investigation [6]. Especially for solutions of trivalent praseodymium compounds, the emission from the $^1\text{D}_2$ level is expected to be far more intense compared to the emission from the level $^3\text{P}_0$ as multiphonon relaxations due to the presence of high frequency oscillators present in or of the solvent lead readily to a depopulation of the $^3\text{P}_0$ level. For example, anhydrous $\text{Pr}(\text{DPM})_3$ (DPM = di-*t*-butyl-1,3-diketonate) shows in absolute DMSO the $^3\text{H}_4 \leftarrow ^1\text{D}_2$ as well as the $^3\text{H}_6 \leftarrow ^3\text{P}_0$ transitions whereas in the presence of water

only the ${}^3\text{H}_4 \leftarrow {}^1\text{D}_2$ transition is observed [7]. It is especially noteworthy that both the solutions of PrI_3 and of $\text{Pr}(\text{Tf}_2\text{N})_3$ in $[\text{bmpyr}][\text{Tf}_2\text{N}]$ show emissions from the ${}^3\text{P}_j$ levels with unusual high intensities, even at room temperature. Usually the radiationless population of the ${}^1\text{D}_2$ level from the excited ${}^3\text{P}_j$ states is preferred at this temperature. The luminescence from the ${}^3\text{P}_0$ level is more intense compared to luminescence from the ${}^1\text{P}_1$ level as its population takes place via the ${}^3\text{P}_1$ level by a strong radiationless relaxation [8]. This usually leads to total quenching of luminescence from the ${}^3\text{P}_1$ level. Even under direct excitation into the ${}^3\text{P}_1$ level often only luminescence from the ${}^3\text{P}_0$ level is observed [9]. Thus, our system is representative for the comparatively rare case where luminescence from the ${}^3\text{P}_1$ state is observed in the liquid state even at room temperature. In case of $\text{Pr}(\text{Tf}_2\text{N})_3$ in $[\text{bmpyr}][\text{Tf}_2\text{N}]$ even the ${}^3\text{H}_4 \leftarrow {}^3\text{P}_1$ and ${}^3\text{H}_4 \leftarrow {}^1\text{I}_6$ transitions can be distinguished.

The emission spectra of the solid compounds $[\text{bmpyr}]_4[\text{PrI}_6][\text{Tf}_2\text{N}]$ (Fig. 8) and $[\text{bmpyr}]_2[\text{Pr}(\text{Tf}_2\text{N})_5]$ (Fig. 9) show – as expected – weaker ${}^3\text{H}_4 \leftarrow {}^1\text{D}_2$ transitions than the solution. This is particularly observed in the iodine compound and can be attributed to the pure iodide surrounding of the rare earth cation and thus the absence of any low frequent oscillator bonds in the surrounding of praseodymium. In this compound predominantly high energy transitions (${}^3\text{H}_4 \leftarrow {}^3\text{P}_1$, ${}^3\text{H}_4 \leftarrow {}^1\text{I}_6$, ${}^3\text{H}_4 \leftarrow {}^3\text{P}_0$) are observed.

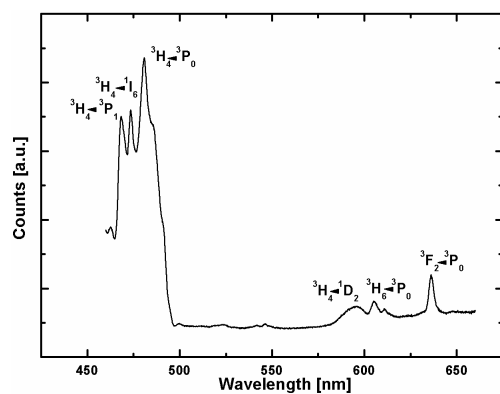


Fig. 8: Emission spectrum of PrI_3 dissolved in $[\text{bmpyr}][\text{Tf}_2\text{N}]$

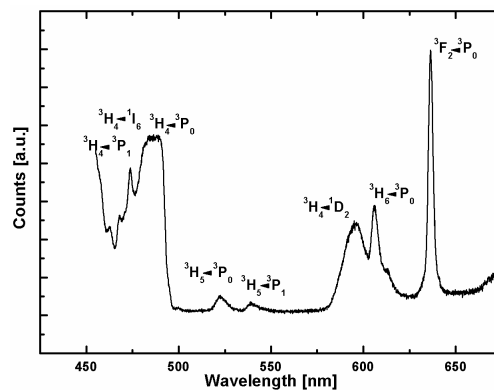
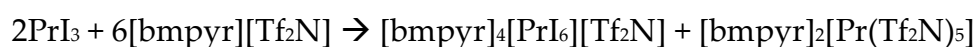


Fig. 9: Emission spectrum of PrI_3 dissolved in $[\text{bmpyr}][\text{Tf}_2\text{N}]$

The emission spectrum of $[\text{bmpyr}]_2[\text{Pr}(\text{Tf}_2\text{N})_5]$ shows broader lines which might be attributed to the lower site symmetry and stronger crystal field around Pr^{3+} . transitions almost exclusively transitions from the $^3\text{P}_j$ levels. Aside from a reversed intensity distribution of the $^3\text{H}_4 \leftarrow ^3\text{P}_0$ and $^3\text{H}_4 \leftarrow ^1\text{D}_2$, the spectrum of $[\text{bmpyr}]_2[\text{Pr}(\text{Tf}_2\text{N})_5]$ shows a close resemblance to the solution spectra. From this it can be derived that in solution the predominant Pr^{3+} species is most probably the complex ion $[\text{Pr}(\text{Tf}_2\text{N})_5]^{2-}$.

2.4 Discussion

According to the reaction equation



PrI_3 dissolves in the ionic liquid $[\text{bmpyr}][\text{Tf}_2\text{N}]$ similar to NdI_3 . Thereby, at least two different praseodymium species are formed. One contains praseodymium octahedrally coordinated by iodine anions, as established by the crystal structure analysis of $[\text{bmpyr}]_4[\text{PrI}_6][\text{Tf}_2\text{N}]$. By reacting $\text{Pr}(\text{Tf}_2\text{N})_3$ with $[\text{bmpyr}][\text{Tf}_2\text{N}]$ we were able to obtain $[\text{bmpyr}]_2[\text{Pr}(\text{Tf}_2\text{N})_5]$ which was be structurally characterized. It shows Pr^{3+} coordinated by nine oxygen atoms of five bis(trifluoromethanesulfonyl)amide ligands in the form of a monocapped square antiprism. In consequence, the remaining praseodymium cations must be solvated by the anion of the ionic liquid. All systems show strong transitions from the $^3\text{P}_j$ levels which can be attributed to the absence of any low frequency oscillators in the immediate neighbourhood of the praseodymium cation. As expected for the solid compounds the intensities for the $^3\text{H}_4 \leftarrow ^3\text{P}_0$ are enhanced compared to the $^3\text{H}_4 \leftarrow ^1\text{D}_2$ transition. Our investigations show that ionic liquids are promising media to study the luminescent properties of rare earth cations in the liquid state as they generally quench to a lesser extend the optical transition than conventional solvents. This may open up the way to new liquid luminescent materials.

The coordination-effect of the Tf_2N -anion can even better be studied in europium-complexes, since the $^5\text{D}_0 \rightarrow ^7\text{F}_4$ transition is sensitive to the local environment of the

Eu³⁺ [10]. Also the effect of lanthanide contraction can yield in different behaviour of the respective trivalent cation in the ionic liquid which is shown in the next chapter.

2.5 Literature

- [1] R.D. Shannon, *Acta Crystallogr., Sect. A.* **1976**, 32, 751.
- [2] D.B. Baudry, A. Dormond, F. Duris, J.M. Bernard, J.R. Desmurs, *J. Fluorine Chem.* **2003**, 121, 233.
- [3] A. Babai, A.-V. Mudring, *J. Alloys Comp.* **2006**, 418, 122.
- [4] G.H. Dieke, *Spectra and energy levels of rare earth ions in crystals*, Interscience Publishers, New York, **1968**; W.T. Carnall, H.M. Crosswhite, H. Crosswhite, *Energy level structure and transition probabilities in the spectra of trivalent lanthanides in LaF₃*. Special Report **1977** (Argonne, IL: Chemistry Division, Argonne National Laboratory).
- [5] A. Ben Ali, E. Antic-Fidancev, B. Viana, P. Aschehough, M. Taibi, J. Aride, A. Boukhari, *J. Phys.: Condens. Matter* **2001**, 13, 9663.
- [6] G. Blasse, B.C. Grabmaier, *Luminescent Materials*, **1994**, Springer-Verlag, Berlin, Heidelberg.
- [7] A.I. Voloshin, N.M. Shavaleev, V.P. Kazakov, *Luminescence* **2001**, 93, 199.
- [8] U. Schäfer, J. Nekum, N. Bodenschatz, J. Heber, *J. Lumin.* **1994**, 60/61, 633.
- [9] P. Boutinad, R. Mahiou, N. Martin, M. Malinowski, *Luminescence* **1997**, 72-74, 809.
- [10] H.C. Aspinall, *Chemistry of f-Block Elements*, **2001**, Gordon and Breach Science Publishers, Amsterdam.

3. Behaviour of Ln(Tf₂N)₃ in [bmpyr][Tf₂N]

3.1 Introduction

In this chapter the focus is set on the structural and physical properties of [Tf₂N]-compounds of a series of rare-earth cations (Sm, Eu, Gd, Tb, Tm, Yb, Lu). The lanthanide contraction leads to a structural transition from [bmpyr]₂[Ln(Tf₂N)₅] (La-Tb, type I) to [bmpyr][Ln(Tf₂N)₄] (Dy-Lu, type II). The complexes are characterized by XRD and elemental analysis. Thermogramms evidence, that the lighter rare-earth cations compose complexes which themselves are ionic liquids, featuring melting points < 100°C. The respective europium and ytterbium compound are chosen as representatives for the type I and II compounds and were investigated further by cyclic voltammetry and spectroscopy. By exchanging the [bmpyr]⁺ cation in [bmpyr]₂[Eu(Tf₂N)₅] by a [bmim]-cation (bmim = 1-butyl-1-methylimidazolium) a RTIL is obtained, consisting of a complex rare-earth anion. The coordination mode of the [Tf₂N] anion is further studied in the respective europium-compound by means of spectroscopy. Addition of the RTIL [bmpyr][OTf] to the systems Ln(Tf₂N)₃/[bmpyr][Tf₂N] leads to ligand exchange within the coordination spheres of the rare-earth ions. This is evidenced by single-XRD, electrochemical methods and spectroscopy.

3.2 Preparation

Ln(Tf₂N)₃: The compounds were synthesized as described before (see 2.2). Anal. data:
Nd(Tf₂N)₃ NdC₆F₁₈N₃O₁₂S₆: C, 7.32; H, 0.00; N, 4.27%. Found: C, 7.34; H, 0.00; N, 4.15%.
Eu(Tf₂N)₃ EuC₆F₁₈N₃O₁₂S₆: C, 7.26; H, 0.00; N, 4.23%. Found: C, 7.23; H, 0.00; N, 4.20%.
Tb(Tf₂N)₃ TbC₆F₁₈N₃O₁₂S₆: C, 7.21; H, 0.00; N, 4.20%. Found: C, 7.31; H, 0.00; N, 4.28%.
Dy(Tf₂N)₃ DyC₆F₁₈N₃O₁₂S₆: C, 7.19; H, 0.00; N, 4.19%. Found: C, 7.12; H, 0.00; N, 4.08%.
Tm(Tf₂N)₃ TmC₆F₁₈N₃O₁₂S₆: C, 7.14; H, 0.00; N, 4.16%. Found: C, 7.28; H, 0.08; N, 4.08%.
Yb(Tf₂N)₃ YbC₆F₁₈N₃O₁₂S₆: C, 7.11; H, 0.00; N, 4.15%. Found: C, 7.26; H, 0.00; N, 4.00%.
Lu(Tf₂N)₃ LuC₆F₁₈N₃O₁₂S₆: C, 7.10; H, 0.00; N, 4.14%. Found: C, 7.34; H, 0.06; N, 4.22%.

[bmpyr]₂[Ln(Tf₂N)₅] (Ln = Y, La-Tb) were synthesized from the respective Ln(Tf₂N)₃ compound (0.5 mmol) and [bmpyr][Tf₂N] (422.4 mg, 1 mmol). The educts were placed in a schlenk tube and stirred for 2 h at 120 °C until a homogeneous compound is obtained. By cooling to room temperature typically pale colored solids are obtained, the color depending on the Ln(Tf₂N)₃. The products were analyzed by powder-XRD and elemental analysis. To obtain single crystals with sufficient quality for XRD, Ln(Tf₂N)₃ (0.125 mmol) and [bmpyr][Tf₂N] (355 mg, 0.25 ml, 0.8 mmol) were placed in a silica tube which was sealed under vacuum. The reaction was carried out at 120°C for 36 h. Single crystals of [bmpyr]₂[Ln(Tf₂N)₅] form as an insoluble product after cooling the reaction mixture to room temperature (5 K/min). Anal. Data:

[bmpyr]₂[Nd(Tf₂N)₅] NdC₂₈H₄₀F₃₀N₇O₂₀S₁₀: C, 18.38; H, 2.20; N, 5.36%. Found: C, 18.79; H, 1.56; N, 5.42%.

[bmpyr]₂[Eu(Tf₂N)₅] EuC₂₈H₄₀F₃₀N₇O₂₀S₁₀: C, 18.31; H, 2.19; N, 5.34%. Found: C, 18.39; H, 2.41; N, 5.36%.

[bmpyr][Ln(Tf₂N)₄] (Ln = Dy-Lu) were synthesized from the respective Ln(Tf₂N)₃ compound (0.5 mmol) and [bmpyr][Tf₂N] (211.2 mg, 0.5 mmol). The educts were placed in a schlenk tube and stirred for 2 h at 120 °C until a homogeneous compound is obtained. By cooling to room temperature a colorless solid is obtained. The products were analyzed by powder-XRD and elemental analysis. To obtain single crystals with sufficient quality for XRD, the procedure for [bmpyr]₂[Ln(Tf₂N)₅] was followed. Anal. data:

[bmpyr][Tm(Tf₂N)₄] TmC₁₇H₂₀F₂₄N₅O₁₆S₈: C, 14.26; H, 1.41; N, 4.89%. Found: C, 14.26; H, 1.31; N, 4.96%.

[bmpyr][Yb(Tf₂N)₄] YbC₁₇H₂₀F₂₄N₅O₁₆S₈: C, 14.22; H, 1.40; N, 4.88%. Found: C, 14.55; H, 1.76; N, 4.91%.

[bmpyr][Lu(Tf₂N)₄] LuC₁₇H₂₀F₂₄N₅O₁₆S₈: C, 14.20; H, 1.40; N, 4.87%. Found: C, 14.62; H, 1.14; N, 4.87%.

[bmpyr][OTf] was prepared following a method of Welton [1]: **[bmim][Cl]** (44.4 g, 0.25 mol) was dissolved in 50 ml CH_2Cl_2 and **Li(OTf)** (39.0 g, 0.25 mol) was added. The suspension was stirred overnight and filtered. The decanted solution was washed with several aliquots of water until no halide residues could be detected (AgNO_3 test). The solvent was removed and the ionic liquid dried in vacuum at 393K overnight. Typical yields > 90%.

[bmim][Tf₂N] was prepared analog to **[bmpyr][Tf₂N]** (see 1.2).

[bmim]₂[Eu(Tf₂N)₅] was synthesized analogously to the respective **[bmpyr]** compound.

3.3 Structural aspects

The type I and type II compounds are case isostructural; therefore only one compound of each type is described. Powder XRD data (Fig. 1) in combination with elemental analysis evidences that exclusively one type of compound is composed depending on the size of the rare-earth cation. Crystallographic data and selected distances are shown in Table 1 and 2. In both cases, the trivalent lanthanide cations are coordinated by oxygen atoms exclusively belonging to the **[Tf₂N]**-ligand and are forming discrete anionic units. The larger lanthanide cations exhibit a nine-fold oxygen coordination which can best be described as a monocapped square antiprism (cf. Fig.2, left). The mean oxygen-lanthanide distances of 248 pm for Nd^{3+} , and 241 pm for Tb^{3+} well reflect the lanthanide contraction and are shorter than in the nonhydrates of the respective trivalent lanthanide cations ($\text{Nd}-\text{O} = 251$ pm, $\text{Tb}-\text{O} = 243$ pm) [2] but can be compared to values found for typical metal-organic complexes with the same coordination number for the respective lanthanide cation as e.g. hexafluoroacetylacetonate complexes of neodymium and terbium [3]. The oxygen surrounding of the f-element cation is achieved by four bidentate bis(trifluoromethanesulfonyl)amide ligands and one monodentate ligand. The monodentate bis(trifluoromethanesulfonyl)amide ligand adopts a *transoid* conformation (with respect to the S-N-S plane) which is also found to be the more stable

conformation for the free Tf_2N anion [4]. For the bidentate ligands both conformations are observed. One of the four ligands adopts a *cisoid*-conformation and another one a *transoid*-conformation, while the other two ligand positions show a mixed occupation by ligands in *cisoid*- and *transoid*-conformations (cf. Fig. 2, right). The *transoid*-chelating coordination mode turns the bis(trifluoromethanesulfonyl)amide into a dissymmetric molecule. One *transoid* chelating ring exhibits a λ -configuration whereas one of the positions with mixed occupancy show a λ -, the other one a δ -configuration. A distinct change of the S—O interatomic distances within bis(trifluoromethanesulfonyl)-amide upon coordination is observed when compared to the free ligand (S—O ~ 141 pm) [5]. For

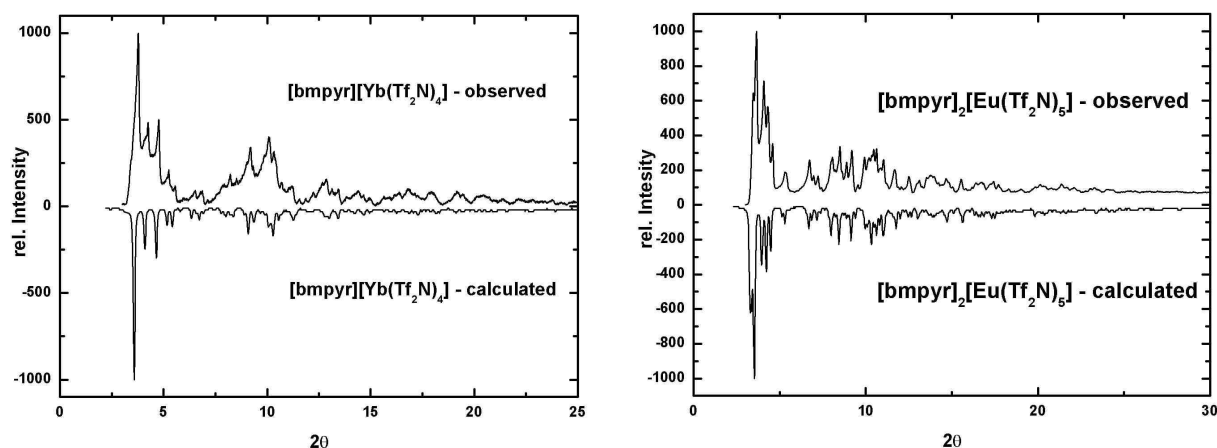


Fig. 1: Powder-XRD of $[\text{bmpyr}][\text{Eu}(\text{Tf}_2\text{N})_5]$ (left) and $[\text{bmpyr}][\text{Yb}(\text{Tf}_2\text{N})_4]$ (right)

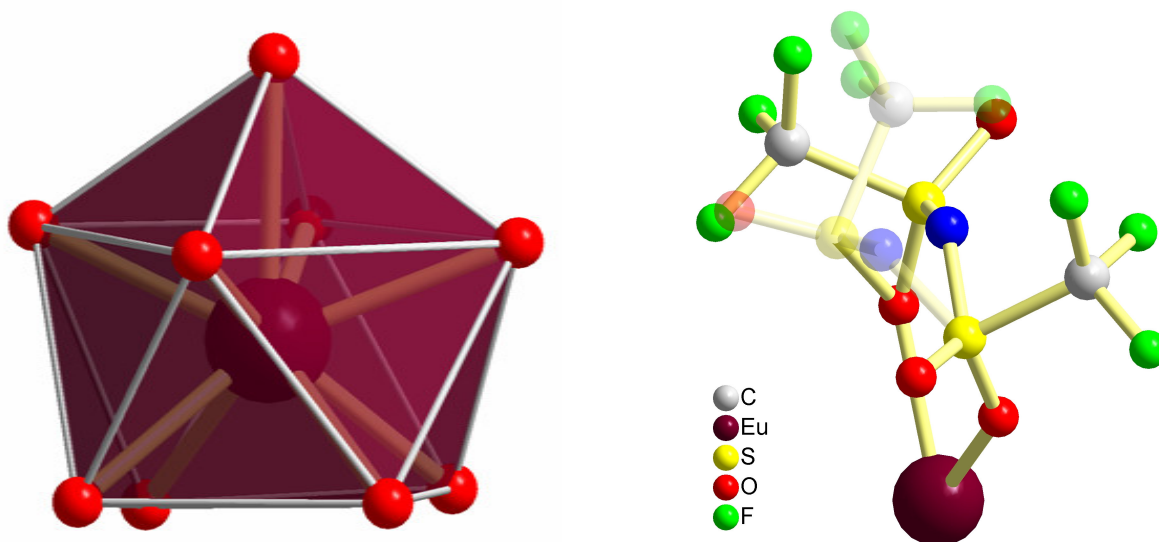


Fig. 2: Coordination of Ln^{3+} by oxygen-atoms in $[\text{bmpyr}]_2[\text{Ln}(\text{Tf}_2\text{N})_5]$ (left) and disorder of the chelating (Tf_2N) -moiety in $[\text{bmpyr}]_2[\text{Eu}(\text{Tf}_2\text{N})_5]$ (right)

[bmpyr]₂[Nd(Tf₂N)₅] the mean S—O interatomic distance of 147 pm is found for a coordinating oxygen atom, the mean “free” S—O interatomic distance is 142 pm.

The same values are found for [bmpyr]₂[Tb(Tf₂N)₅]. A mean N-S-N angle of 127°, and a mean S—N distances of 156 pm are found for [bmpyr]₂[Nd(Tf₂N)₅], for [bmpyr]₂[Tb(Tf₂N)₅] values of 126° and 157 pm are found. These values match well the values found for the free ligand (126° and 157 pm).

While the larger trivalent lanthanide cations Pr³⁺-Tb³⁺ show a ninefold coordination by oxygen, the smaller lanthanide cations Dy³⁺-Lu³⁺ prefer an eightfold coordination by oxygen (Fig. 3). The asymmetric unit of the crystal structure of [bmpyr][Ln(Tf₂N)₄], Ln = Tm, Yb, Lu, contains two crystallographically distinct lanthanide cations. Both exhibit an oxygen surrounding which resembles a trigonal dodecahedron. This coordination polyhedron is most times preferred over a cube when ligand-ligand repulsion becomes important for coordination number eight. The mean oxygen—f-element distances in [bmpyr][Ln(Tf₂N)₄] lie with values of 231 pm for Tm³⁺ and 230 pm for Lu³⁺ in the expected range and can be compared acetylacetonato complexes [6].

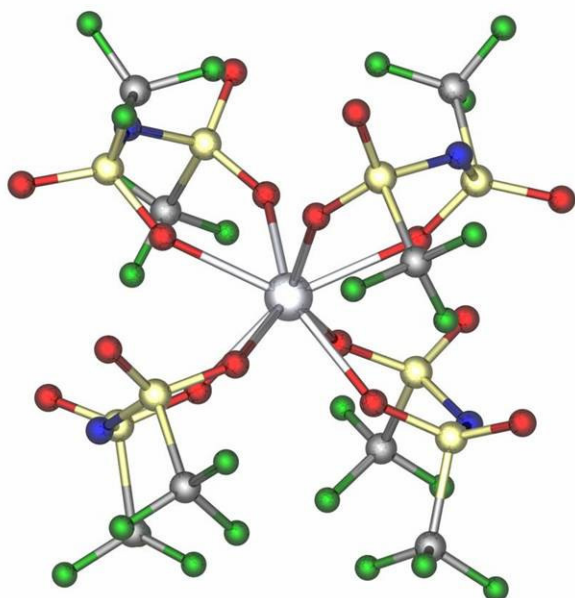


Fig. 3: Coordination of Ln³⁺ by oxygen-atoms in [bmpyr][Ln(Tf₂N)₄]

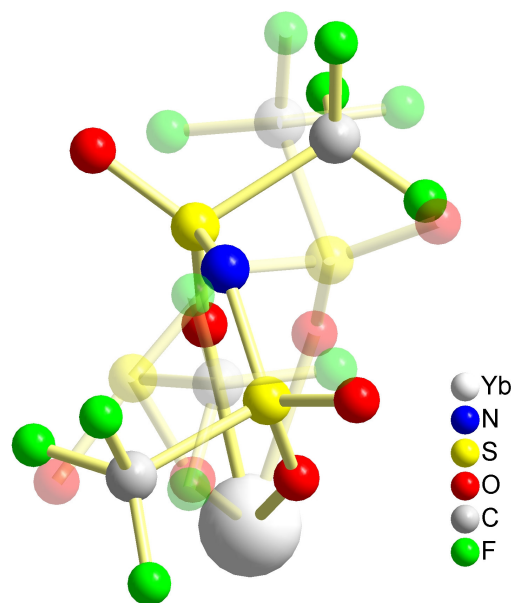


Fig. 4: Disorder of the chelating (Tf₂N)-moiety in [bmpyr][Yb(Tf₂N)₄]

One crystallographically independent lanthanide cation is coordinated by four chelating Tf₂N-ligands with two ligands in a *cisoid*- and two in a *transoid*-conformation. The *transoid*-Tf₂N ligands both have λ configuration. The other crystallographically independent lanthanide cation in [bmpyr][Ln(Tf₂N)₄] is, again, coordinated by four chelating Tf₂N-ligands of which two adopt a *cisoid*- and two a *transoid*-conformation. But here disorder between λ - and δ - configured *transoid* ligands is observed (see Fig. 4).

As noted above for [bmpyr]₂[Ln(Tf₂N)₅] a distinct change of the S—O interatomic distances within the bis(trifluoromethanesulfonyl)amide ligand upon coordination can be detected. For [bmpyr][Tm(Tf₂N)₄] the mean interatomic distance of 147 pm is found for S—O involving a coordinating oxygen atom, whereas the mean S—O interatomic distance for the “free” S—O bonds is 141 pm. For [bmpyr][Lu(Tf₂N)₄] values of 146 pm and 140 pm are found. A mean N-S-N angle of 127° is found for [bmpyr][Tm(Tf₂N)₄] with and a mean S—N distances of 156 pm. For [bmpyr][Lu(Tf₂N)₄] the values are 126° and 156 pm, respectively. Thus, for compounds of the compositions [bmpyr]₂[Ln(Tf₂N)₅] and [mppypr][Ln(Tf₂N)₄] coordination of the bis(trifluoromethanesulfonyl)amide anion to trivalent f-element cations leads to a significant lengthening of the S—O bond involving the coordinating oxygen atom basically unchanged when compared to the free anion. The change of the S—O bond distance is far more pronounced in the trivalent complex compounds than in the analogous divalent complex compound [mppypr]₂[Yb(Tf₂N)₄] where values of 144 pm for the S—O bond with the coordinating oxygen atom and 141 pm for the non-coordination were observed [4]. This indicates together with a shorter Yb—O interatomic distance (in [mppypr]₂[Yb(Tf₂N)₄] a Yb²⁺—O interatomic distance of 250 pm is found) a stronger interaction of the bis-(trifluoromethanesulfonyl)amide oxygen atoms with the lanthanide. In all cases no significant change neither in the mean N-S-N angle nor in the S—N bonding distance could be observed.

Table 4: Crystallographic and refinement details for [bmpyr]₂[Ln](Tf₂N)₅ and [bmpyr] [Ln](Tf₂N)₄

	[bmpyr]₂[Nd(Tf₂N)₅]	[bmpyr]₂[Eu(Tf₂N)₅]	[bmpyr]₂[Tb(Tf₂N)₅]	[bmpyr][Tm(Tf₂N)₄]	[bmpyr][Yb(Tf₂N)₄]	[bmpyr][Lu(Tf₂N)₄]
Emp. Formula	Nd ₁ C ₂₈ H ₄₀ F ₃₀ N ₇ O ₂₀ S ₁₀	Eu ₁ C ₂₈ H ₄₀ F ₃₀ N ₇ O ₂₀ S ₁₀	Tb ₁ C ₂₈ H ₄₀ F ₃₀ N ₇ O ₂₀ S ₁₀	Tm ₁ C ₁₇ H ₂₀ F ₂₄ N ₅ O ₁₆ S ₈	Yb ₁ C ₁₇ H ₂₀ F ₂₄ N ₅ O ₁₆ S ₈	Lu ₁ C ₁₇ H ₂₀ F ₂₄ N ₅ O ₁₆ S ₈
Form.weight	1829.51	1837.23	1844.19	1431.79	1435.90	1437.83
Crystal system	triclinic	triclinic	triclinic	Monoclinic	monoclinic	monoclinic
Space group	<i>P</i> $\bar{1}$ (no. 2)	<i>P</i> $\bar{1}$ (no. 2)	<i>P</i> $\bar{1}$ (no. 2)	<i>P</i> 2/ <i>c</i> (no. 13)	<i>P</i> 2/ <i>c</i> (no. 13)	<i>P</i> 2/ <i>c</i> (no. 13)
Cell dim.	<i>a</i> = 1230.18(11) pm <i>b</i> = 1242.50(11) pm <i>c</i> = 2258.91(19) pm α = 94.401(7) $^\circ$ β = 102.493(7) $^\circ$ γ = 105.768(7) $^\circ$	<i>a</i> = 1232.26(13) pm <i>b</i> = 1235.77(13) pm <i>c</i> = 2263.7(2) pm α = 95.244(8) $^\circ$ β = 102.786(8) $^\circ$. γ = 106.066(8) $^\circ$	<i>a</i> = 1231.56(10) pm <i>b</i> = 1236.23(11) pm <i>c</i> = 2258.06(19) pm α = 95.260(7) $^\circ$ β = 102.886(7) $^\circ$. γ = 106.036(7) $^\circ$	<i>a</i> = 2015.75(19) pm <i>b</i> = 1488.47(8) pm <i>c</i> = 1619.68(12) pm β = 113.234(6) $^\circ$.	<i>a</i> = 2013.33(15) pm <i>b</i> = 1486.17(9) pm <i>c</i> = 1620.65(11) pm β = 112.971 (5) $^\circ$.	<i>a</i> = 2010.47 (12) pm <i>b</i> = 1485.72 (8) pm <i>c</i> = 1621.22 (11) pm β = 102.786(8) $^\circ$.
Volume	3210.2(5)·10 ⁶ pm ³	3187.2(6) ·10 ⁶ pm ³	3177.5(5) ·10 ⁶ pm ³	4465.5(6) ·10 ⁶ pm ³	4457.7(5) ·10 ⁶ pm ³	3187.2(6) ·10 ⁶ pm ³
Z	2	2	2	4	4	4
Density (calc.)	1.893 g·cm ⁻³	1.914 g·cm ⁻³	1.928 g·cm ⁻³	2.130 g·cm ⁻³	2.140 g·cm ⁻³	2.142 g·cm ⁻³
Abs. coefficient	1.290 mm ⁻¹	1.468 mm ⁻¹	1.599 mm ⁻¹	2.528 mm ⁻¹	2.649 mm ⁻¹	2.756 mm ⁻¹
Refl. collected	42148	36883	48596	65568	68174	50262
Ind. Refl. / R _{int}	13981 / 0.0621	10618 / 0.0775	13850 / 0.0620	9747/ 0.0682	9973/ 0.0743	6999 / 0.0537
Abs. correction	numerical	numerical	Numerical	Numerical	numerical	numerical
Data/Param.	13981/890	10618/977	13850/877	9747/580	9973/626	6999/625
GooF on F ²	1.069	0.894	1.038	1.066	1.048	1.082
R ind. [I>2 σ (I)]	R ₁ = 0.0671 wR ₂ = 0.1839	R ₁ = 0.0470 wR ₂ = 0.0875	R ₁ = 0.0647 wR ₂ = 0.1680	R ₁ = 0.0938 wR ₂ = 0.2520	R ₁ = 0.0913 wR ₂ = 0.2412	R ₁ = 0.0770 wR ₂ = 0.2134
R ind. (all data)	R ₁ = 0.0831 wR ₂ = 0.1974	R ₁ = 0.0859 wR ₂ = 0.0979	R ₁ = 0.0946 wR ₂ = 0.1835	R ₁ = 0.1212 wR ₂ = 0.2796	R ₁ = 0.1229 wR ₂ = 0.2690	R ₁ = 0.0881 wR ₂ = 0.2240

Table 5: Selected distances (pm) in [bmpyr]_n[Ln(Tf₂N)_{n+3}] (disordered atoms are omitted)

	Ln = Nd	Ln = Eu	Ln = Tb		Ln = Tm	Ln = Yb	Ln = Lu
Ln(1)-O(31)#	242.1(5)	237.6(4)	235.4(5)	Ln(1)-O(11)	233.7(7)	2.334(7)	2.334(7)
Ln(1)-O(41)	248.1(5)	244.5(4)	241.8(5)	Ln(1)-O(12)	228.3(6)	2.272(6)	2.263(7)
Ln(1)-O(51)	253.5(4)	252.7(4)	252.9(5)	Ln(1)-O(21)	231.6(8)	2.303(7)	2.306(7)
Ln(1)-O(61)	248.9(4)	244.3(4)	241.1(5)	Ln(1)-O(22)	228.4(7)	2.275(7)	2.273(8)
Ln(1)-O(71)	249.1(4)	246.1(4)	243.3(5)				
Ln(1)-O(43)	249.9(4)	246.1(4)	243.1(5)				
Ln(1)-O(53)	246.4(4)	242.6(4)	239.2(5)				
Ln(1)-O(63)	244.0(4)	240.0(4)	238.3(4)				
Ln(1)-O(72)	245.8(4)	241.0(4)	238.2(5)				
S(31)-O(31)*	144.8(5)	144.9(4)	145.0(6)	S(11)-O(11)*	145.8(8)	145.7(8)	1.458(8)
S(31)-O(32)	141.7(5)	141.6(5)	141.8(6)	S(11)-O(14)	144.1(9)	142.8(9)	1.438(9)
S(32)-O(33)	142.0(5)	142.5(5)	142.1(6)	S(12)-O(12)*	145.7(7)	145.0(7)	1.447(8)
S(32)-O(34)	142.9(5)	143.2(5)	142.8(6)	S(12)-O(13)	140.7(8)	140.4(8)	1.410(9)
S(41)-O(41)*	145.4(5)	144.6(4)	144.8(5)	S(21)-O(22)*	148.2(9)	147.3(9)	1.467(9)
S(41)-O(42)	141.4(6)	142.7(5)	140.7(7)	S(21)-O(23)	140.0(9)	139.9(9)	1.401(9)
S(42)-O(43)*	144.2(5)	144.2(4)	145.1(5)	S(22)-O(21)*	149.6(9)	148.5(9)	1.465(9)
S(42)-O(44)	142.0(6)	142.9(5)	142.4(6)	S(22)-O(24)	140.8(2)	141.6(9)	1.419(0)
S(51)-O(51)*	145.1(4)	145.1(4)	145.5(5)				
S(51)-O(52)	141.2(5)	141.9(4)	140.9(6)				
S(52)-O(53)*	146.0(4)	145.6(4)	146.1(5)				
S(52)-O(54)	139.4(5)	141.0(5)	140.6(6)				
S(61)-O(61)*	146.0(4)	145.6(4)	145.6(5)				
S(61)-O(62)	140.8(5)	141.6(5)	141.8(6)				
S(72)-O(72)*	144.1(5)	144.4(4)	145.3(6)				
S(72)-O(73)	140.1(9)	144.0(6)	142.5(8)				

#) = monodentate coordination *) = oxygen bond to metal-atom

3.4 Thermal investigations

The structurally characterized substances of the general formula $[\text{bmpyr}]_n[\text{Ln}(\text{Tf}_2\text{N})_{3+n}]$ were examined further by DSC measurements. The Sm, Eu, Gd and Tb compounds exhibit melting points $< 100^\circ\text{C}$ and can therefore be qualified as an ionic liquid. The heavier rare-earth ions compose complexes with melting points up to 105°C . The compound $[\text{bmpyr}]_2[\text{Sm}(\text{Tf}_2\text{N})_5]$ shows a very simple thermogram. The substance melts at 83.8°C and crystallizes at 43.3°C . The super-cooling of approx. 40°C is a common feature in ionic liquid compounds [7].

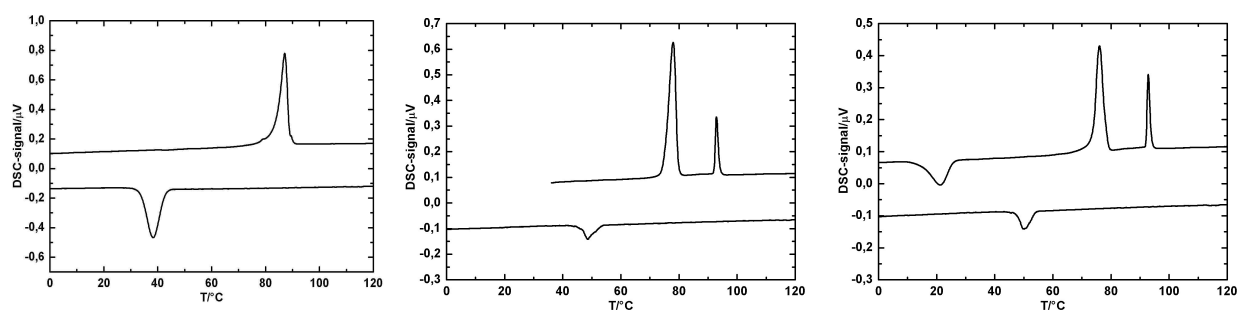


Fig. 5: Thermograms of $[\text{bmpyr}]_2[\text{Ln}(\text{Tf}_2\text{N})_5]$ a) Sm (left) b) Eu, 1st cycle (middle) c) Eu, 2nd cycle (left)

The Eu and Gd compound exhibit a more complicated thermal behavior. The compounds show a strong endothermic peak at 73.9°C and 61.1°C respectively. The europium-compound then melts at 92.1°C and the gadolinium-compound at 94.7°C (see Fig. 5 b), c) & 6 a)). The endothermic peaks prior to the melting peaks could be caused by a structural transition involving a change in the stereochemistry of the $[\text{Tf}_2\text{N}]$ -moieties, however, further investigations are required to verify this hypothesis. Upon cooling, again supercooling is observed and the compounds turn to a solid at 53.6°C (Eu) and 44.3°C (Gd). Surprisingly the crystallization appears not to be complete, after further cooling to -50°C and reheating, an exothermic peak is observed at 14.4°C (Eu, Fig. 5 b)) and 22.2°C (Gd, data not shown). This peak is shifted to higher temperatures

by changing the heating rate from 5°C/min to 10°C/min and is therefore likely to be an effect of post crystallization.

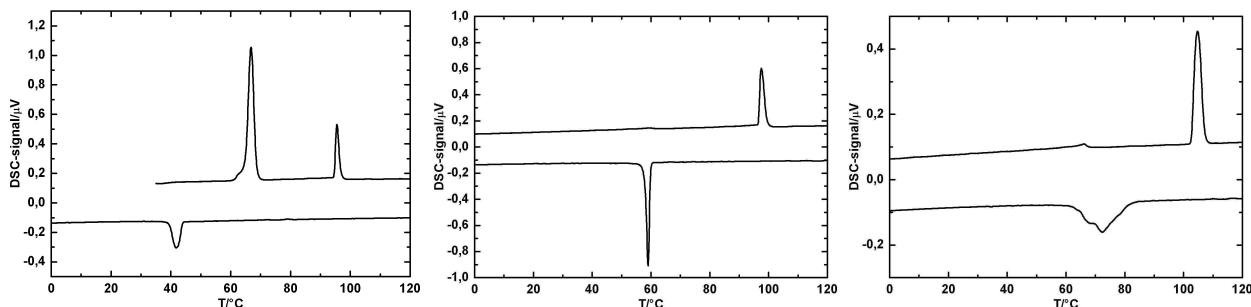


Fig. 6: Thermograms of [bmpyr]_n[Ln(Tf₂N)_{n+3}] a) Gd (left) b) Tb (middle) c) Tm (left)

The other compounds show a more simple thermogram, bearing melting points between 96.°C (Tb) and 105.1°C (Lu). In all cases a very weak endothermic peak prior to the melting peak is observed, while upon cooling the compounds crystallize in one step without post crystallization upon reheating.

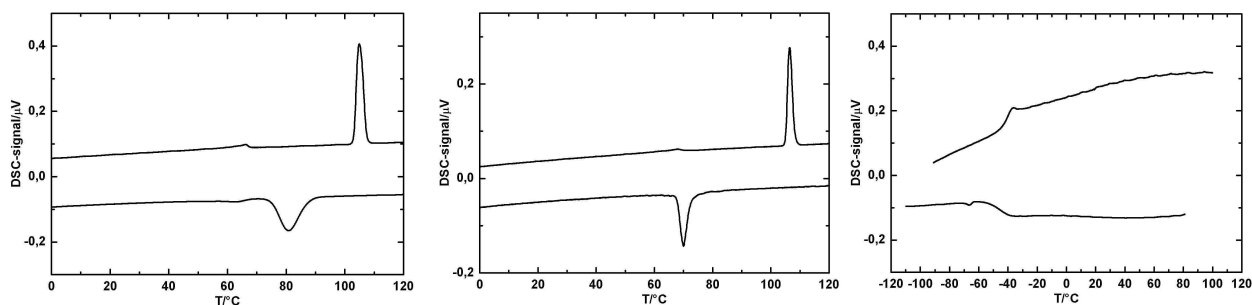


Fig. 7: Thermograms of [bmpyr][Ln(Tf₂N)₄] a) Yb (left) b) Tm (middle) and [bmim]₂[Eu(Tf₂N)₅] (left)

By exchanging the [bmpyr]-cation in [bmpyr]₂[Eu(Tf₂N)₅] by a [bmim]-cation, a RTIL is obtained. Upon cooling the compound [bmim]₂[Eu(Tf₂N)₅], a glass-transition is observed at -50°C which is followed by a weak exothermic peak which could turn up due to partial crystallization. The heating curve shows the solid → liquid transition at the same temperature as the glass formation occurred upon cooling. The pure [bmim][Tf₂N] exhibits a similar thermogram, the glass-transition point being shifted to lower temperatures (-80°C). It appears that the lower tendency of the [bmim]-cation to crystallize composes a europium-based RTIL which is liquid even at temperatures

below 0°C. However, an applicable viscosity of the ionic liquid is reached at elevated temperatures (~ 50°C).

In Figure 8 the increase of the melting points of $[\text{bmpyr}]_n[\text{Ln}(\text{Tf}_2\text{N})_{3+n}]$ dependent on the rare-earth ion is shown. The higher the mass of the incorporated rare-earth ion, the higher is the melting point of the substance. Surprisingly the structural transition from $[\text{bmpyr}]_2[\text{Ln}(\text{Tf}_2\text{N})_5]$ to $[\text{bmpyr}][\text{Ln}(\text{Tf}_2\text{N})_4]$ has little influence on the melting points of the substances.

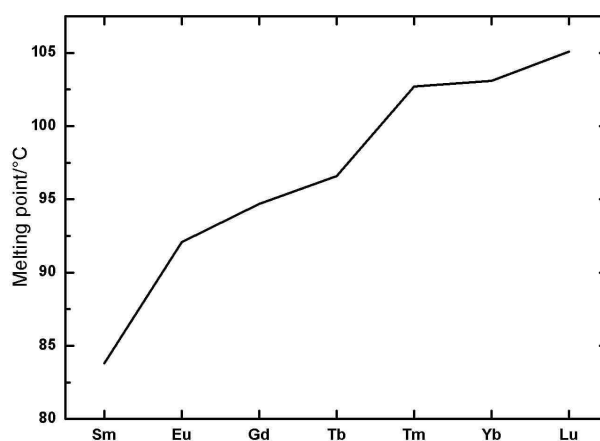


Fig. 8: Ion mass-dependence of the melting point of $[\text{bmpyr}]_n[\text{Ln}(\text{Tf}_2\text{N})_{3+n}]$

3.4 Spectroscopical investigations

The crystal structure of $[\text{bmpyr}]_2[\text{Eu}(\text{Tf}_2\text{N})_5]$ features a nine-coordinated europium atom, surrounded by the oxygen-atoms of five $[\text{Tf}_2\text{N}]$ -anions. Billard et al. investigated the system $\text{Eu}(\text{Tf}_2\text{N})$ - $[\text{bmim}][\text{Tf}_2\text{N}]$ by means of EXAFS-spectroscopy and molecular dynamic simulation [8]. The conclusion of their measurements leads to a europium-ion which is coordinated by five $[\text{Tf}_2\text{N}]$ -anions, the coordination-number being $9.8(\pm 20\%)$. The question which arises is: Is there a difference between the coordination numbers of the europium ion in a solution of $\text{Eu}(\text{Tf}_2\text{N})_3$ in $[\text{bmpyr}][\text{Tf}_2\text{N}]$, the solid

[bmpyr]₂[Eu(Tf₂N)₅], and the RTIL [bmim]₂[EuTf₂N)₅]? The hypersensitive ⁵D₀→⁷F₄ transition of europium gives information on the local surrounding of the luminescent centre and allows to compare the modes of coordination on the europium-ion. The spectra were measured of a solution of Eu(Tf₂N)₃/[bmpyr][Tf₂N], pure [bmpyr]₂[Eu(Tf₂N)₅] and pure [bmim]₂[EuTf₂N)₅]. All spectra show the most intense ⁵D₀→⁷F₄ transition at 622 nm (data not shown). The regions between 670-720 nm are displayed in Fig 9.

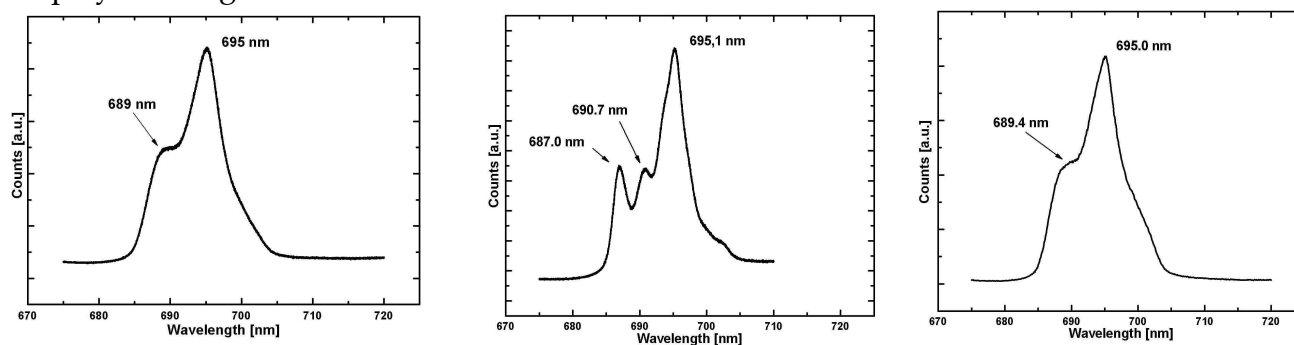


Fig. 9: Hypersensitive transition of Eu³⁺ in a solution of Eu(Tf₂N)₃ in [bmpyr][Tf₂N] (left), [bmpyr]₂[Eu(Tf₂N)₅] (middle) and [bmim]₂[Eu(Tf₂N)₅] (right)

The RTIL [bmim]₂[EuTf₂N)₅] exhibits a similar hypersensitive transition as a solution of Eu(Tf₂N)₃ in [bmpyr][Tf₂N] does. The maximum is located at 695 nm and there is a shoulder at 689 nm which overlaps with the main peak. In the solid [bmpyr]₂[Eu(Tf₂N)₅], the main peak is also located at 695 nm. The peak at lower energy is split in two shoulders, which have their maxima at 687 and 690 nm. This differs significantly from the constitution of the other peaks and indicates a different local surrounding compared to the other two samples. It appears that it is not only the better resolution of the solid-state measurement which makes the two shoulder-peaks appear: at 689 nm, where the maximum of the liquid samples are located, the solid sample exhibits a minimum. Therefore it can be concluded that the Eu³⁺ coordination in [bmim]₂[Eu(Tf₂N)₅] and in solutions of Eu³⁺ in [bmpyr][Tf₂N] is similar (C.N. 9.8 ± 20%), while in the solid compound the europium shows a nine fold coordination by oxygen-atoms, one ligand only coordinating monodentate. One possible explanation of these difference could be

the monodentate ligand binding in a chelating mode to the metal-centre, when the $[\text{Eu}(\text{Tf}_2\text{N})_5]^{2-}$ moiety is more flexible (liquid state, dissolved state) and all five ligands can bind in a chelating mode. In the solid state, there appears not to be enough space around the Eu^{3+} to accommodate five $[\text{Tf}_2\text{N}]$ -units in a chelating fashion.

3.5 Ligand exchange reactions

By adding $[\text{bmpyr}][\text{OTf}]$, which is a RTIL, to the system $\text{Yb}(\text{Tf}_2\text{N})_3 - [\text{bmpyr}][\text{Tf}_2\text{N}]$, ligand exchange is evidenced by the formation of the compound $[\text{bmpyr}]_4[\text{Yb}(\text{OTf})_6][\text{Tf}_2\text{N}]$. Consequentially the compound $[\text{bmpyr}]_3[\text{Yb}(\text{OTf})_6]$ is synthesized, a homoleptic rare-earth triflate compound. Attempts to synthesize the analogue europium-compound in order to elucidate its structure by single-XRD presumably failed as a result of the polymeric nature of the formed compounds. However, ligand exchange could be evidenced by electrochemical methods in solution. Further, the possible combinations of solutions of $\text{Eu}(\text{Tf}_2\text{N})_3$, $\text{Eu}(\text{OTf})_3$, $\text{Yb}(\text{Tf}_2\text{N})_3$, $\text{Yb}(\text{OTf})_3$ in the ionic liquids $[\text{bmpyr}][\text{OTf}]$ and $[\text{bmpyr}][\text{Tf}_2\text{N}]$ were investigated by electrochemical methods.

3.5.1 Structural investigations

By dissolving $\text{Yb}(\text{Tf}_2\text{N})_3$ in $[\text{bmpyr}][\text{OTf}]$ a compound with the composition $[\text{bmpyr}]_4[\text{Yb}(\text{OTf})_6][\text{Tf}_2\text{N}]$ was crystallized. Single crystal structure determination shows the Yb-atom to be coordinated octahedrally by triflate-anion. The $[\text{Tf}_2\text{N}]$ -anion is incorporated in the structure in a non-coordinating manner (cf. Fig. 10, circled). The structure suffers from disorder (cf. Table 2, right); therefore bond lengths and distances are not discussed further. Nevertheless the connectivities are well determined and the asymmetric unit reveals that all $[\text{Tf}_2\text{N}]$ -ligands within the coordination sphere of Yb^{3+} are displaced by $[\text{OTf}]$.

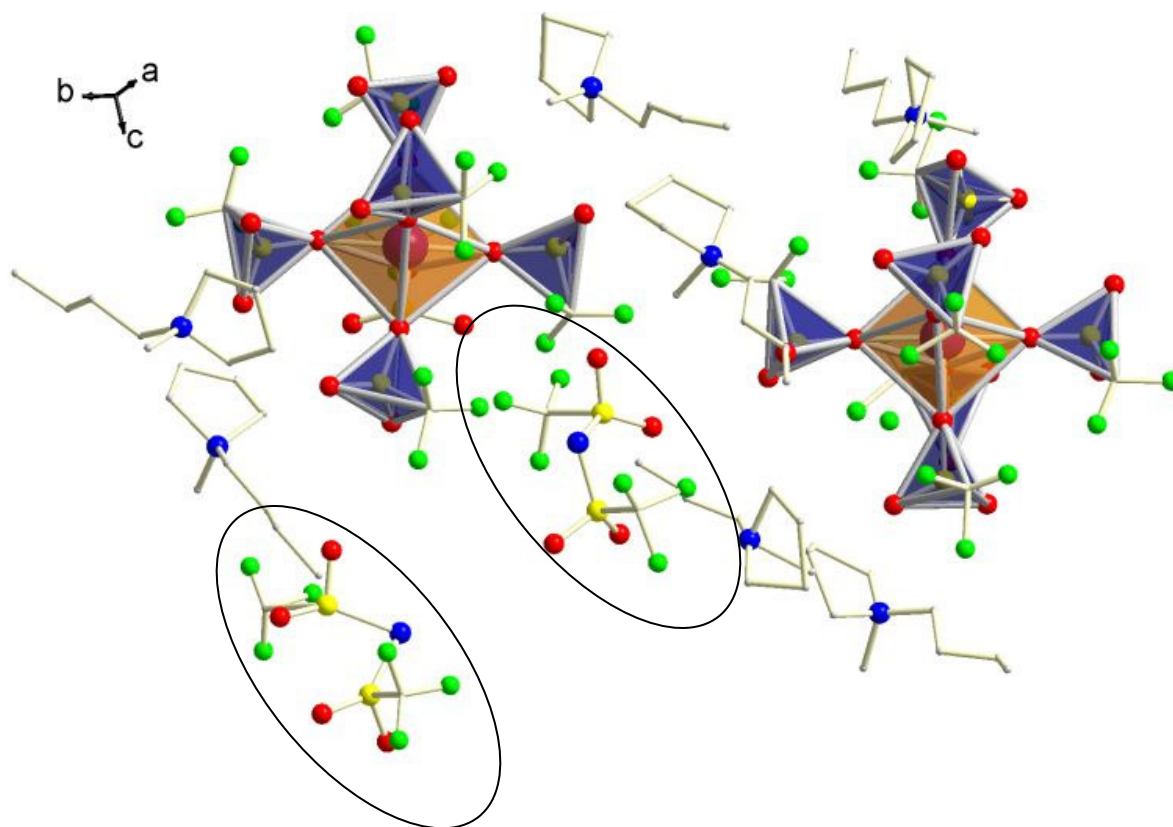


Fig. 10: Asymmetric unit of $[\text{bmpyr}]_4[\text{Yb}(\text{OTf})_6][\text{Tf}_2\text{N}]$

In order to obtain more reliable data of the triflate coordination on Yb^{3+} , the $[\text{Tf}_2\text{N}]$ -free compound $[\text{bmpyr}]_3[\text{Yb}(\text{OTf})_6]$ was synthesized from $\text{Yb}(\text{OTf})_3$ and $[\text{bmpyr}][\text{OTf}]$. From single crystal data (cf. Table 2) it is evidenced, that the structure is very similar to $[\text{bmpyr}]_4[\text{Yb}(\text{OTf})_6][\text{Tf}_2\text{N}]$. The compound $[\text{bmpyr}]_3[\text{Yb}(\text{OTf})_6]$ crystallizes in the

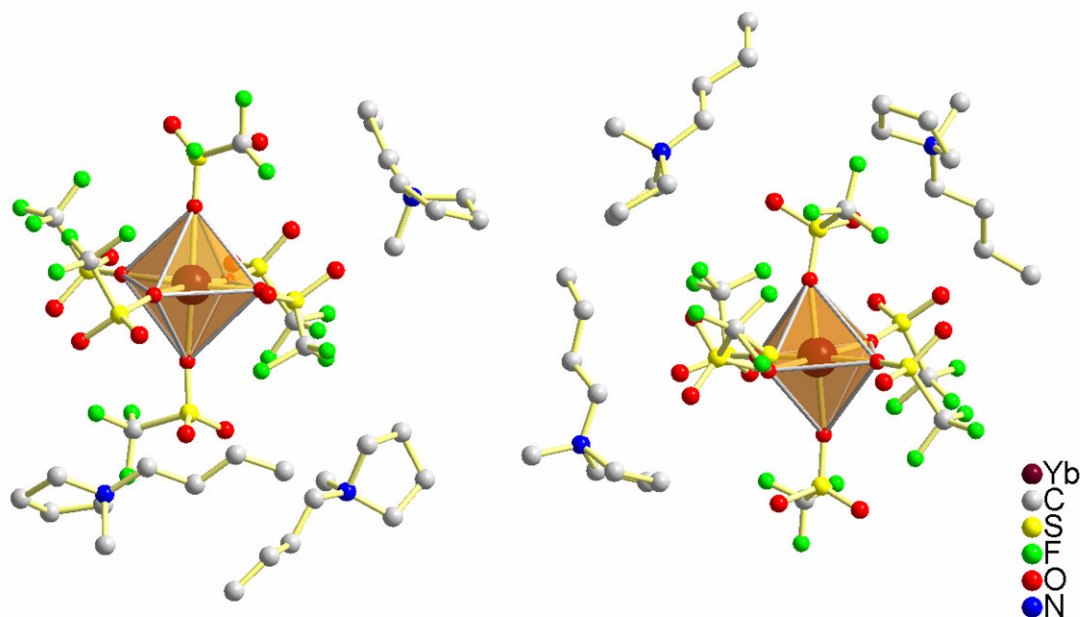


Fig. 11: Asymmetric unit of $[\text{bmpyr}]_3[\text{Yb}(\text{OTf})_6]$

monoclinic spacegroup $P2_1/c$ with four formula units in the unit cell. The asymmetric unit consist of two $[\text{Yb}(\text{OTf})_6]^{3-}$ units which are surrounded by $[\text{bmpyr}]$ cations (see. Fig. 5). All $[\text{OTf}]$ -ligands coordinate monodentately in a non-bridging fashion which yields to isolated octahedra, embedded in a $[\text{bmypr}]$ -matrix. The triflate anions are all-trans arranged – in a way that steric repulsion in minimized (see. Fig 6). In the equatorial positions, the CF_3 -groups are directed in opposite directions in way, that the trans-regiochemistry is also realized with the axial CF_3 -groups.

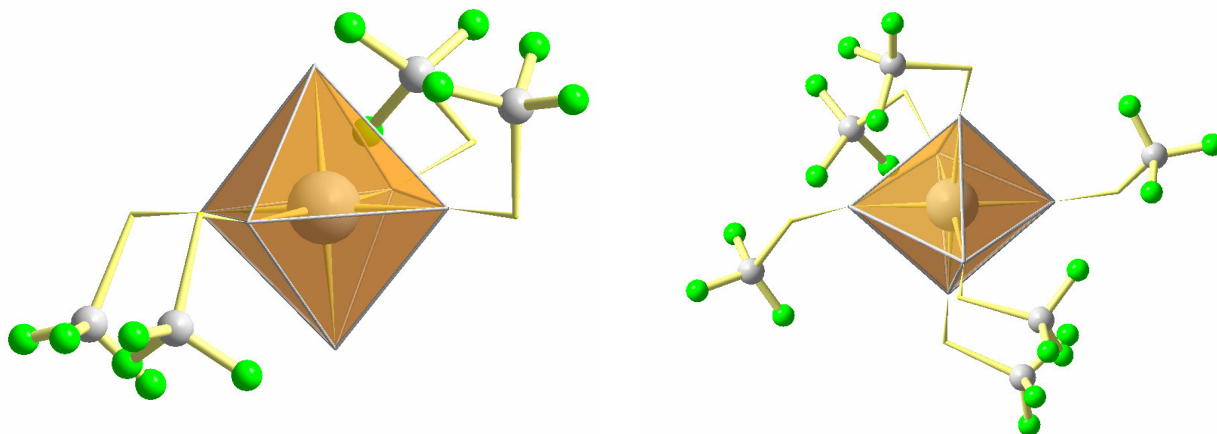


Fig. 12: All-trans conformation of the triflate-groups in $[\text{Yb}(\text{OTf})_6]^{3-}$

The Yb-O distances are in a range of 215.7(7) – 219.5(7) pm for Yb(1) and 216.7(7) – 219.3(6) for Yb(2). These values are in agreement with the sum of ionic radii according to Shannon [9] and significantly shorter than observed in $[\text{bmpyr}][\text{Yb}(\text{Tf}_2\text{N})_5]$ (cf. Tab 5). The S-O bond distances of the coordinating oxygen-atoms are slightly elongated (145 pm in average) in contrast to the “free” oxygen atoms (see Table 4). The triflate-anion is known as a weakly basic anion (weakly coordinating) and is suggested to be used as a substitute for perchlorate-anions whenever possible [10]. The $[\text{Tf}_2\text{N}]$ anion is also known as a weakly coordinating anion, therefore it is of interest which is anion is the less basic one. It is possible to measure the lewis-basicity, or donor-number, of a donor molecule by electrochemical methods. This will be described in the next paragraph.

Table 6: Crystallographic details for [bmpyr]₃[Yb(OTf)₆] and [bmpyr]₄[Yb(OTf)₆][Tf₂N]

	[bmpyr] ₃ [Yb(OTf) ₆]	[bmpyr] ₄ [Yb(OTf) ₆][Tf ₂ N]
Empirical formula	Yb ₂ S ₁₂ F ₃₆ O ₃₆ N ₆ C ₆₆ H ₁₂₀	Yb ₂ S ₁₄ F ₄₂ O ₄₀ N ₈ C ₇₇ H ₁₄₀
Formula weight	2988.49	3410.90
Crystal system	monoclinic	monoclinic
Space group	<i>P2₁/c</i> (no. 14)	<i>P2₁/c</i> (no. 14)
Unit cell dimensions	<i>a</i> = 2539.07(13) pm <i>b</i> = 2027.26(6) pm <i>c</i> = 2472.95(13) pm β = 119.493(4) $^\circ$	<i>a</i> = 2542.0(3) pm <i>b</i> = 2056.78(12) pm <i>c</i> = 2967.3(3) pm β = 91.990(8) $^\circ$
Volume	11489.8(9)·10 ⁶ pm ³	15504(2)·10 ⁶ pm ³
Z	4	4
Absorption coefficient	1.972 mm ⁻¹	0.306 mm ⁻¹
Reflections collected	61158	81633
Independent reflections / <i>R</i> _{int}	15020 / 0.0424	14473 / 0.1484
Absorption correction	numerical	numerical
Data/Parameters	15020 / 1437	14473 / 1727
GooF on <i>F</i> ²	1.063	1.048
Final <i>R</i> indices [<i>I</i> > 2σ(<i>I</i>)]	<i>R</i> ₁ = 0.0568, <i>wR</i> ₂ = 0.1407	<i>R</i> ₁ = 0.0886, <i>wR</i> ₂ = 0.2021
<i>R</i> indices (all data)	<i>R</i> ₁ = 0.0806, <i>wR</i> ₂ = 0.1508	<i>R</i> ₁ = 0.1810, <i>wR</i> ₂ = 0.2352

Table 7 Selected distances (pm) in [bmpyr]₃[Yb(OTf)₆] (disordered atoms are omitted)

Yb(1)-O(40)	215.7(7)	S(10)-O(10)*	144.2(7)	S(100)-O(102)	142.0(9)
Yb(1)-O(50)	217.5(7)	S(30)-O(30)*	141.3(8)	S(100)-O(100)*	145.3(8)
Yb(1)-O(20)	218.3(7)	S(30)-O(31)	140.6(9)	S(200)-O(202)	140.8(9)
Yb(1)-O(30)	218.6(7)	S(30)-O(32)	166.2(9)	S(200)-O(201)	142.8(9)
Yb(1)-O(60)	218.9(7)	S(40)-O(41)	137.0(9)	S(200)-O(200)*	146.3(7)
Yb(1)-O(10)	219.5(7)	S(40)-O(42)	141.7(9)	S(300)-O(301)	140.9(8)
Yb(2)-O(300)	216.7(7)	S(40)-O(40)*	144.1(8)	S(300)-O(302)	142.5(8)
Yb(2)-O(400)	218.1(6)	S(50)-O(52)	141.2(7)	S(300)-O(300)*	144.9(7)
Yb(2)-O(600)	218.3(7)	S(50)-O(51)	141.4(8)	S(400)-O(401)	129.4(9)
Yb(2)-O(200)	219.0(6)	S(50)-O(50)*	144.4(8)	S(400)-O(400)*	142.7(7)
Yb(2)-O(100)	219.1(7)	S(60)-O(62)	137.1(9)	S(400)-O(402)	146.4(9)
Yb(2)-O(500)	219.3(6)	S(60)-O(60)*	145.8(8)	S(600)-O(601)	141.4(7)
S(10)-O(12)	141.4(7)	S(60)-O(61)	146.6(9)	S(600)-O(602)	142.2(8)
S(10)-O(11)	142.4(8)	S(100)-O(101)	141.5(8)	S(600)-O(600)*	145.1(7)

*) = oxygen bond to ytterbium

3.5.2 Electrochemical investigations

Figure 13, left side, shows the cyclic voltammograms of a 0.025 M solution of $\text{Yb}(\text{Tf}_2\text{N})_3$ in $[\text{bmpyr}][\text{Tf}_2\text{N}]$. The cathodic peak at -1.21 V is assigned to the reduction of trivalent Ytterbium to the divalent state. The anodic peak at -0.95 V points the back-oxidation to the trivalent state.

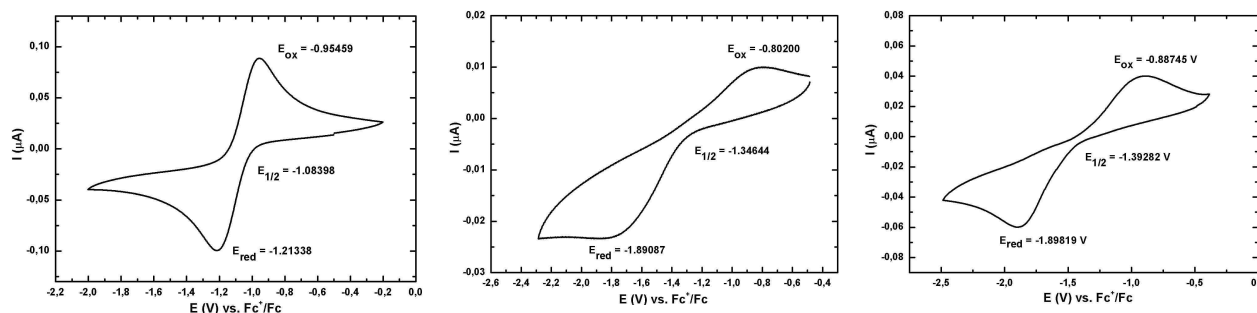


Fig. 13: CV of $\text{Yb}(\text{Tf}_2\text{N})_3/[\text{bmpyr}][\text{Tf}_2\text{N}]$ (left), $\text{Yb}(\text{Tf}_2\text{N})_3/[\text{bmpyr}][\text{OTf}]$ (middle) and $\text{Yb}(\text{OTf})_3/[\text{bmpyr}][\text{OTf}]$ (right)

The separation of the current peaks is 0.26 V and exceeds the theoretical value for a one electron transfer reaction which is electrochemically reversible (58 mV) [11]. Therefore it can be concluded that the electron-transfer is quasireversible or irreversible. If $\text{Yb}(\text{Tf}_2\text{N})_3$ is dissolved in $[\text{bmpyr}][\text{OTf}]$, the reduction peak shifts to more negative values (-1.89 V) and the oxidation peak to more positive (0.80 V). The peak separation is increased (1.09 V) indicating the poor reversibility. By comparing the cyclic voltammogram of $\text{Yb}(\text{Tf}_2\text{N})_3/[\text{bmpyr}][\text{OTf}]$ (middle) with $\text{Yb}(\text{OTf})_3/[\text{bmpyr}][\text{OTf}]$ (left) it strikes that the reduction peaks of the trivalent species are both located at -1.89 V. Also the halfwavepotentials are very similar (-1.35 V, -1.39 V respectively) and differ significantly from the observed one for the pure $[\text{Tf}_2\text{N}]$ -sample (-1.08 V). This observation is in good agreement with the reported structures in 3.5.2: The $[\text{OTf}]$ anion is a stronger donor compared to $[\text{Tf}_2\text{N}]$. It displaces the $[\text{Tf}_2\text{N}]$ ligands and shifts the halfwavepotential towards lower values because of the stronger Lewis basicity.

In case of the Europium-samples, the situation is similar. The pure $[\text{Tf}_2\text{N}]$ -system exhibits a reduction peak at -1.04 V, the back oxidation proceeds at -0.08 V. Again the separation of the peak potentials exceeds the theoretical value for a reversible one elec-

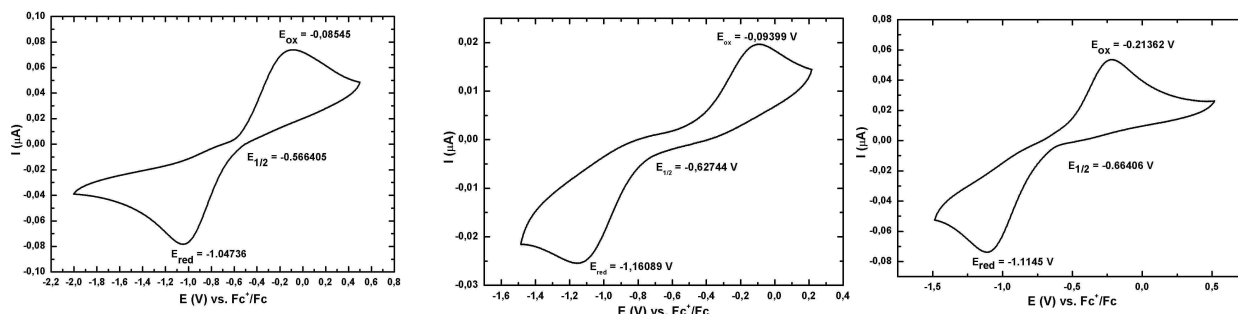


Fig. 14: CV of $\text{Eu}(\text{Tf}_2\text{N})_3/[\text{bmpyr}][\text{Tf}_2\text{N}]$ (left), $\text{Eu}(\text{Tf}_2\text{N})_3/[\text{bmpyr}][\text{OTf}]$ (middle) and $\text{Eu}(\text{OTf})_3/[\text{bmpyr}][\text{OTf}]$ (right)

tron transfers process. By dissolving $\text{Eu}(\text{Tf}_2\text{N})_3$ in $[\text{bmpyr}][\text{OTf}]$ (Fig. 14, middle) a halfwavepotential of -0.63 V is observed, while in the pure $[\text{OTf}]$ -system (right) the halfwavepotential is located at -0.66 V. Again these values are very similar, whereas the first sample (left) shows a lower halfwavepotential at -0.57 V. It can be assumed that in the Europium compounds the $[\text{Tf}_2\text{N}]$ -ligand is also displaced by triflate upon adding $[\text{bmpyr}][\text{OTf}]$. Several attempts to crystallize a Europium-triflate compound failed due to the texture of the composed products. Reactions of $\text{Eu}(\text{Tf}_2\text{N})_3$ with $[\text{bmpyr}][\text{OTf}]$ yielded in jelly-like products, also in the system $\text{Eu}(\text{OTf})_3/[\text{bmpyr}][\text{OTf}]$ with different stoichiometries and temperatures a crystalline phase could not be isolated. From spectroscopical data the formed species could not be identified clearly.

3.6 Literature

- [1] T. Welton, *Chem. Commun.* **2005**, 3, 13.
- [2] T. Timofte, A. Babai, G. Meyer, A.-V. Mudring, *Acta Crystallogr.* **2005**, E61, i94;
T. Timofte, A. Babai, G. Meyer, A.-V. Mudring, *Acta Crystallogr.* **2005**, E61, i87.
- [3] J.C.Plakatouras, C. Kavounis, C.J. Cardin, *Acta Crystallogr.* **2003**, E59, m838;
W.J.Evans, D.G. Giarikos, M.A. Johnston, M.A. Greci, J.W. Ziller, *Dalton Trans.* **2002**, 520; S.R. Drake, A. Lyons, D.J. Otway, D.J. Williams, *Inorg. Chem.* **1994**, **33**, 1230.
- [4] A.-V. Mudring, A. Babai, S. Arenz, R. Giernoth, *Angew. Chem.* **2005**, 117, 5621; *Int. Ed.* **2005**, 44, 5485.
- [5] A. Haas, C. Klare, P. Betz, J. Bruckmann, C. Kruger, Y.-H. Tsay, F. Aubke, *Inorg. Chem.* **1996**, 35, 1918.
- [6] M.D. Danford, J.H. Burns, C.E. Higgins, J.R. Stokely, W.H. Baldwin, *Inorg. Chem.* 1970, 9, 1953; S. Cheng, *Jiegou Huaxue (Chin.) (Chinese J. Struct. Chem.)* **1997**, 16, 371.
- [7] H.L. Ngo, K.Le Compte, L. Hargens, A.B. Mc Ewen, *Thermochim. Acta* **2000**, 357, 97.
- [8] C. Gaillard, I. Billard, A. Chaumont, S. Mekki, A. Ouadi, M.A. Denecke, G. Moutiers, G. Wipf, *Inorg. Chem.* **2006**, 44, 8355.
- [9] R.D. Shannon, *Acta Crystallogr.* **1976**, A32, 751.
- [10] *Inorg. Chem.*, **2006**, 45, 20A.
- [11] J. Heinze, *Angew. Chem.* **1984**, 96, 823.

III. Divalent (pseudo) rare-earth compounds in ILs

1. YbI₂ in Tf₂N-based ionic liquids

1.1 Introduction

The electrochemical data in II-3.5.2 indicate, that divalent rare-earth species should be stable in [OTf] and [Tf₂N]-based ionic liquids. Especially the CV of Yb(Tf₂N)₃/[bmpyr][Tf₂N] shows the least irreversible reaction Yb(III) + e⁻ → Yb(II) and it can be assumed that there is no onward-reaction of the divalent species which is generated at the working-electrode. Therefore a metathesis strategy for characterizing the divalent species in [Tf₂N]-types of ionic liquids was acquired. In principle, there are two possibilities of obtaining a divalent Yb-species in [bmpyr][Tf₂N]. Either a trivalent species is dissolved and afterwards reduced to the divalent, or a divalent species is directly used as an educt. In order to keep the number of components in the ionic liquids as low as possible, the latter procedure was utilized. Ytterbiumdiodide is readily available from YbI₃ by subliming the solid at 800°C in high-vacuum [1]. By dissolving the compound in [bmpyr][Tf₂N], the iodides are displaced by the [Tf₂N]-anions and a colorless compound crystallizes after oversaturation. This compound could not be examined by XRD, since the crystals suffered from twinning and were of bad quality. By slightly changing the cationic structure of the ionic liquid and displacing the butyl chain by a propyl-chain – crystals of sufficient quality could be grown to analyse the compound by single-XRD. According to the equation



a homoleptic divalent rare-earth ionic liquid compound is composed.

1.2 Preparation

YbI₂ was prepared from the respective amounts of the elements which were placed in a silica tube that was sealed off under vacuum and subsequently heated for 30 h at 200 °C. The crude product (purple YbI₃) was sublimed under high vacuum at 800°C to give bright yellow YbI₂.

[mppyr][Tf₂N] was synthesized as described before (cf. I, 1.2)

[mppyr]₂[Yb(Tf₂N)₄]: The reaction of YbI₂ (0.2 mmol, 87 mg) with [mppyr][Tf₂N] (4.8 mmol, 1 g) was carried out in an evacuated and sealed silica tube at 393K for 48 h.

Colorless single crystals of [mppyr]₂[Yb(Tf₂N)₄] form as the single, insoluble product after subsequent cooling (2 K/min) to room temperature. The product was separated by filtration. Estimated yield: 66%; melting point: 107°C; IR (KBr): 1473(s), 1433(s), 1352(vs), 1331(vs), 1231(vs), 1197(vs), 1144(vs), 1058(vs), 972(w), 940(w), 797(m), 763(w), 742(m), 652(s), 618(s), 608(s), 599(s), 574(s), 515(s) cm⁻¹

1.3 Structural aspects

The title compound crystallizes in the monoclinic space group $P2_1/n$ with four formula units in the unit cell. The asymmetric unit of the crystal structure shows Yb(II) being coordinated by four Tf₂N⁻ anions (Figure 1, left) and two cations of the ionic liquid to compensate the charge. The coordination by Tf₂N⁻ is accomplished through the oxygen-atoms. The Yb atom is surrounded by eight oxygen atoms forming a distorted square antiprism (Figure 1, right). The cations surround the anionic [Yb(Tf₂N)₄]²⁻ units ($d(\text{N}(5)\text{--}\text{N}(3)) = 473.3$ pm, $d(\text{N}(5)\text{--}\text{N}(4)) = 631.0$ pm; $d(\text{N}(6)\text{--}\text{N}(1)) = 625.3$ pm, $d(\text{N}(6)\text{--}\text{N}(2)) = 453.4$ pm) (Figure 2) forming a honeycomb-like structure.

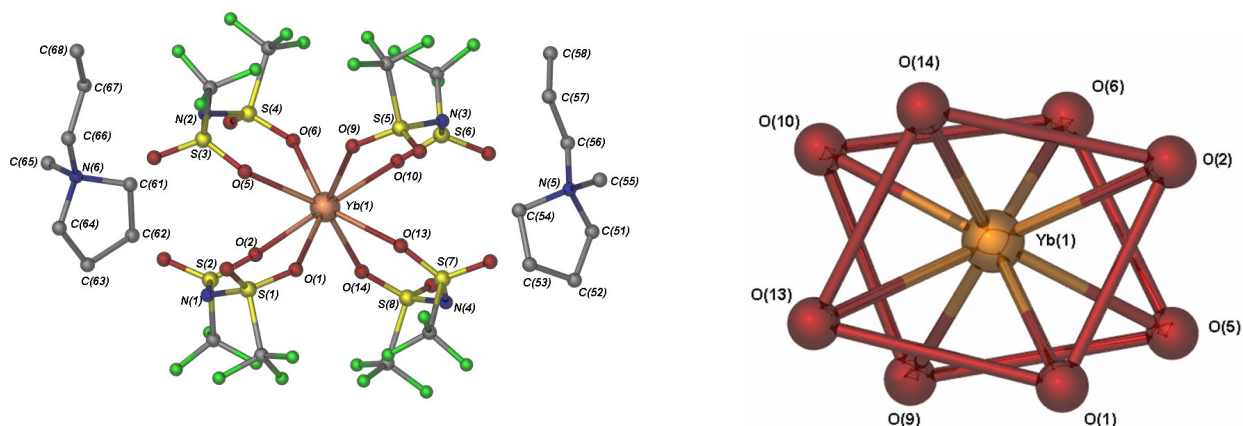


Fig. 1: Molecular structure of [mppyr]₂[Yb(Tf₂N)₄] (left) and first coordination sphere of Yb(II) (right)

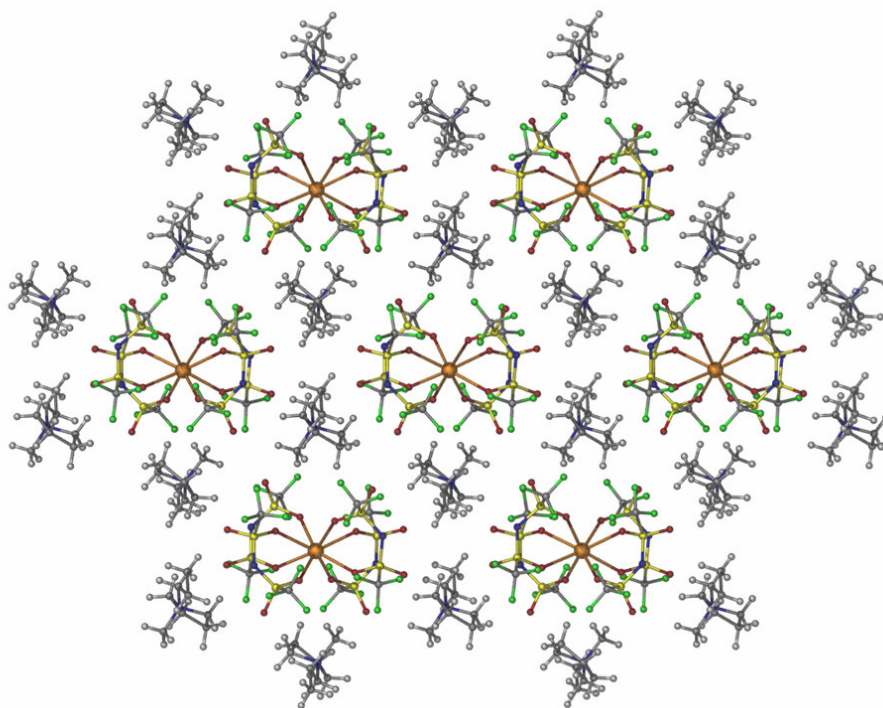


Fig. 2: Crystal structure of [mppyr]₂[Yb(Tf₂N)₄], view along b-axis

The Y-O distances range from 241.0 to 251.7 pm, the latter being assumably the so far largest observed Yb(II)-O bonding distance. In aryloxo-ytterbium complexes, distances of 210-217 pm are found, Yb-O distances with bridging aryloxo-ligands lie in the range of 224-234 pm [2]. With the neutral THF (tetrahydrofuran) as a ligand Yb-O distances of 238-239 pm are reported for [Yb(THF)₆]²⁺ [3]. Unfortunately there are no structural data

for Yb(II)-1,3-diketone complexes available for comparison. Considering that the ionic radius of eightfold coordinate Yb²⁺ corresponds to the one for eightfold coordinated La³⁺ one might compare the average Yb-O distance of 246.1 pm in [mppyr]₂[Yb(Tf₂N)₄] to *d*(La-O) of 247 found for [La(acac)₃(H₂O)₂] [4].

Surprisingly, all the ligands show a *cisoid*-conformation with respect to the –CF₃ groups, which pinches the [Yb(Tf₂N)₄]²⁻ antiprisms along the crystallographic *b*-axis (Figure 2). This is in contrast to the coordination modes in the trivalent compounds. The free acid [Tf₂N]H (i.e. (CF₃SO₂)₂NH) crystallizes with the –CF₃ groups being *transoid*-oriented towards each other.[5] The corresponding base [Tf₂N] (i.e. (CF₃SO₂)₂N⁻) prefers the *transoid*-conformation as well in the absence of suitable coordination centers [6, 7]. This observation is backed by theoretical calculations (*transoid*-[Tf₂N]H is about 8 kJ/mol more stable than *cisoid*-[Tf₂N]H, *transoid*-[Tf₂N⁻] compared to *cisoid*-[Tf₂N⁻] about 4 kJ/mol) [7 m]). There from it can be concluded that the *cisoid*-conformation of the [Tf₂N]-anion in [mppyr][Tf₂N] is decisively determined by Yb-[Tf₂N] interactions. As a result of the very weak interaction between the metal center and the oxygen atoms, the average S-O distances of the sulfur-oxygen bond [144.3 pm (coordinating oxygen atoms) and 141.6 pm (non coordinating oxygen atoms)] are only slightly affected upon coordination to Yb²⁺ – even when compared to the neutral amine (*d*(S-O) = 140.1 pm and 141.7 pm) [8].

Table 8 Selected distances and angles in [mppyr]₂[Yb(Tf₂N)₄]

Yb(1)-O(1)	242.1(3)	S(1)-O(1)	144.5(3)	S(1)-N(1)	156.3(4)	S(5)-O(9)	145.0(3)
Yb(1)-O(2)	247.6(3)	S(1)-O(3)	142.1(4)	S(2)-N(1)	156.4(4)	S(5)-O(11)	141.6(3)
Yb(1)-O(5)	251.7(3)	S(2)-O(2)	144.3(3)	S(3)-N(2)	156.5(4)	S(6)-O(10)	144.1(3)
Yb(1)-O(6)	243.5(3)	S(2)-O(4)	141.9(3)	S(4)-N(2)	156.7(4)	S(6)-O(12)	141.5(4)
Yb(1)-O(9)	241.0(3)	S(3)-O(5)	143.9(3)	S(5)-N(3)	156.8(4)	S(7)-O(13)	143.6(3)
Yb(1)-O(10)	247.0(3)	S(3)-O(7)	142.0(3)	S(6)-N(3)	155.8(4)	S(7)-O(15)	141.7(3)
Yb(1)-O(13)	250.2(3)	S(4)-O(6)	144.7(3)	S(7)-N(4)	156.2(4)	S(8)-O(14)	144.1(3)
Yb(1)-O(14)	245.6(3)	S(4)-O(8)	140.5(4)	S(8)-N(4)	156.8(4)	S(8)-O(16)	141.8(4)

Table 9 Crystallographic and refinement details for [mppyr]₂[Yb(Tf₂N)₄]

	[mppyr] ₂ [Yb(Tf ₂ N) ₄]
Empirical formula	C ₂₄ H ₃₆ YbF ₂₄ N ₆ O ₁₆ S ₈

Formula weight	1550.11
Crystal system	monoclinic
Space group	$P2_1/n$ (no. 14)
Unit cell dimensions	$a = 1122.01(4)$ pm $b = 2260.21(9)$ pm $c = 2188.47(9)$ pm $\beta = 102.209(3)^\circ$
Volume	$5.4244(4)$ nm ³
Z	4
Density (calculated)	1.8978
Absorption coefficient	2.177 mm ⁻¹
Reflections collected	56375
Independent reflections / R_{int}	11822 / 0.1138
Absorption correction	numerical
T_{max} / T_{min}	0.4976 / 0.2904
Parameters	316
Goof on F^2	0.963
Final R indices [$I > 2\sigma(I)$]	$R_1 = 0.046$, $wR_2 = 0.105$
R indices (all data)	$R_1 = 0.0654$, $wR_2 = 0.1136$

1.4 Literature

- [1] G. Meyer, *Chem. Rev.* **1988**, *88*, 93; J.D Corbett, *Inorg. Synth.* **1983**, *22*, 31.; G. Meyer, in: *Synthesis of Lanthanide and Actinide Compounds* (G. Meyer, L.R. Morss, eds.), Kluwer Acad. Publ., Dordrecht/NL **1991**, 135.
- [2] G.B. Deacon, C.M. Forsyth, P.C. Junk, B.W. Skelton, A. White, *Chem. Eur. J.* **1999**, *5*, 1452.
- [3] C.E. Plečnik, S. Liu, J. Liu, X. Chen, E.A. Meyers, S. G. Shore, *Inorg. Chem.* **2002**, *41*, 4936.
- [4] T. Phillips, D.E. Sands, W.F. Wagner, *Inorg. Chem.* **1968**, *7*, 2295.
- [5] A. Haas, C. Klare, P. Betz, J. Bruckmann, C. Kruger, Y.-H. Tsay, F. Aubke, *Inorg. Chem.* **1996**, *35*, 1918.
- [6] Crystal structures purely organic: J.J. Golding, D.R. MacFarlane, L. Spiccia, M. Forsyth, B.W. Skelton, A.H. White, *Chem. Commun.* **1998**, *15*, 1593;
V. Montanari, D.D. DesMareteau, W.T. Pennigton, *J. Mol. Struct.* **2000**, *550/551*, 337;

- C.M. Forsyth, D.R. MacFarlane, J.J. Golding, J. Huang, J. Sun, M. Forsyth, *Chem. Mater.* **2002**, *14*, 2103; J.A. Schlueter, U. Geiser, H.H. Wang, A.M. Kini, B.H. Ward, J.P. Parakka, R.G. Daugherty, M.E. Kelly, P.G. Nixon, R.W. Winter, G.L. Gard, L.K. Montgomery, H.-J. Koo, M.-H. Whangbo, *J. Solid State Chem.* **2002**, *168*, 524; M.G. Davidson, P.R. Raithby, A.L. Johnson, P.D. Bolton, *Eur. J. Inorg. Chem.* **2003**, 3445; D.D. DesMarteau, W.T. Pennington, V. Montanari, B.H. Thomas, *J. Fluorine Chem.* **2003**, *122*, 57; J.D. Holbrey, W.M. Reichert, R.D. Rogers, *Dalton Trans.* **2004**, 2267.
- [7] Crystal structures of metal-[Tf₂N] compounds: J.L. Nowinski, P. Lightfoot, P.G. Bruce, *J. Mater. Chem.* **1994**, *4*, 1579; A. Haas, C. Klare, P. Betz, J. Bruckmann, C. Kruger, Y.-H. Tsay, F. Aubke, *Inorg. Chem.* **1996**, *35*, 1918; L. Xue, C.W. Padgett, D.D. DesMareau, W.T. Pennington, *Solid State Sci.* **2002**, *4*, 1535; D. Brouillette, D.E. Irish, N.J. Taylor, G. Perron, M. Odziemkowski, J.E. Desnoyers, *PCCP* **2002**, *4*, 6063; Z. Zak, A. Ruzicka, *Z. Kristallogr.* **1998**, *213*, 217; M.G. Davidson, P.R. Raithby, A.L. Johnson, P.D. Bolton, *Eur. J. Inorg. Chem.* **2003**, 3445; L. Xue, C.W. Padgett, D.D. DesMarteau, W.T. Pennington, *Acta Crystallogr.* **2004**, *C60*, m200; L. Xue, D.D. DesMarteau, W.T. Pennington, *Solid State Sci.* **2005**, *7*, 311; D.D. DesMarteau et al., CCDC247563, private communication; A. Babai, A.-V. Mudring, *J. Alloys Comp.* **2006**, *418*, 122; A. Babai, A.-V. Mudring, *Chem. Mat.* **2005**, *17*, 6230; A. Babai, A.-V. Mudring, *Inorg. Chem.* **2006**, *45*, 3249; A. Babai, A.-V. Mudring, *Dalton Trans.* **2006**, 1828; A.-V. Mudring, A. Babai, S. Arenz, R. Giernoth *Angew. Chem.* **2005**, *117*, 5621; *Angew. Chem. Int. Ed.* **2005**, *44*, 5485.
- [8] A. Haas, C. Klare, P. Betz, J. Bruckmann, C. Kruger, Y.-H. Tsay, F. Aubke, *Inorg. Chem.* **1996**, *35*, 1918.

2. SmI_2 and NdI_2 in $[\text{S}(\text{Et})_3][\text{Tf}_2\text{N}]$

2.1 Introduction

It has been well established that the redox potentials of divalent rare earth cations cover a wide range and can reach values similar to alkali metals [1, 2]. Particularly, investigations on the reactivity of SmI_2 in different ionic liquids are of eminent interest as SmI_2 , the so-called Kagan reagent, is one of the most versatile reduction reagents used in organic chemistry [3]. As shown in chapter 1.1 it is possible to stabilize divalent Ytterbium in the ionic liquid $[\text{mppy}][\text{Tf}_2\text{N}]$. SmI_2 dissolves in this ionic liquid to giving a deep-red, long-time stable solution which was evidenced by UV-spectroscopy (see appendix 2). In contrast, a solution of SmI_2 (as well as a solution of NdI_2) in the sulfonium-based ionic liquid $[\text{SEt}_3][\text{Tf}_2\text{N}]$ leads to the reduction of the cation of the ionic liquid. The ionic liquid decomposes to a dark brown liquid of higher viscosity and evolves a smell reminiscent of garlic when exposed to the atmosphere [4]. In order to determine the product of decomposition on the side of the rare earth cation the respective rare earth diiodides, LnI_2 , $\text{Ln} = \text{Nd}, \text{Sm}$ were reacted with $[\text{SEt}_3][\text{Tf}_2\text{N}]$ at elevated temperatures. After slow cooling the reaction mixture to room temperature crystals of sufficient quality for single crystal X-ray structure analysis were obtained, which were identified as the trivalent compounds $[\text{S}(\text{Et})_3]_3[\text{LnI}_6]$ $\text{Ln} = \text{Sm}, \text{Nd}$.

2.2 Preparation

$[\text{SEt}_3][\text{Tf}_2\text{N}]$ was prepared from $[\text{S}(\text{Et})_3]\text{I}$ and $\text{Li}[\text{Tf}_2\text{N}]$ following the procedure described in 1.2.

LnI_2 ($\text{Ln} = \text{Sm}, \text{Nd}$) was prepared by reduction of LnI_3 with the corresponding Ln metal in a sealed tantalum container, jacketed with an evacuated silica tube. LnI_3 was prepared from metal and iodine according to the procedure described in the literature [5].

[SEt₃]₃[LnI₆]: The reaction of LnI₂ (0.22 mmol, ~ 88 mg) with [SEt₃][Tf₂N] (1.8 mmol, 0.73g, 0.5 ml) was carried out in an evacuated and sealed silica tube at 393 K for 12 h. Yellow (Sm) and pale green (Nd) single crystals of [SEt₃]₃[LnI₆] form as an insoluble product after subsequent cooling (2 K/min) to room temperature. The product was separated by filtration. Estimated yields: ~15%.

2.3 Structural aspects

The structures of the isotopic compounds [SEt₃]₃[LnI₆], Ln = Nd, Sm (Fig. 1) are characterized by nearly ideal [LnI₆]³⁻ octahedra. The mean interatomic distances of $d(\text{Nd-I}) = 311$ pm and $d(\text{Sm-I}) = 309$ pm are well in the expected range and reflect the radii contraction along the series of trivalent rare earth cations.

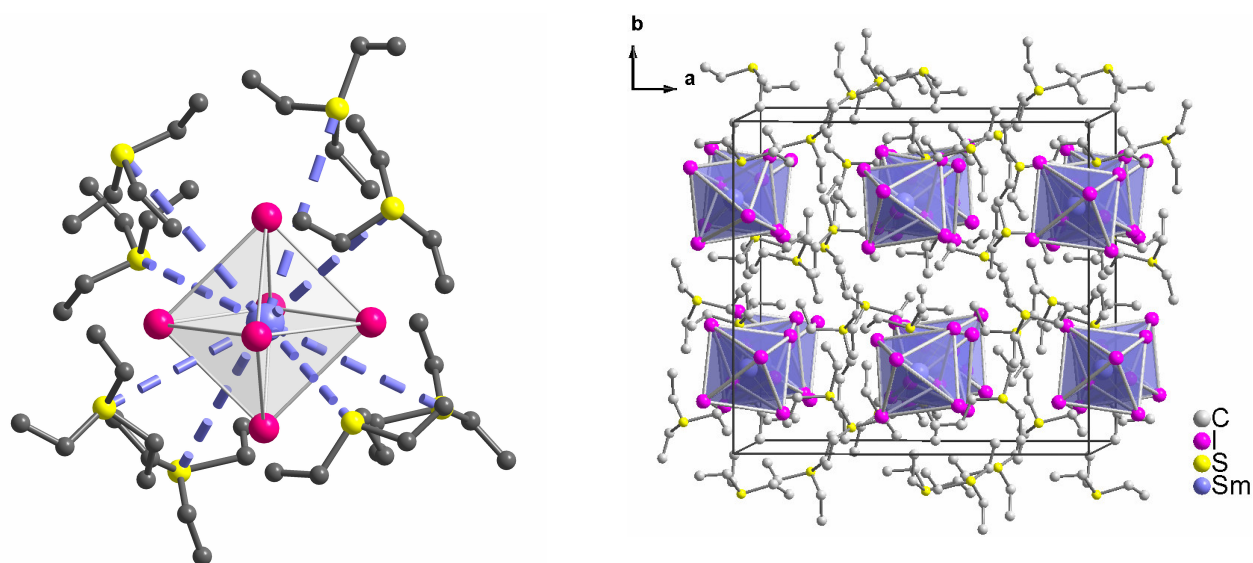


Fig 1: Coordination sphere of Sm³⁺ (left) and crystal structure (right) in [S(Et)₃][LnI₆]

Especially noteworthy is the second coordination sphere of the rare earth cations. Each of the triangular faces of the [LnI₆]³⁻ octahedron is capped by a triethylsulfonium cation leading to the formation of a (distorted) cube (Fig. 2). This structural feature has already been predicted by molecular dynamic studies to occur for [LnCl₆]³⁻ in imidazolium ionic liquids [6] and has been observed in compounds obtained from the ionic liquid

[mppyr][Tf₂N] (mppyr = 1-methyl-1-propylpyrrolidinium) [7]. A similar structural motif has recently been found for [PF₆]⁻ in the ionic liquid [dmim][PF₆] (dmim = 1,3-dimethylimidazolium) [8]. Therefrom the general conclusion can be drawn that for anionic octahedral units as [MX₆]⁻ a second coordination sphere of a cube of cations (of the ionic liquid) is a common structural feature.

Table 10: Crystallographic details for [SEt₃]₃[LnI₆], Ln = Nd, Sm

	[SEt ₃] ₃ [NdI ₆]	[SEt ₃] ₃ [SmI ₆]
Empirical formula	S ₃ C ₉ H ₄₅ NdI ₆	S ₃ C ₉ H ₄₅ SmI ₆
Formula weight	1251.3	1257.4
Crystal system	orthorhombic	orthorhombic
Space group	<i>Pbca</i> (no. 61)	<i>Pbca</i> (no. 61)
Unit cell dimensions	<i>a</i> = 1942.6(2) pm <i>b</i> = 1816.3(3) pm <i>c</i> = 2143.5(4) pm	<i>a</i> = 1936.8(1) pm <i>b</i> = 1807.07(7) pm <i>c</i> = 2116.47(8) pm
Volume	7563.1(2) · 10 ⁶ pm ³	7407.47(6) · 10 ⁶ pm ³
Z	8	8
Absorption coefficient	6.442 mm ⁻¹	6.761 mm ⁻¹
Reflections collected	71340	79255
Independent reflections / <i>R</i> _{int}	8902 / 0.404	8117 / 0.101
Absorption correction	numerical	numerical
Data/Parameters	8902 / 163	8117 / 263
GooF on <i>F</i> ²	0.572	0.946
Final <i>R</i> indices [<i>I</i> > 2σ(<i>I</i>)]	<i>R</i> ₁ = 0.0926, w <i>R</i> ₂ = 0.1589	<i>R</i> ₁ = 0.0511, w <i>R</i> ₂ = 0.0765
<i>R</i> indices (all data)	<i>R</i> ₁ = 0.4693, w <i>R</i> ₂ = 0.3147	<i>R</i> ₁ = 0.0906, w <i>R</i> ₂ = 0.0842

The high conformational flexibility of the triethylsulfonium cation, which on one hand is a prerequisite for a cation of an ionic liquid becomes a crucial problem when trying to get crystals of sufficient quality for X-ray structure analysis. As already been noted for the Tf₂N⁻ anion conformational flexibility and well shielded or delocalized charge often leads to strong disorder in the crystal. However, in the case of [SEt₃]₃[NdI₆] we were able to obtain high quality crystals, which allowed not only positioning of the cations, but also their anisotropic refinement and even refinement of hydrogen positions after the riding model. Thus, the structure of the triethylsulfonium cation could be determined reliably. Awareness has to be drawn to the fact that the cation is far from being planar as

it has been mentioned occasionally in the literature [9, 10] but shows a strong tetrahedralization at the central sulfur atom with S-C bonding angles of about 101°.

2.4 Literature

- [1] G. Meyer, *Chem. Rev.* **1988**, *88*, 93.
- [2] L. Morss in *Handbook of the Physics and Chemistry of Rare Earth* (K.A. Gschneidner, L. Eyring, G.R. Choppin and G. H. Lander, Eds.) **1994**, Vol. 8, Chapter 122; P. Strange, A. Svane, W.M. Temmermann, Z. Szotek and H. Winter, *Nature* **1999**, *399*, 756.
- [3] M.B. Smith, J. March (Eds), *March's Advanced Organic Chemistry: Reactions, Mechanisms, and Structure*, Wiley Interscience, **2001**; H.B. Kagan, *New J. Chem.* **1990**, 14.
- [4] So far the exact identity of the decomposition products, which is of a complex nature is not determined. Reduction of the triethylsulfonium cation apparently leads to cleavage of the S-C bond and subsequent polymerization. When exposed to atmosphere hydrolysis takes place and sulfanes are formed.
- [5] J.D. Corbett, *Inorg. Synth.* **1983**, *22*, 31; G. Meyer in *Synthesis of Lanthanide and Actinide Compounds* (G. Meyer, L. Morss, Eds.), Kluwer Acad. Publ. Dordrecht /NL, **1991**, 135.
- [6] A. Chaumont, G. Wipff, *J. Phys. Chem. B* **2004**, *108*, 3311.
- [7] A. Babai, A.-V. Mudring, *J. Alloys Comp.* **2006**, *418*, 122.
- [8] Ch. Hardacre, S.E.J. McMath, M. Niewenhuyzen, D.T. Bowron, A.K. Soper, *J. Phys.: Condens. Matter* **2003**, *15*, 159.
- [9] H. Stegemann, A. Rode, A. Reiche, A. Schnittke and H. Füllbier, *Electrochim. Acta*, **1990**, *37*, 379; H. Paulsson, A. Hagfeldt, L. Kloo, *J. Phys. Chem. B*, **2003**, *107*, 13665;

H. Paulsson, M. Berggrund, E. Vantesson, A. Hagfeldt, L. Kloo, *Solar Engergy Mat. and Solar Cells*, **2004**, 82, 345; X.Li, K.E. Johnson, *Can. J. Chem.* **2004**, 82, 491.

[10] H. Matsumoto, T. Matsuda and Y. Miyazaki, *Chem. Lett.* **2000**, 1430.

3. Alkaline-earth diiodides in [mppy_r][Tf₂N]

3.1 Introduction

In order to elucidate the behavior of simple salts of divalent rare-earth metals in Tf₂N-based RTILs the interaction of alkaline earth iodides AEI₂ (AE = Ca, Sr and Ba) with the ionic liquid [mppy_r][Tf₂N] is investigated. As mentioned in the last chapter is possible to stabilize divalent ytterbium and samarium compounds in [mppy_r][Tf₂N]. The ytterbium-complex [mppy_r]₂[Yb(Tf₂N)₄] is characterized by single-XRD. The samarium-species did not crystallize under similar conditions, and variation of the cation of the ionic liquid leads to oxidation of Sm²⁺ to Sm³⁺ in [S(Et)₃][SmI₆] (cf. 2.2).

Further motivation for the study of alkaline-earth metals compounds in this type of ionic liquid comes from spectroscopic and chemical investigations of the behavior of divalent rare earth cations in this class of solvents as Ca²⁺ / Yb²⁺ and Sr²⁺ / Eu²⁺ have similar ionic radii and often behave similar in systems where the ions are substituted by each other. A plethora of isotypic compounds of rare-earth and the respective alkaline-earth metals are known [1]. Thus alkaline earth cations are ideal model systems for the highly reducing divalent lanthanides. [mppy_r]₂[Ca(Tf₂N)₄], [mppy_r]₂[Sr(Tf₂N)₄] and [mppy_r][Ba(Tf₂N)₃], were crystallized from a solution of the respective alkaline-earth diiodide and the ionic liquid [mppy_r][Tf₂N]). The effect of the coordination is further examined by Raman spectroscopy.

3.2 Preparation

AEI₂: The alkaline earth iodides, [AE]I₂, AE = Ca, Sr, Ba were synthesized by dissolving the corresponding carbonate or oxide in aqueous HI. The anhydrous compound was obtained by removing the solvent and excess acid in high vacuum at 250 °C.

[mppy_r][Tf₂N] was synthesized as described before (cf. I, 1.2).

Synthesis of the AE-complexes: CaI_2 (0.17 mmol, 50 mg) and $[\text{mppyr}][\text{Tf}_2\text{N}]$ (4 mmol, 1.63 g, ~ 1.1 ml) were placed in a silica tube which was sealed under vacuum. The reaction mixture was heated at 393 K for 48 h. Colorless transparent single crystals of $[\text{mppyr}]_2[\text{Ca}(\text{Tf}_2\text{N})_4]$ form as an insoluble product after cooling the reaction mixture to room temperature (2 K/min). The product was separated by cannula-filtration from the ionic liquid. Estimated yield: 80%. The analogous procedure with SrI_2 (1 mmol, 340 mg) and $[\text{mppyr}][\text{Tf}_2\text{N}]$ (4 mmol, 1.63 g, ~ 1.1 ml) resulted in the formation of colorless transparent single crystals of $[\text{mppyr}]_2[\text{Sr}(\text{Tf}_2\text{N})_4]$ (estimated yield: 80%). BaI_2 (1 mmol, 390 mg) and $[\text{mppyr}][\text{Tf}_2\text{N}]$ (4 mmol, 1.63 g, ~ 1.1 ml) gave $[\text{mppyr}][\text{Ba}(\text{Tf}_2\text{N})_3]$ in an estimated yield of 25%.

3.3 Structural aspects

Colourless, transparent crystals of the general composition $[\text{mppyr}]_2[\text{AE}(\text{Tf}_2\text{N})_4]$ for AE = Ca, Sr and $[\text{mppyr}][\text{Ba}(\text{Tf}_2\text{N})_3]$ are obtained from oversaturated solutions of the respective alkaline earth iodide in the ionic liquid $[\text{mppyr}][\text{Tf}_2\text{N}]$.

The calcium and strontium compounds crystallize in the monoclinic space group $P2_1/c$ with four formula units in the unit cell. Both structures are not isotypic but homootypic, since the structures are similar but the fractional coordinates and the lattice constants are slightly different and the monoclinic angle is widened in $[\text{mppyr}]_2[\text{Ca}(\text{Tf}_2\text{N})_4]$ ($107.74(1)^\circ$ compared to $105.73(1)^\circ$ in $[\text{mppyr}]_2[\text{Sr}(\text{Tf}_2\text{N})_4]$) (see Tab. 1). The asymmetric units of both crystal structures show the AE(II)-ions being coordinated by four Tf_2N^- anions forming a distorted square antiprism (see Fig. 1 for $[\text{Ca}(\text{Tf}_2\text{N})_4]^{2-}$) and two cations of the ionic liquid to compensate the charge.

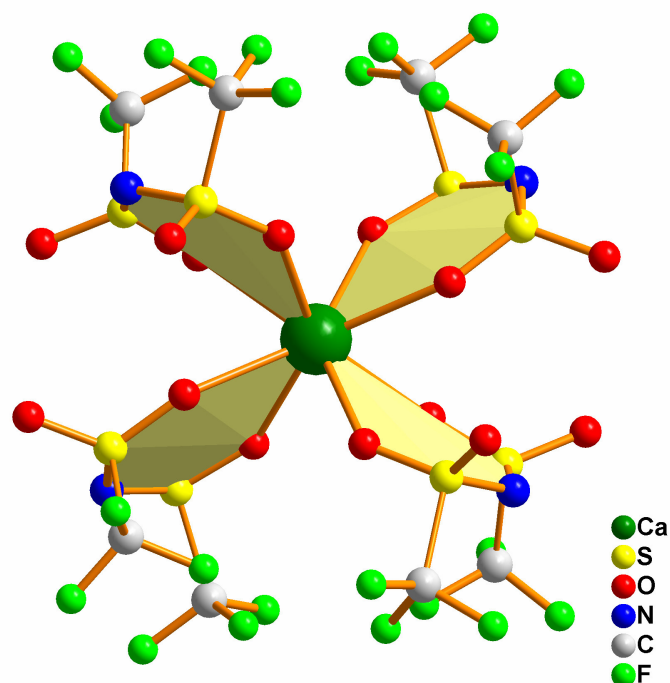


Fig. 1: Coordination of Ca^{2+} by four Tf_2N^- ligands in the crystal structure of $[\text{mppyr}]_2[\text{Ca}(\text{Tf}_2\text{N})_4]$

The Ca-O distances range from 237.0(4) pm to 248.2(4) pm (c.f. Table 2). With a mean Ca-O distance of 241 pm these are slightly shorter than the calcium-oxygen distance of oxygen atoms belonging to the bis(trifluoromethanesulfonyl)amide ligand in the hydrated calcium-bis(trifluoromethanesulfonyl)amide, $\text{Ca}(\text{H}_2\text{O})_4(\text{Tf}_2\text{N})_2$, (246.6(4) pm and 250.2(4) pm) [2]. This might be attributed to the fact that in the homoleptic compound $[\text{mppyr}]_2[\text{Ca}(\text{Tf}_2\text{N})_4]$ the Tf_2N^- ligands compete only with themselves whereas in the hydrated calcium-bis(trifluoromethanesulfonyl)amide, the weak $[\text{Tf}_2\text{N}]^-$ ligand is forced to compete with the stronger coordinating oxygen donor atoms of the additional water molecules leading to larger Ca-O interatomic distances and, in turn to a weaker Ca-O bond whenever the $[\text{Tf}_2\text{N}]^-$ ligand oxygen atoms are involved.

Due to the strong delocalization of the negative charge over all atomic centers and the high conformational flexibility of the C-S-N-S-C backbone, the Tf_2N ligand is regarded as a weakly coordinating anion (WCA). This is supported by the fact that, so far, for most known Tf_2N compounds the interatomic S-O distances within the

bis(trifluoromethanesulfonyl)amide anion are equal or close to those in the free anion. This generally holds true for structures with “non coordinating” cations [3]. In contrast to this common observation in [mppy_r]₂[Ca(Tf₂N)₄] a rather significant elongation of the S-O interatomic distances on the binding site of the ligands compared to the S-O distances on the non-binding site (144.7(4) – 145.8(4) pm *vs.* 142.1(4) – 143.6(4) pm). This effect appears to be quite remarkable – especially as such a pronounced difference between the S-O interatomic distances between the metal-bonded and unbound oxygen atoms is not observed in Ca(H₂O)₄(Tf₂N)₂ [2]. This backs our hypothesis that the Ca-O(Tf₂N) bond is weakened in the presence of stronger coordinating ligands such as water while in the pure presence of just bis(trifluoromethanesulfonyl)amide calcium is solely interacting with the oxygen atoms belonging to the [Tf₂N]-ligand. The same observation is made for the compounds [mppy_r]₂[Ln(Tf₂N)₅], Ln = Pr, Nd, Tb and [mppy_r]₂[Ln(Tf₂N)₅], Ln = Tm, Lu compared to La(Tf₂N)₃(H₂O)₃ as described in chapter I, 2 & 3.

All Tf₂N⁻ ligands show a *cisoid* conformation with respect to the –CF₃ groups in [mppy_r]₂[Ca(Tf₂N)₄] which pinches the [AE(Tf₂N)₄]²⁻ antiprisms along the crystallographic *b*-axis (Fig. 2 (a)). The S-N interatomic distances ($d_{\text{mean}}(\text{N-S}) = 157$ pm) as well as the S-N-S –bonding angles ($\langle_{\text{mean}}(\text{S-N-S}) = 128^\circ$) are similar to the values found for the free ligand and in good agreement with theoretical calculations. The crystal structure of [mppy_r]₂[Ca(Tf₂N)₄] (Fig. 2 (b)) is similar (though not isotypic) to the structure of [mppy_r]₂[Yb(Tf₂N)₄] (cf. II, 1.3), where the anionic parts are surrounded with the cations in a honeycomb like lattice.

Table 11: Selected crystallographic data and refinement parameters.

	[mppyr] ₂ [Ca(Tf ₂ N) ₄]	[mppyr] ₂ [Sr(Tf ₂ N) ₄]	[mppyr] ₂ [Ba(Tf ₂ N) ₃]
Empirical formula	C ₂₄ H ₃₆ CaF ₂₄ N ₆ O ₁₆ S ₈	C ₂₄ H ₃₆ SrF ₂₄ N ₆ O ₁₆ S ₈	C ₁₄ H ₁₈ BaF ₁₈ N ₄ O ₁₂ S ₆
Formula weight	1417.15	1446.69	1106.02
Crystal system	monoclinic	monoclinic	orthorhombic
Space group	<i>P</i> 2 ₁ / <i>c</i>	<i>P</i> 2 ₁ / <i>c</i>	<i>Pbca</i>
Unit cell dimensions	<i>a</i> = 11.200(1) Å <i>b</i> = 22.447(3) Å <i>c</i> = 22.390(2) Å β = 107.74(1)°	<i>a</i> = 11.488(1) Å <i>b</i> = 22.151(1) Å <i>c</i> = 23.534(1) Å β = 105.73(1)°	<i>a</i> = 12.376(1) Å <i>b</i> = 24.043(1) Å <i>c</i> = 23.052(1) Å
Volume	5361.6(1) Å ³	5764.8(6) Å ³	7144.7(6) Å ³
Z	4	4	8
Density (calculated)	1.756 g cm ⁻³	1.688 g cm ⁻³	2.056 g cm ⁻³
Absorption coefficient	0.576 mm ⁻¹	1.362 mm ⁻¹	1.613 mm ⁻¹
Reflections collected	59083	78537	102336
Independent reflections / <i>R</i> _{int}	11669 / 0.1553	12677 / 0.0784	7984 / 0.0633
Absorption correction	numerical	numerical	numerical
<i>T</i> _{max} / <i>T</i> _{min}	0.9593 / 0.8120	0.8611 / 0.5515	0.8597 / 0.6502
Parameters	857	716 (28 restraints)	498
Goof on <i>F</i> ²	0.818	0.904	1.001
Final <i>R</i> indices [<i>I</i> > 2σ(<i>I</i>)]	<i>R</i> ₁ = 0.0543, <i>wR</i> ₂ = 0.1057	<i>R</i> ₁ = 0.0625, <i>wR</i> ₂ = 0.1559	<i>R</i> ₁ = 0.0281, <i>wR</i> ₂ = 0.0625
<i>R</i> indices (all data)	<i>R</i> ₁ = 0.1673, <i>wR</i> ₂ = 0.1414	<i>R</i> ₁ = 0.1522, <i>wR</i> ₂ = 0.1985	<i>R</i> ₁ = 0.0456, <i>wR</i> ₂ = 0.0691

Table 12: Selected interatomic distances (pm) and angles (°).

[mppyr] ₂ [Ca(Tf ₂ N) ₄]				[mppyr] ₂ [Sr(Tf ₂ N) ₄]				[mppyr][Ba(Tf ₂ N) ₃]			
Ca-O1	237.0(4)	N1-S1	155.8(5)	Sr-O1	256.1(4)	N1-S1	154.9(5)	Ba1-O1	281.8(2)	N1-S1	157.4(2)
Ca-O2	238.4(4)	N1-S2	157.9(7)	Sr-O2	256.9(4)	N1-S2	155.9(7)	Ba1-O2	272.7(2)	N1-S2	157.4(2)
Ca-O3	239.1(4)	N2-S3	156.5(5)	Sr-O3	254.2(4)	N2-S3	155.5(5)	Ba1-O3	276.4(2)	N2-S3	156.5(2)
Ca-O4	240.5(3)	N2-S4	156.6(7)	Sr-O4	257.6(4)	N2-S4	156.3(7)	Ba1-O4	278.8(2)	N2-S4	157.8(2)
Ca-O5	242.7(4)	N3-S6	157.0(5)	Sr-O5	256.1(4)	N3-S6	154.3(7)	Ba1-O5	279.9(2)	N3-S5	156.6(3)
Ca-O6	244.6(4)	N3-S5	157.1(6)	Sr-O6	255.2(4)	N3-S5	156.5(9)	Ba1-O6	280.9(2)	N3-S6	157.7(3)
Ca-O7	246.8(4)	N4-S8	156.2(7)	Sr-O7	256.0(4)	N4-S7	155.4(7)	Ba1-O11	269.8(2)		
Ca-O8	248.2(4)	N4-S7	157.0(5)	Sr-O8	255.2(4)	N4-S8	155.8(6)	Ba1-O13	278.2(2)		
								Ba1-O15	274.6(2)		
S1-O1	145.1(4)	S1-N1-S2	128.4(3)	S1-O1	140.5(4)	S1-N1-S2	127.87(34)	S1-O1	143.4(2)	S1-N1-S2	126.72(16)
S1-O11	142.7(4)	S3-N2-S4	128.3(3)	S1-O11	139.2(6)	S3-N2-S4	127.49(34)	S1-O11	142.8(2)	S3-N2-S4	127.07(16)
S2-O2	145.8(4)	S6-N3-S5	127.2(3)	S2-O2	141.5(4)	S6-N3-S5	128.61(49)	S2-O2	142.9(2)	S5-N3-S6	125.81(17)
S2-O12	142.9(4)	S8-N4-S7	129.0(3)	S2-O12	143.1(6)	S7-N4-S8	127.99(40)	S2-O12	142.2(2)		
S3-O3	145.7(4)			S3-O3	140.5(4)			S3-O3	143.2(2)		
S3-O13	143.5(4)			S3-O13	141.5(6)			S3-O13	143.0(2)		
S4-O4	145.3(4)			S4-O4	141.1(4)			S4-O4	142.8(2)		
S4-O14	143.2(4)			S4-O14	140.6(5)			S4-O14	142.2(2)		
S5-O5	145.1(4)			S5-O5	142.7(4)			S5-O5	143.2(2)		
S5-O15	143.5(4)			S5-O15	140.8(6)			S5-O15	142.9(2)		
S6-O6	145.3(4)			S6-O6	142.2(4)			S6-O6	143.4(2)		
S6-O16	142.1(4)			S6-O16	145.4(9)			S6-O16	142.3(2)		

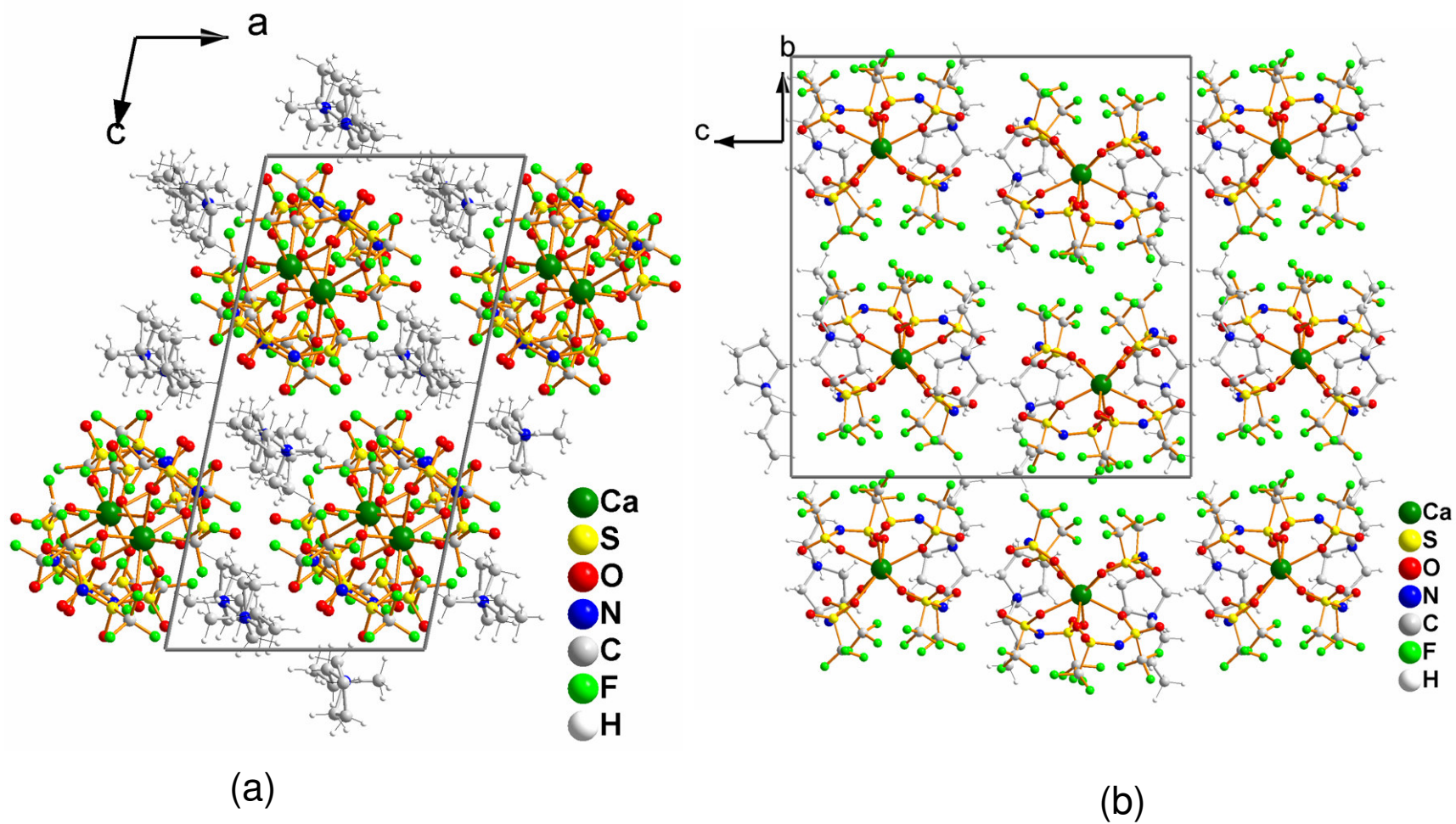


Fig. 2: Projection of the crystal structure of $[\text{mppyr}]_2[\text{Ca}(\text{Tf}_2\text{N})_4]$ along the crystallographic (a) b - and (b) a -axes

In [mppy₂][Sr(Tf₂N)₄] the Sr-O distances range from 254.2(4) to 257.6(4) pm (see Table 2). With a mean value of 256 pm they are slightly smaller than in the “binary” Sr(Tf₂N)₂ (d(S-O) = 258 pm). However, when comparing metal-oxygen distances of ligands which exhibit the same coordinating mode, for bidentately chelating [Tf₂N]-ligands in Sr(Tf₂N)₂ similar distances are found as in [mppy₂][Sr(Tf₂N)₄], whereas S-O distances involving bridging [Tf₂N]-ligands seem to be generally larger. The influence of coordination on the S-O bond distance is far less pronounced than in the analogous calcium compound. As in [mppy₂][Ca(Tf₂N)₄], in [mppy₂][Sr(Tf₂N)₄] the N-S distances (156 pm) and S-N-S angles (128°) are unchanged upon coordination.

Due to the larger ionic radius of Sr²⁺ when compared to Ca²⁺, the Sr-O distances in [mppy₂][Sr(Tf₂N)₄] are significantly larger than the metal-oxygen distance in [mppy₂][Ca(Tf₂N)₄]. Thus, the propeller-like arrangement of the anions is widened in [mppy₂][Sr(Tf₂N)₄] when compared to the Ca compound. In consequence the heterocyclic cations have more space to order within the fluorine segregated layers which are stacked along the crystallographic *a*-axis (see Fig. 3). In [mppy₂][Sr(Tf₂N)₄] the cations are located in hydrophobic channels which are composed by the perfluoralkyl groups of the bis(trifluoromethanesulfonyl)amide ligands. The F--H-C distances are too large (d(F--H-C) ~ 2.6 Å) for significant hydrogen bonding [4]. Furthermore, the cations, although they are clearly identified from the difference fourier-map, exhibit high displacement parameters after anisotropic refinement of the carbon skeleton even at low temperatures. This is taken as an indicator for weak interactions between the cationic and anionic parts of the structure.

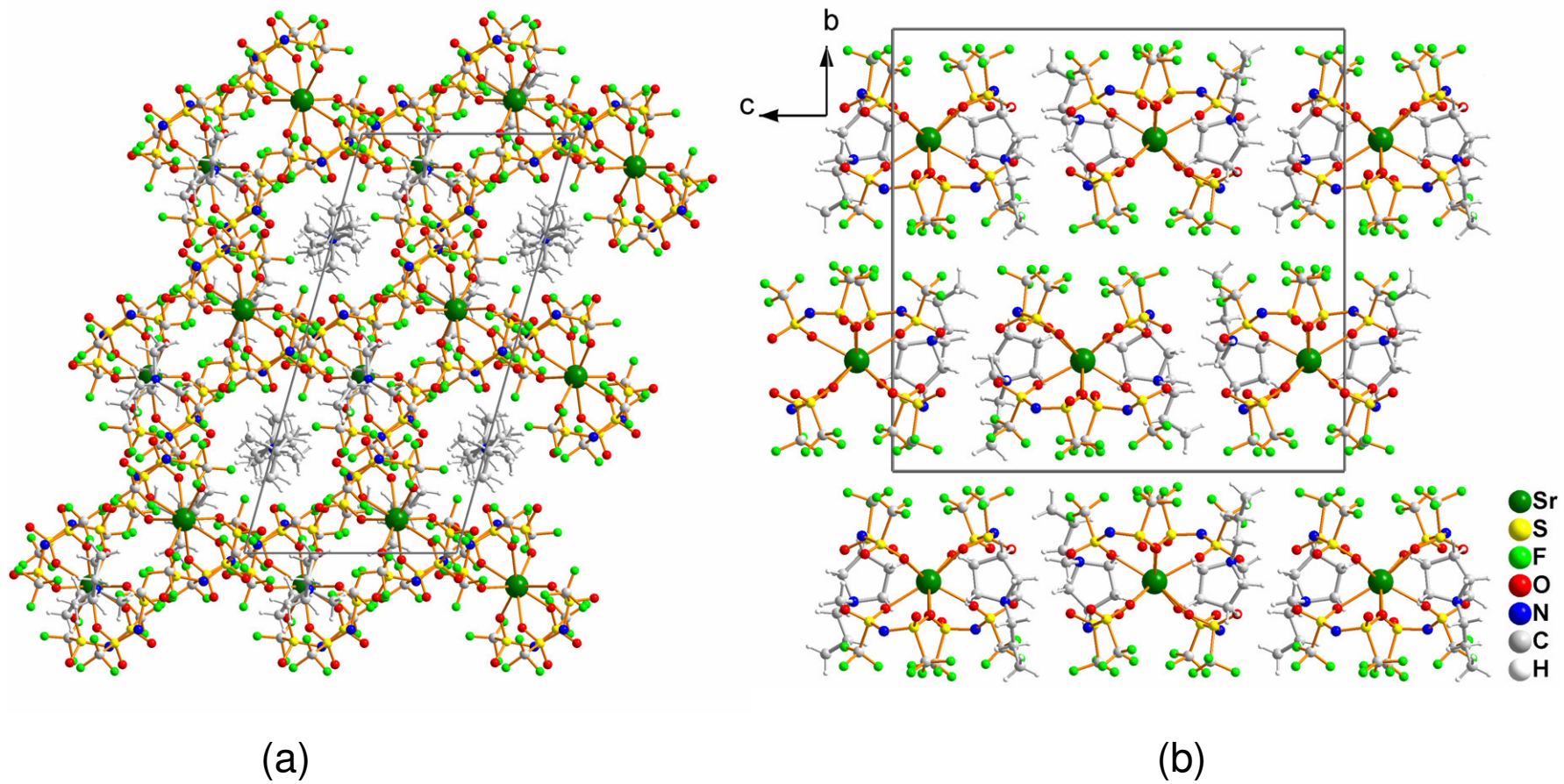


Fig. 3: Projection of the crystal structure of $[\text{mppyr}]_2[\text{Sr}(\text{Tf}_2\text{N})_4]$ along the crystallographic (a) b - and (b) a -axes

In contrast to Ca^{2+} and Sr^{2+} which are coordinated by eight oxygen atoms of four Tf_2N^- ligands forming discrete anionic moieties, the larger alkaline earth metal cation Ba^{2+} prefers a coordination number of nine. The barium–oxygen distances range from 269.8(2) to 281.8(2) pm with a mean value of 277 pm. This value is significantly less than the mean $\text{Ba-O}(\text{Tf}_2\text{N})$ distance of 281 pm reported for $\text{Ba}(\text{H}_2\text{O})(\text{Tf}_2\text{N})_2$ [2]. This can, as previously pointed out for $[\text{mppyr}]_2[\text{Ca}(\text{Tf}_2\text{N})_4]$ compared to $\text{Ca}(\text{H}_2\text{O})_4(\text{Tf}_2\text{N})_2$, attributed to the fact that in $\text{Ba}(\text{H}_2\text{O})(\text{Tf}_2\text{N})_2$ obviously the $\text{Ba-O}(\text{Tf}_2\text{N})$ bond gets weakened in the presence of coordinating water.

In $[\text{mppyr}][\text{Ba}(\text{Tf}_2\text{N})_3]$ the alkaline earth metal cation interacts with six oxygen atoms belonging to three Tf_2N^- anions which coordinate in a bidentately chelating mode and three further oxygen atoms which show mono-hapto ligand-metal interactions. The mono-hapto ligands are linking the Ba^{2+} cations to infinite chains along the a -axis (Fig. 4).

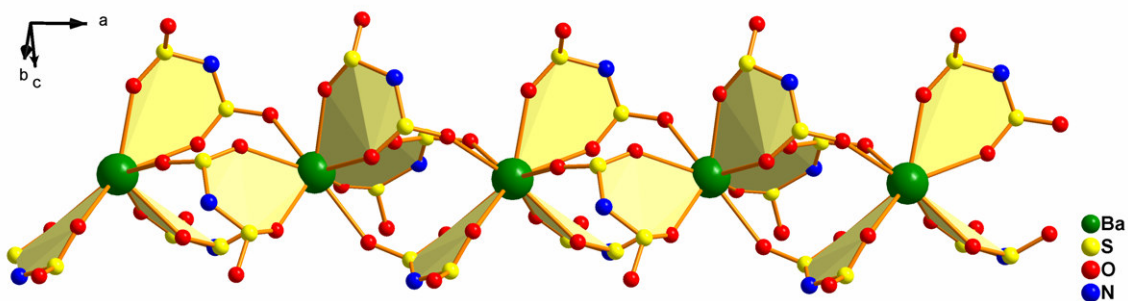


Fig. 4: $[\text{Ba}(\text{Tf}_2\text{N})_3]$ strands in $[\text{mppyr}][\text{Ba}(\text{Tf}_2\text{N})_3]$ (CF_3 -groups are omitted for reasons of clarity)

These chains form an hexagonal arrangement (see Fig. 5). The $[\text{mppyr}]$ -cations are packed alongside the anionic chains in the crystal structure. The S-O interatomic distance within the bis(trifluoromethanesulfonyl)amide ligand gets lengthened slightly upon coordination (143 vs. 142 pm) whereas the N-S (157 pm) and S-N-S angle (127°) virtually remain unchanged when compared to the free ligand. Again, all $[\text{Tf}_2\text{N}]$ -anions adopt a *cisoid* conformation.

It has been previously proposed, that the $[\text{Tf}_2\text{N}]$ anion would coordinate in a chelating mode through oxygen atoms including nitrogen-metal interaction if the cation size is large enough as in the case of Ba^{2+} [5]. Neither in $[\text{mppyr}][\text{Ba}(\text{Tf}_2\text{N})_3]$ nor in $\text{Ba}(\text{H}_2\text{O})(\text{Tf}_2\text{N})_2$ any nitrogen-metal interaction is observed [6]. This can not only be proven by the single crystal X-ray structures but even better by Raman spectroscopic studies.

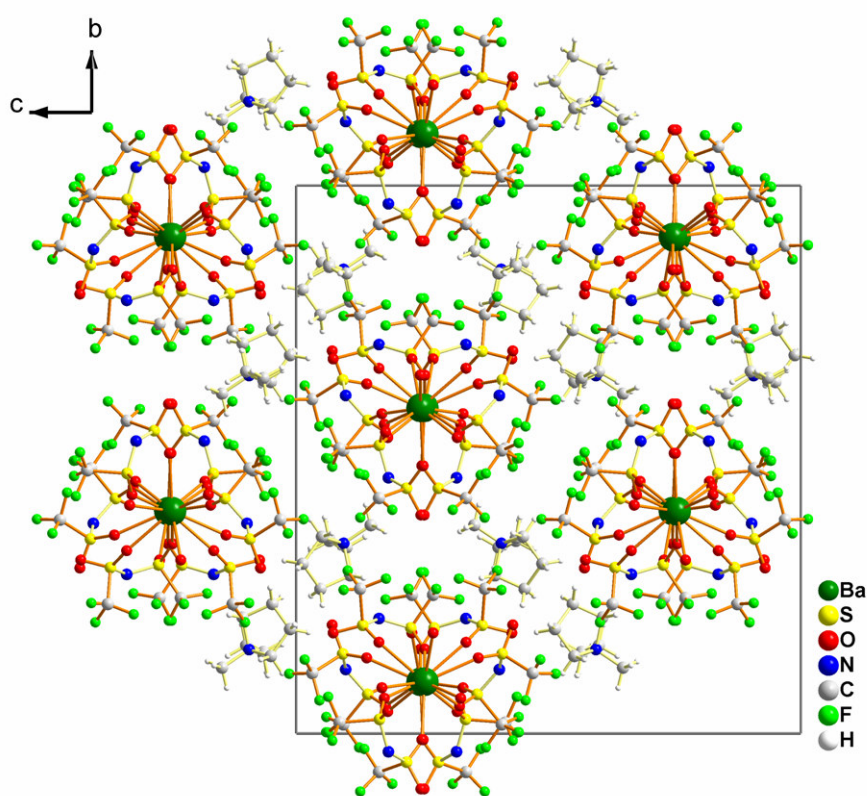


Fig. 5: Hexagonal packing of the $[\text{Ba}(\text{Tf}_2\text{N})_3]$ strands in $[\text{mppyr}][\text{Ba}(\text{Tf}_2\text{N})_3]$

3.4 Raman investigations

Raman spectra were obtained from the bulk solids recorded at 150 mW on a Bruker IFS-FRA-106/s. For the measurement the respective samples were sealed under an argon atmosphere in glass capillaries and recorded at room temperature.

[mppyr]₂[Ca(Tf₂N)₄]: 135(w), 212(w), 247(w), 291(m), 331(m), 353(m), 409(w), 553(w), 574(w), 746(vs), 902(m), 1041(w), 1149(m), 1246(s), 1329(m), 1454(s) [cm⁻¹].

[mppyr]₂[Sr(Tf₂N)₄]: 133(w), 208(w), 239(w), 289(m), 329(m), 353(m), 409(w), 553(w), 574(w), 744(vs), 902(m), 1045(w), 1145(m), 1242(s), 1327(m), 1454(s) [cm⁻¹].

[mppyr][Ba(Tf₂N)₃]: 108(s), 208(w), 231(w), 287(m), 329(m), 349(m), 411(w), 553(w), 571(w), 744(vs), 902(m), 1043(w), 1136(m), 1158(m), 1246(s), 1309(m), 1448(s) [cm⁻¹].

The characteristic Raman bands of the ionic liquid [mppyr][Tf₂N] [5] as well as of the free acid HTf₂N [7] are well known and have been assigned previously so that the coordination of the anion can be easily verified for bulk samples of the AE-complexes.

The $\nu_s(\text{SNS})$ as well as the $\nu_s(\text{SO}_2)$ vibrations are the most relevant ones to study as they should be most influenced by interactions of the bis(trifluoromethanesulfonyl)-amide with the metal cation. It has been claimed that upon deprotonation of HTf₂N the S-N bonds within the Tf₂N moiety are strengthened and gain partially a double bond character. Indeed the expected shift of the $\nu_s(\text{SNS})$ band can be observed in the Raman spectra [7]. For the "free" Tf₂N⁻ in the ionic liquid [mppyr][Tf₂N] itself, the $\nu_s(\text{SNS})$ band is found at 740 cm⁻¹. Under complexation, the $\nu_s(\text{SNS})$ band of the anion shifts in the Ba and Sr-complex to 744 cm⁻¹. The Ca-complex shows the same shift to higher energy at 746 cm⁻¹ (see Fig. 6). In the free acid HTf₂N, the $\nu_s(\text{SNS})$ band is found around ~770 cm⁻¹ [8]. Thus, under complexation the frequency of the $\nu_s(\text{SNS})$ rises slightly when compared to the free anion.

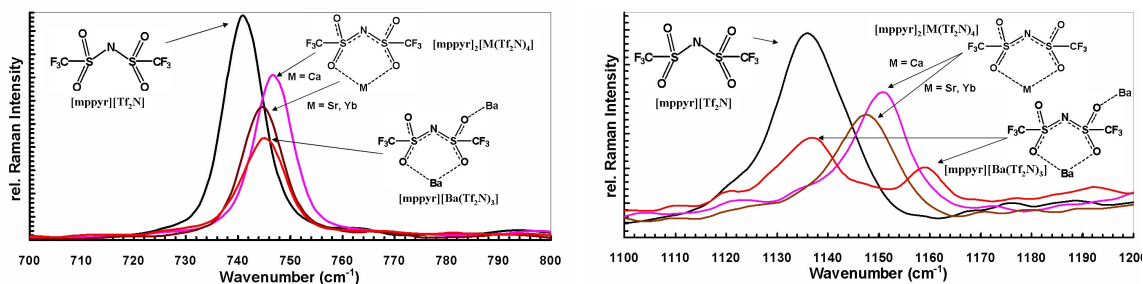


Fig. 6: Raman spectra of $[\text{mppyr}][\text{AE}(\text{Tf}_2\text{N})_4]$ (AE = Ca, Sr, Yb) and $[\text{mppyr}][\text{Ba}(\text{Tf}_2\text{N})_3]$

The $\nu_s(\text{SO}_2)$ which should be directly influenced by coordination of the sulfonyl-oxygen to a metal center is observed for the free and quasi non interacting Tf_2N^- anion at 1136 cm^{-1} . In $[\text{mppyr}]_2[\text{Ca}(\text{Tf}_2\text{N})_4]$ the band is located at 1149 cm^{-1} , see Fig. 6. In the strontium compound the band is shifted to 1145 cm^{-1} . Furthermore, for $[\text{mppyr}][\text{Ba}(\text{Tf}_2\text{N})_3]$ the $\nu_s(\text{SO}_2)$ band is split in two peaks at 1136 cm^{-1} and 1158 cm^{-1} . Hence, the position of the $\nu_s(\text{SO}_2)$ band sensitive to both, the mode of coordination and the coordinated metal itself. Apparently a stronger coordinative bond towards the metal center shifts the frequencies of the symmetric S-O stretching vibration to higher energy.

Judging from the Raman spectra any contamination of the samples with $[\text{mppyr}][\text{I}]$, which is a by-product of the reaction, can be excluded as none of the reported Raman frequencies of $[\text{mppyr}][\text{I}]$ could be detected.

3.5 Discussion

In the absence of any stronger competing ligands such as water, the homoleptic alkaline earth metal – bis(trifluoromethanesulfonyl)amide complexes $[\text{mppyr}]_2[\text{Ca}(\text{Tf}_2\text{N})_4]$, $[\text{mppyr}]_2[\text{Sr}(\text{Tf}_2\text{N})_4]$ and $[\text{mppyr}][\text{Ba}(\text{Tf}_2\text{N})_3]$ were obtained from the respective alkaline earth metal iodide and the ionic liquid $[\text{mppyr}][\text{Tf}_2\text{N}]$. These compounds belong to the first examples of homoleptic alkaline earth metal bis(trifluoromethanesulfonyl)amides. Compared to the previously described water containing alkaline earth metal bis(trifluoromethanesulfonyl)amides $[\text{Ca}(\text{H}_2\text{O})_4(\text{Tf}_2\text{N})_2]$ and $[\text{Ba}(\text{H}_2\text{O})(\text{Tf}_2\text{N})_2]$ a small but significant elongation of the sulfur-oxygen bond distance involving the coordinating oxygen is observed when compared to the free ligand. Furthermore, the interatomic EA- $\text{O}(\text{Tf}_2\text{N})$ distances are less

in the homoleptic compounds than in the heteroleptic ones which may be indicative for a stronger metal-ligand interaction in the homoleptic compounds due to the absence of stronger donor ligands like water. At the same time, upon coordination, the frequency of the symmetric S-O stretching vibration gets slightly shifted to larger values the stronger the metal is coordinating. The effect of complex formation on the S-N-S bonding angles and distances is negligible. The $\nu_s(\text{SNS})$ frequencies gets slightly shifted to larger values upon complexation when compared to the free anion. Altogether these observations confirm once more that the bis(trifluoromethanesulfonyl)amide ligand can be regarded as comparatively weakly coordinating. While chelating *transoid* structures are known (cf. chapter I, 3), there appears to be a tendency that the Tf_2N anion prefers a *cisoid* conformation when coordinating in a chelating mode while for the free anion the *transoid* conformation is strongly preferred (calculations show the *transoid* structure of the free anion to be more stable by 4 kJ/mol compared to the *cisoid* one). But structural data for Tf_2N complex compounds are still scarce to allow for a generalization. Common and typical for all structures now characterized is extensive fluorine segregation which results in the formation of hydrophilic and hydrophobic structure parts.

3.6 Literature

- [1] L. Maron, L. Perrin, O. Eisenstein, R.A. Andersen, *J. Am. Chem. Soc.* **2002**, *124*, 5614.
- [2] L. Xue, D.D. DesMarteau, W.T. Pennington, *Solid State Sci.* **2005**, *7*, 311.
- [3] J.J. Golding, D.R. MacFarlane, L. Spiccia, M. Forsyth, B.W. Skelton, A.H. White *Chem. Commun.* **1998**, *15*, 1593; V. Montanari, D.D. DesMarteau, W.T. Pennington, *J. Mol. Struct.* **2000**, *550/551*, 337; C. Forsyth, D.R. MacFarlane, J. Golding, J. Huang, J. Sun, M. Forsyth, *Chem. Mater.* **2002**, *14*, 2103; J.A. Schlueter, U. Geiser, H.H. Wang, A.M. Kini, B.H. Ward, J.P. Parakka, R.G. Daugherty, M.E. Kelly, P.G. Nixon, R.W. Winter, G.L. Gard, L.K. Montgomery, H.-J. Koo, M.-H. Whangbo, *J. Solid State Chem.* **2002**, *168*, 524; M.G. Davidson, P.R. Raithby, A.L. Johnson, P.D. Bolton, *Eur. J. Inorg. Chem.* **2003**, 3445;

- D.D. DesMarteau, W.T. Pennington, V. Montanari, B.H. Thomas, *J. Fluorine Chem.* **2003**, *122*, 57; J.D. Holbrey, W.M. Reichert, R.D. Rogers, *J. Chem. Soc., Dalton Trans.* **2004**, 2267.
- [4] T. Steiner, *Angew. Chem.* **2002**, *114*, 50.
- [5] M. Castriota, T. Caruso, R.G. Agostino, E. Cazzanelli, W.A. Henderson, S. Passerini, *J. Phys. Chem. A* **2005**, *109*, 92.
- [6] Note that a η^2 -N,O coordination mode has been described for (cymene)-Ru(Tf₂N)₂: D.B. Williams, M.E. Stoll, B.L. Scott, D.A. Costa, *Chem. Commun.* **2005**, 1438.
- [7] J. Foropoulos, D.D. DesMarteau, *Inorg. Chem.* **1984**, *23*, 3720.
- [8] I. Rey, P. Johansson, J Lindgren, J.C Lassegues, J. Grondin, L. Servant, *J. Phys. Chem. A* **1998**, *102*, 3249.

IV Summary

The aim of this work was to get a deeper understanding of the interaction of rare-earth ions with triflate- and bis(trifluoromethanesulfonyl)amide-based ionic liquids. The solvent-solute interactions were investigated by X-ray methods, optical and vibrational spectroscopy and by electrochemical methods. Particularly the confirmation of the formed complexes by X-ray methods is valuable.

The trivalent rare-earth iodides, LnI_3 ($\text{Ln} = \text{La}, \text{Pr}, \text{Nd}, \text{Sm}, \text{Dy}, \text{Er}$) dissolve in 1-butyl-1-methylpyrrolidinium-bis(trifluoromethanesulfonyl)amide ($[\text{bmpyr}][\text{Tf}_2\text{N}]$) by composing the sparingly soluble compound $[\text{bmpyr}]_4[\text{LnI}_6][\text{Tf}_2\text{N}]$. The lanthanides are six coordinated by iodines, the second coordination sphere is accomplished by eight $[\text{bmpyr}]^+$ cations located tangentially on each face of the $[\text{LnI}_6]^{3-}$ -octahedra. The $[\text{Tf}_2\text{N}]^-$ -anion is co-crystallized in a non-coordinating fashion (see Fig. 1)

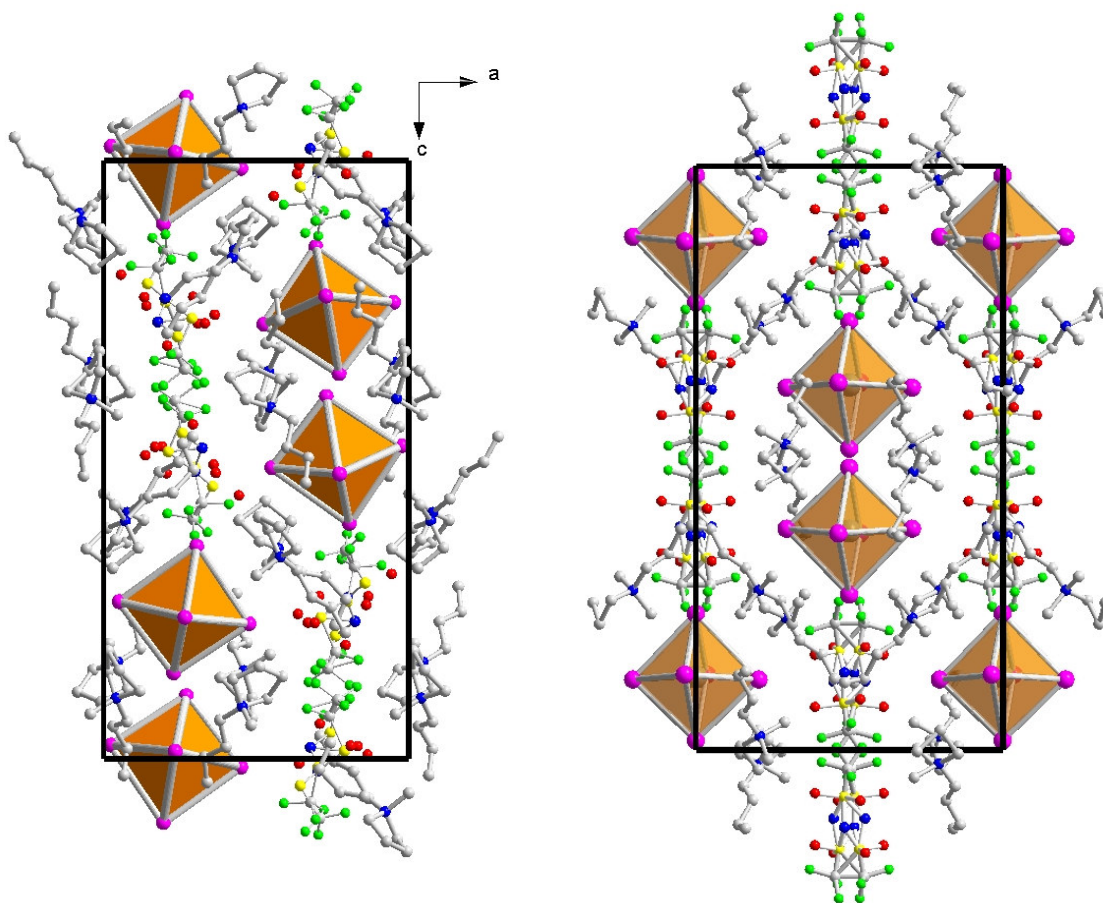


Fig. 1: Unit cell of $[\text{bmpyr}][\text{LnI}_6][\text{Tf}_2\text{N}]$ (left: La, Pr; right: Nd, Sm, Dy, Er)

Considering the stoichiometries of the reaction, also a Ln-[Tf₂N] complex must form which remains in solution, where the rare-earth-ion is surrounded by anions of the ionic liquid. By interacting Ln(Tf₂N)₃ (Ln = Pr, Nd, Sm, Eu, Tb, Dy, Tm, Yb, Lu) with [bmpyr][Tf₂N] the compounds [bmpyr]₂[Ln(Tf₂N)₅] (Ln = Pr-Tb) and [bmpyr][Ln(Tf₂N)₄] (Ln = Dy-Lu) were be crystallized. The larger lanthanides are nine coordinated by four ligands binding chelating, and one anion coordinating monodentately to the metal (see Fig.2).

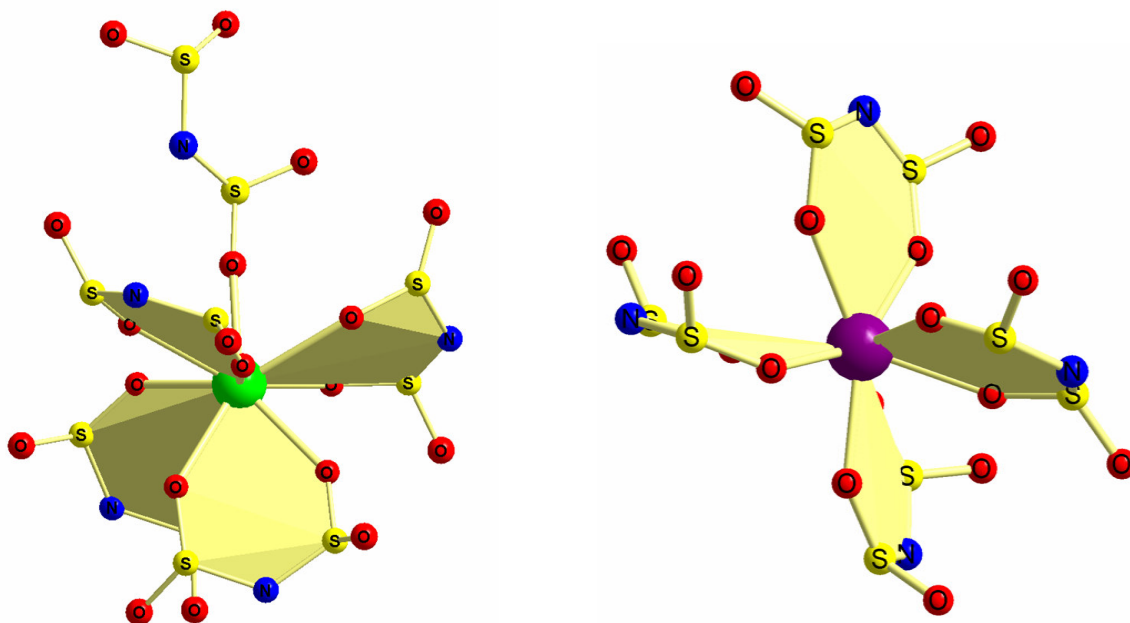


Fig. 2: Coordination mode of [Tf₂N] in [bmpyr]₂[Ln(Tf₂N)₅] (left) and [bmpyr][Ln(Tf₂N)₄] (right)

The formed complexes [bmpyr]₂[Ln(Tf₂N)₅] (Ln = Pr-Gd) are ionic liquids themselves, exhibiting melting points < 100°C. The smaller lanthanides prefer a coordination number of eight, which is realized by four anions binding in a chelating fashion. The luminescent properties of the Pr-compounds [bmpyr]₄[PrI₆][Tf₂N] and [bmpyr]₂[Pr(Tf₂N)₅] were investigated in solutions as well as in the solid state. After excitation into the ³P₁ level strong luminescence not only from the ¹D₂ level but also from the ³P₀ and even from the ³P₁ level are observed. Remarkably in the case of the solid compounds and even more astonishing for a solution of Pr(Tf₂N)₃ in [bmpyr][Tf₂N] the strongest luminescence transitions start from the ³P₀ level. In

conventional solvents, these energy levels are quenched by radiationless deactivation of the high energy levels to the 1D_2 level.

By reacting $\text{Yb}(\text{Tf}_2\text{N})_3$ with the ionic liquid 1-butyl-1-methylpyrrolidinium-trifluoromethanesulfonate $[\text{bmpyr}][\text{OTf}]$ ligand exchange could be evidenced by crystallizing the compound $[\text{bmpyr}]_4[\text{Yb}(\text{OTf})_6][\text{Tf}_2\text{N}]$, in which the $[\text{Tf}_2\text{N}]$ -anions are incorporated in a non-coordinating fashion in the crystal structure. The ytterbium atoms are surrounded octahedrally solely by triflates. By utilizing cyclic voltammetry, ligand displacement could be also be verified in solutions of $\text{Yb}(\text{Tf}_2\text{N})_3$ in $[\text{bmpyr}][\text{OTf}]$ (see Fig. 3). The stronger lewis acidity of the triflate groups shifts the halvewave potential of the $\text{Yb}(\text{III})/\text{Yb}(\text{II})$ couple towards lower potentials (-1,34 V), compared to the potentials measured in the pure $\text{Yb}(\text{Tf}_2\text{N})_3/[\text{bmpyr}][\text{Tf}_2\text{N}]$ -system (-1.08 V). By reacting $\text{Yb}(\text{OTf})_3$ with $[\text{bmpyr}][\text{OTf}]$, the $[\text{Tf}_2\text{N}]$ -free compound $[\text{bmpyr}]_3[\text{Yb}(\text{OTf})_6]$ was obtained. Like in $[\text{bmpyr}]_4[\text{Yb}(\text{OTf})_6][\text{Tf}_2\text{N}]$, the metal-ions are coordinated octahedrally by monodentately binding triflate-anions.

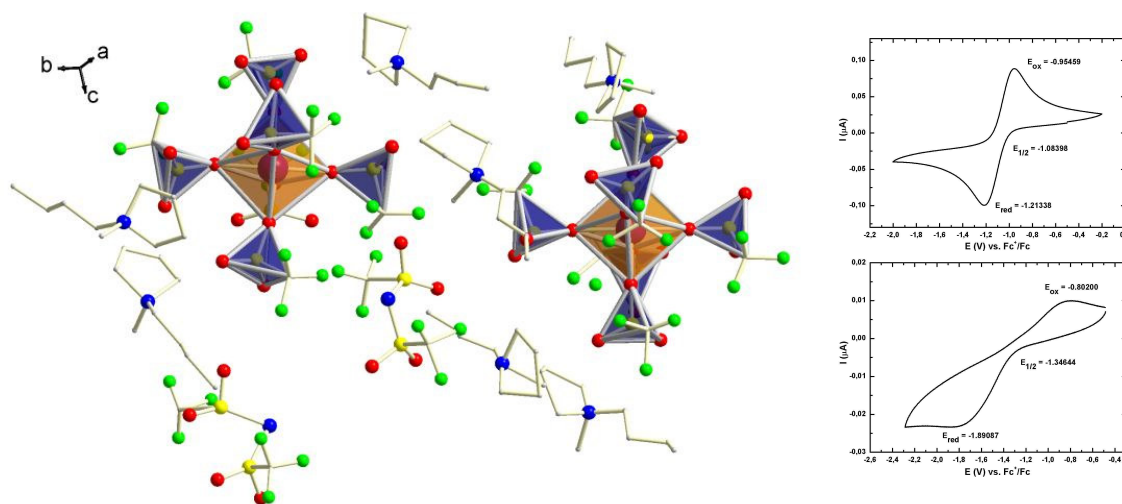


Fig. 3: Asymmetric unit of $[\text{bmpyr}]_4[\text{Yb}(\text{OTf})_6][\text{Tf}_2\text{N}]$ (left) and CVs of $\text{Yb}(\text{Tf}_2\text{N})_3$ in $[\text{bmpyr}][\text{Tf}_2\text{N}]$ (top left) and $[\text{bmpyr}][\text{OTf}]$ (bottom left)

To obtain structural data for divalent rare-earth-species, YbI_2 was reacted with 1-methyl-1-propylpyrrolidinium-bis(trifluoromethanesulfonyl)amide ($[\text{mppyr}][\text{Tf}_2\text{N}]$) to give $[\text{mppyr}][\text{Yb}(\text{Tf}_2\text{N})_4]$. Surprisingly the coordination sphere is built up by four $[\text{Tf}_2\text{N}]$ -anions, as it is in the trivalent compound $[\text{bmpyr}]_2[\text{Yb}(\text{Tf}_2\text{N})_4]$ although the

ionic radius for Yb(II) is comparable to that of Pr(III), which is coordinated by five ligands in $[\text{bmpyr}]_2[\text{Pr}(\text{Tf}_2\text{N})_5]$. This indicates the structural flexibility of the $[\text{Tf}_2\text{N}]$ -ligand, showing all-cis conformation in $[\text{mppyr}]_2[\text{Yb}(\text{Tf}_2\text{N})_4]$ and a cis/trans-disordered conformation in $[\text{bmpyr}][\text{Yb}(\text{Tf}_2\text{N})_4]$ (see Fig. 4).

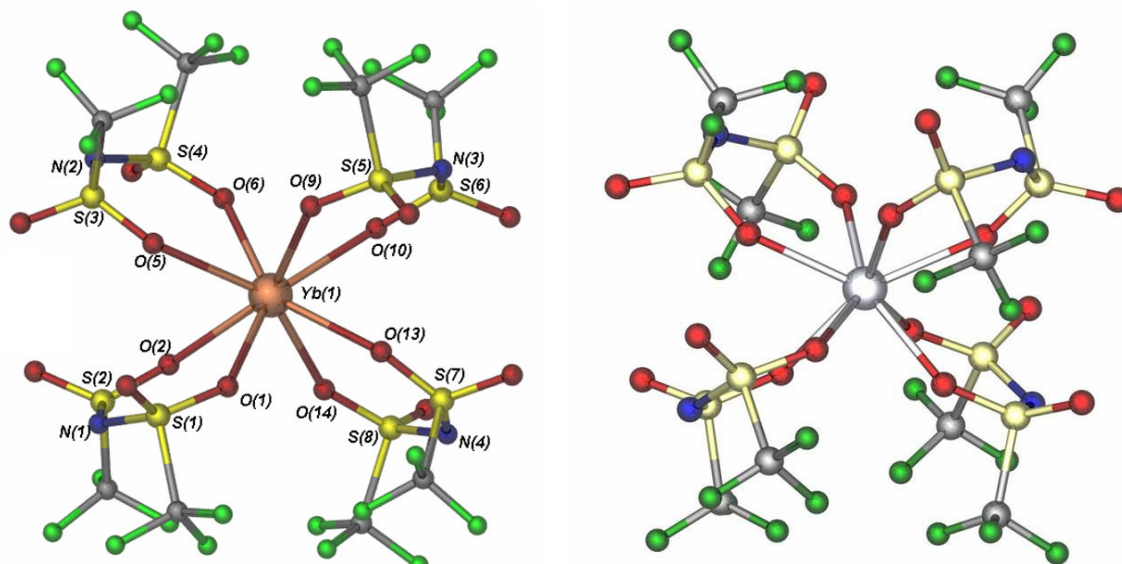


Fig. 4: Comparison of $[\text{Yb}(\text{Tf}_2\text{N})_4]^{2-}$ (left) and $[\text{Yb}(\text{Tf}_2\text{N})_4]$ (right)

In case of the dedicated Sm compound, the divalent species could only be confirmed in solution by UV-spectroscopy (cf. appendix 2). NdI_2 shows no reactivity toward pyrrolidinium-based ionic liquids, therefore triethylsulfonium-bis(trifluoromethanesulfonyl)amide $[\text{S}(\text{Et})_3][\text{Tf}_2\text{N}]$ as an alternative was synthesized. Reaction with NdI_2 as well as SmI_2 lead to decomposition of the ionic liquid, only the trivalent species $[\text{S}(\text{Et})_3][\text{LnI}_6]$ could be isolated (see Fig. 5).

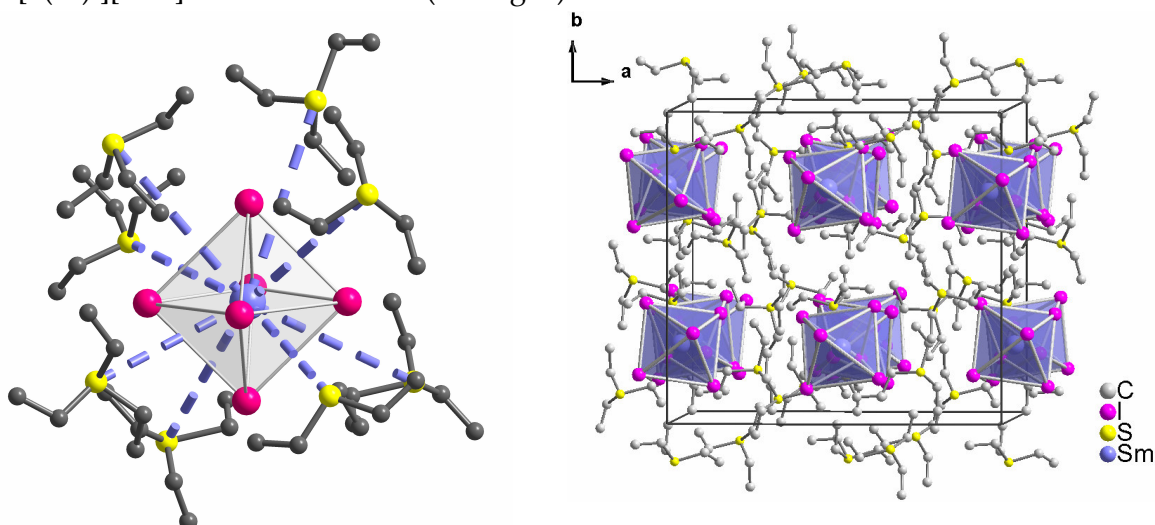


Fig 5: Coordination sphere of Sm^{3+} (left) and crystal structure (right) in $[\text{S}(\text{Et})_3][\text{LnI}_6]$

As redox-stable model compounds for Sm and Eu-complexes, AEI_2 (AE = alkaline earth metal Ca, Sr, Ba) were used as educts for the synthesis of $[Tf_2N]$ -complexes. $[mppy]_2[Ca(Tf_2N)_4]$, $[mppy]_2[Sr(Tf_2N)_4]$ and $[mppy][Ba(Tf_2N)_3]$, were crystallized from a solution of the respective alkaline earth diiodide and the ionic liquid $[mppy][Tf_2N]$. In the calcium and strontium compounds the alkaline earth metal (AE) is coordinated by four bidentately chelating $[Tf_2N]$ ligands to form isolated (distorted) square anti-prismatic $[AE(Tf_2N)_4]^{2-}$ which are separated by N-methyl-N-propyl-pyrrolidinium cations. This corresponds to the rare-earth species $[mppy][Yb(Tf_2N)_4]$. The ionic radius of Ca^{2+} is similar to the one of Yb^{2+} . The larger Sr^{2+} which has a radius comparable to Sm^{2+} still exhibits an eightfold coordination. In contrast to Yb^{2+} , Ca^{2+} and Sr^{2+} , the barium compound, $[mppy][Ba(Tf_2N)_3]$, forms an extended structure. Here the alkaline earth cation is surrounded by six oxygen atoms belonging to three Tf_2N -anions which coordinate bidentately chelating. Three further oxygen atoms of the same ligands are linking the Ba^{2+} cations to infinite $[\text{Ba}(Tf_2N)_3]$ chains. The different coordination modes were also investigated by Raman-spectroscopy.

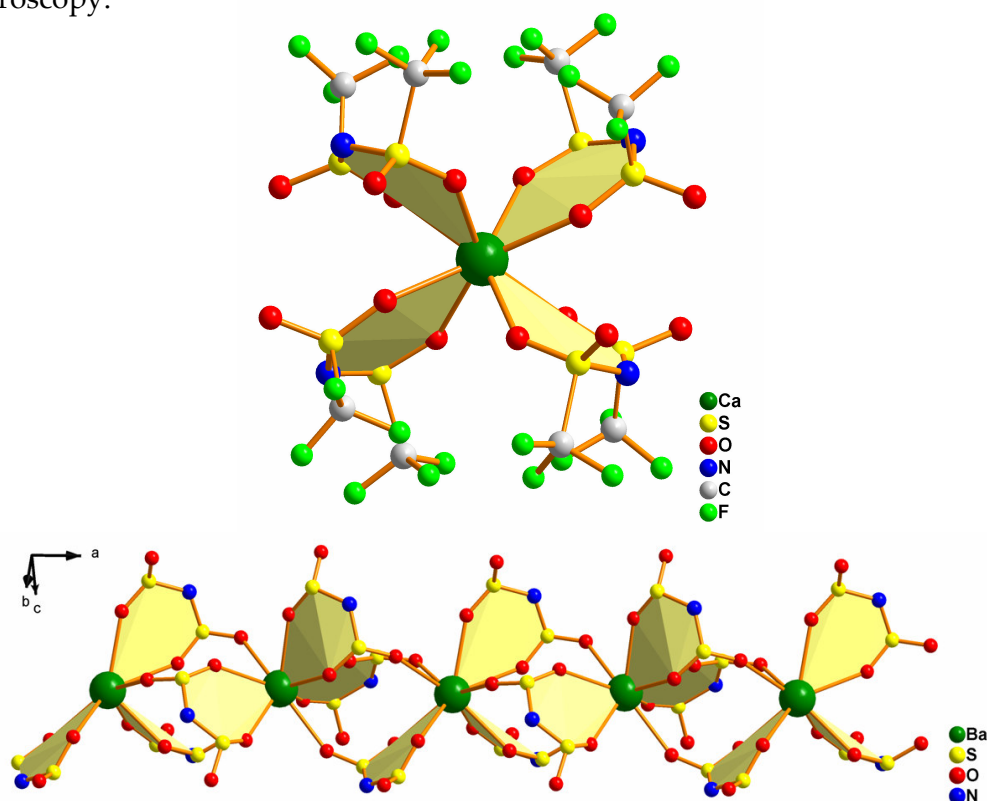
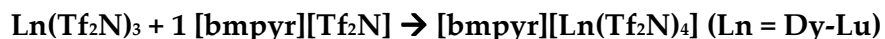
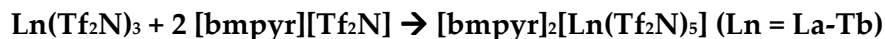


Fig. 6: Coordination mode of $[Tf_2N]^-$ in $[bmpyr][Ca(Tf_2N)_4]$ (top) and $[bmpyr][Ba(Tf_2N)_3]$ (bottom)

Putting all the gained information together the following reaction paths can be concluded for dissolving rare-earth-compounds in [Tf₂N] and [OTf]-based ionic liquids:



These observations are important, as many reactions in these type of solvents may be crucially influenced by complexation. The formation of *-ate* complexes leads to a different behaviour of Ln-ions dissolved in ionic liquids compared to neutral, molecular solvents. By using rare-earth compounds as synthetic reagents in ionic liquids, one should be aware how the structure of “active” species looks like, and that it differs significantly from the ones observed in molecular solvents.

- [1] D.B. Baudry, A. Dormond, F. Duris, J.M. Bernard, J.R. Desmurs, *J. Fluorine Chem.* **2003**, *121*, 233.
- [2] Generally the crystallization of lanthanide-sulfonylamines seems to be difficult: K. Mikami, O. Kotera, Y. Motoyama, M. Tanaka, *Inorg. Chem. Comm.* **1998**, *1*, 10.

V Appendix

1. General Methods

1.1 Experimental techniques

The compounds synthesized in this work as well as the educts are air and moisture sensitive. Therefore the materials were prepared and stored under inert gas conditions. Reactions were carried out using either standard *Schlenk*-technique at a vacuum/argon line or using glass ampoules in an argon-glovebox (MBraun, Garching). Reaction ampoules were sealed under dynamic vacuum conditions outside the glovebox, connected to a vacuum-line. All reaction vessels were carefully dried several hours in a drying cupboard and evacuated in the chamber of the argon-glovebox prior to use. The LnI_3 and $\text{Ln}(\text{Tf}_2\text{N})_3$ educts were sublimed prior to use, the ionic liquids were purified until they exhibited CV-grade purity and dried for at least 24 hours at $120^\circ\text{C} / 10^{-3}$ mbar.

1.2 XRD-methods

Powder diffraction data were recorded on a Huber G670, (Huber, Rimsting, Germany) with Mo-radiation. The samples were powdered and filled in glass-capillaries which were sealed under argon atmosphere. Single crystal data was obtained from a image plate diffraction system with graphite monochromated MoK_α radiation (IPDS, Stoe&Cie, Darmstadt, Germany). Crystal structure solution was accomplished by direct methods using SHELXS-97 [1]. Subsequent difference Fourier analyses and least squares refinements with SHELXL-97 [2] allowed the localization of the remaining atom positions. Data reduction was carried out with the program package X-Red [3], numerical absorption corrections with the program X-Shape [4]. For crystal structure drawings the program Diamond was employed [5].

1.3 Absorption-, Emission- and Raman-spectroscopy

Absorption spectra were recorded on a two-beam spectrometer Cary 05E (Varian, Palo Alto, USA). The visible and near-infrared radiation is generated by a quartz-iodine lamp, the UV-radiation by a deuterium-lamp.

Emission spectra were recorded on a Spex Fluoromax-3 Spectrofluorometer (Jobin Yvon Inc., Longjumeau cedex / France) which is equipped with a xenon lamp (250-850 nm excitation energy). Two Czerny-Tuner monochromators focus the excitation and emission beam, the signals are detected with a R928P-Photomultiplier tube and corrected by a UV-Silicon photo-diode.

Raman spectra were obtained from the bulk solids recorded at 150 mW on a Bruker IFS-FRA-106/s. For the measurement the respective samples were sealed under an argon atmosphere in glass capillaries and recorded at room temperature.

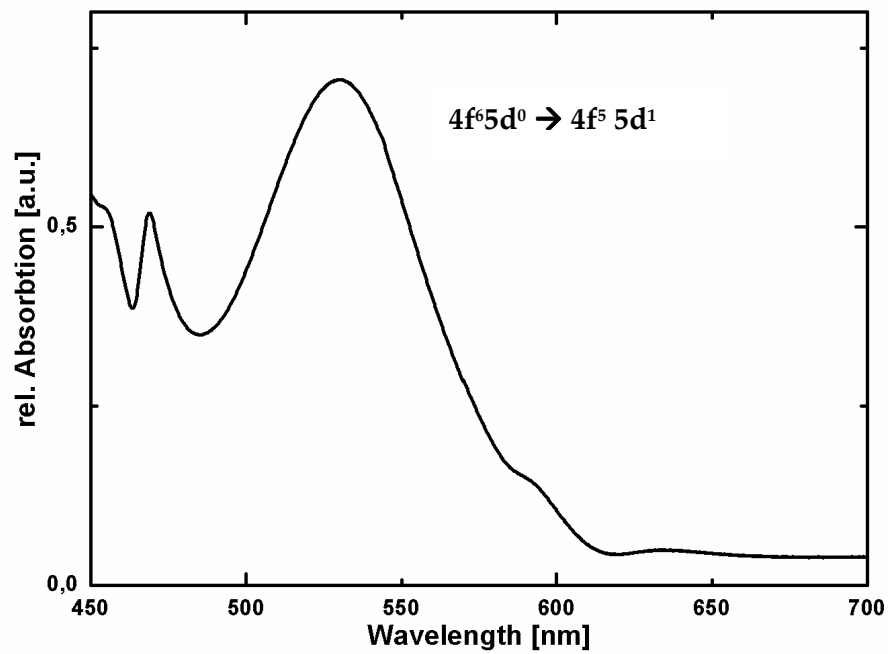
1.4 DSC and cyclic voltammetry

DSC thermograms were measured on a DSC 204 F1 Phoenix (Netzsch, Selb, Germany) equipped with a τ -sensor and nitrogen cooling. All samples were put in aluminum crucibles which were sealed under argon atmosphere. The reference was an empty aluminum crucible with a pierced lid. The measuring unit and the heating furnace were held in an argon stream during the measurement (20 ml/min, 70ml/min respectively). The heating rate was in all cases 5K/min, typical sample-masses are 10-20 mg. The temperature programs were all applied several times on each sample, all transitions were reversible and appeared at the same temperatures.

Cyclic voltammograms were measured on an Autolab PGStat-12 (Metrohm, Filderstadt, Germany). A platinum working electrode (12.57 mm²), a glassy carbon counter electrode and a silver-rod quasi reference electrode were used as a setup. All measurements were carried under an argon atmosphere with a scan rate of 100 mV/s. The electrodes were polished after each measurement with CeO₂, washed with acetone and deionized water, and dried in vacuum prior use.

- [1] SHELXS-97, W.S. Sheldrick, Universität Göttingen, 1997.
- [2] SHELXL-97, W.S. Sheldrick, Universität Göttingen, 1997.
- [3] X-RED, Stoe & Cie, Darmstadt, 2002.
- [4] X-Shape, Stoe & Cie, Darmstadt, 2002.
- [5] Diamond Version 2.1e, Crystal Impact GbR, 1996-2001.

2. VIS-Spectrum of Sm^{2+} in $[\text{bmpyr}][\text{Tf}_2\text{N}]$



3. List of Abbreviations

IL	ionic liquid
RTIL	room temperature ionic liquid
°C	degree celcius
K	Kelvin
V	Volt
A	Ampere
h	hour
min	minutes
IR	infrared
VIS	visible
mp	melting point
CV	cyclic voltamogramm
DSC	difference scanning calorimetry
Ln	Lanthanide (La-Lu)
bmpyr	1-butyl-1-methylpyrrolidinium
mppy	1-propyl-1-methylpyrrolidinium
bmim	1-butyl-1-methylpyrrolidinium
S(Et) ₃	triethylsulfonium
OTf	triflate = trifluomethanesulfonate
Tf ₂ N	bis(trifluormethanesulfonyl)amide

4. Chemicals

Iodine, sublimed	Merck, Darmstadt (D)
Ammoniumiodide p.a.	Merck, Darmstadt (D)
Nd, La 99,9%	Aldrich, Milwaukee, (USA)
Pr, Sm, Eu, Gd, Tb, Dy, Yb 99,9%	Chempur, Karlsruhe (D)
Tm 99,9 %	Acros, New Jersey (USA)
Lu 99,9 %	Smart Elements, Vienna (A)
N-Methylpyrrolidin, N-Methylimidazol 98%	Aldrich, München (D)
Triethylsulfoniumiodide	Lancaster, Karlsruhe (D)
Lithium-bis(trifluormethanesulfonyl)amide 97%	Fluka, Seelze (D)
Lithium-trifluoromethanesulfonate 98+%	Lancaster, Karlsruhe (D)
Bis(trifluoromethanesulfon)imide 95%	Fluka, Seelze (D)
Alkyl-halides 99+%	Fluka, Seelze (D)
Aluminiumoxide	Acros Organics, Geel (BE)

5. Publications

A.-V. Mudring, A. Babai, S. Arenz, R. Giernoth: "The „non-coordinating“ anion bis(trifluoromethanesulfonyl)amide (BTA) coordinating to Yb²⁺: the first structurally characterized bis(trifluoromethanesulfonyl)-amid complex [mppyr]₂[Yb(BTA)₄] from the ionic liquid [mppyr][BTA]" *Angew. Chem.* **2005**, *117*, 5621; *Angew. Chem. Int. Ed.* **2005**, *44*, 5485.

A. Babai, A.-V. Mudring: "Rare Earth Halides in Ionic Liquids - [SEt₃]₃[LnI₆], Ln = Nd, Sm" *Inorg. Chem.* **2005**, *44*, 8168.

A. Babai, A.-V. Mudring: "Anhydrous PrI₃ in the ionic liquid [bmpyr][Tf₂N] : Solid state structure of [bmpyr]₄[PrI₆][Tf₂N] and luminescence of Pr³⁺ in the liquid [bmpyr][Tf₂N] phase" *Chem. Mat.* **2005**, *17*, 6230.

A. Babai, A.-V. Mudring: "The First Homoleptic Bis(trifluoromethanesulfonyl)amide Complex Compounds Of Trivalent f-Elements" *Dalton Trans.* **2006**, *15*, 1828.

A. Babai, A.-V. Mudring: "Homoleptic Alkaline Earth Metal Bis(trifluoromethanesulfonyl)amide Complex Compounds Obtained From an Ionic Liquid" *Inorg. Chem.* **2006**, *45*, 3249.

A. Babai, A.-V. Mudring: "Crystal Engineering in Ionic Liquids. The Crystal Structures of [mppyr]₃[NdI₆] and [bmpyr]₄[NdI₆][Tf₂N]" *Inorg. Chem.* **2006**, *45*, 4847.

Ich versichere, dass ich die von mir vorgelegte Dissertation selbstständig angefertigt, die benutzten Quellen und Hilfsmittel vollständig angegeben und die Stellen der Arbeit - einschließlich Tabellen, Karten und Abbildungen -, die anderen Werken in Wortlaut oder dem Sinn nach entnommen sind, in jedem Einzelfall als Entlehnung kenntlich gemacht habe; dass diese Dissertation noch keiner anderen Fakultät oder Universität zur Prüfung vorgelegen hat; dass sie noch nicht veröffentlicht worden ist; dass ich eine solche Veröffentlichung vor Abschluss des Promotionsverfahrens nicht vornehmen werde.

Die Bestimmungen der geltenden Promotionsordnung sind mir bekannt. Die von mir vorgelegte Dissertation ist von Frau Priv.-Doz. Dr. Anja-Verena Mudring betreut worden.

Köln, 28. August 2006

Curriculum Vitae

Persönliche Daten:

Name	Arash Babai
Geburtstag	31.07.1977
Geburtsort	Trier
Anschrift	Salierring 33 – D-50677 Köln
Nationalität	deutsch
Familienstand	ledig

Bildungsweg:

Seit 09/2004	Promotion, Universität zu Köln
09/2004	Diplom, Universität zu Köln
05/2004 – 09/2004	Diplomarbeit, Universität zu Köln
05/2004	Diplomprüfungen, Universität zu Köln
05/2002	Vordiplom, Universität zu Köln
10/1999	Immatrikulation an der Universität zu Köln
06/1999	Allg. Hochschulreife, Goethegymnasium Hildesheim
1994 – 1999	Goethegymnasium Hildesheim, Hildesheim
1990 – 1994	Gymnasium Josephinum, Hildesheim
1987 – 1990	Orientierungsstufe St.-Augustinus, Hildesheim
1983 – 1987	Grundschule St. Nikolaus, Hildesheim

Aktivitäten an der Universität:

Seit 09/2004	Wissenschaftlicher Mitarbeiter, Universität zu Köln
10/2002 – 09/2004	Studentische Hilfskraft, Universität zu Köln

Köln, 28.08.2006

